STRUCTURE AND STABILITY OF HYDROXY-Cr AND -Al INTERLAYERS IN MONTMORILLONITE

BY

WILLIAM E. DUBBIN

A Thesis
Submitted to the Faculty of Graduate Studies
in Partial Fulfillment of the Requirements
for the Degree of

DOCTOR OF PHILOSOPHY

Department of Soil Science
University of Manitoba
Winnipeg, Manitoba

ISBN 0-612-13092-4

Name _____

Dissertation Abstracts International is arranged by broad, general subject categories. Please select the one subject which most nearly describes the content of your dissertation. Enter the corresponding four-digit code in the spaces provided.

Mineralogy
SUBJECT TERM

0411
SUBJECT CODE

U·M·I

Subject Categories

THE HUMANITIES AND SOCIAL SCIENCES

COMMUNICATIONS AND THE ARTS
Architecture 0729
Art History 0377
Cinema 0900
Dance 0378
Fine Arts 0357
Information Science 0723
Journalism 0391
Library Science 0399
Mass Communications 0708
Music 0413
Speech Communication 0459
Theater 0465

EDUCATION
General 0515
Administration 0514
Adult and Continuing 0516
Agricultural 0517
Art 0273
Bilingual and Multicultural 0282
Business 0688
Community College 0275
Curriculum and Instruction 0727
Early Childhood 0518
Elementary 0524
Finance 0277
Guidance and Counseling 0519
Health 0680
Higher 0745
History of 0520
Home Economics 0278
Industrial 0521
Language and Literature 0279
Mathematics 0280
Music 0522
Philosophy of 0998
Physical 0523
Psychology 0525
Reading 0535
Religious 0527
Sciences 0714
Secondary 0533
Social Sciences 0534
Sociology of 0340
Special 0529
Teacher Training 0530
Technology 0710
Tests and Measurements 0288
Vocational 0747

LANGUAGE, LITERATURE AND LINGUISTICS
Language
- General 0679
- Ancient 0289
- Linguistics 0290
- Modern 0291

Literature
- General 0401
- Classical 0294
- Comparative 0295
- Medieval 0297
- Modern 0298
- African 0316
- American 0591
- Asian 0305
- Canadian (English) 0352
- Canadian (French) 0355
- English 0593
- Germanic 0311
- Latin American 0312
- Middle Eastern 0315
- Romance 0313
- Slavic and East European 0314

PHILOSOPHY, RELIGION AND THEOLOGY
Philosophy 0422
Religion
- General 0318
- Biblical Studies 0321
- Clergy 0319
- History of 0320
- Philosophy of 0322

Theology 0469

SOCIAL SCIENCES
American Studies 0323
Anthropology
- Archaeology 0324
- Cultural 0326
- Physical 0327

Business Administration
- General 0310
- Accounting 0272
- Banking 0770
- Management 0454
- Marketing 0338

Canadian Studies 0385
Economics
- General 0501
- Agricultural 0503
- Commerce-Business 0505
- Finance 0508
- History 0509
- Labor 0510
- Theory 0511

Folklore 0358
Geography 0366
Gerontology 0351
History
- General 0578
- Ancient 0579
- Medieval 0581
- Modern 0582
- Black 0328
- African 0331
- Asia, Australia and Oceania 0332
- Canadian 0334
- European 0335
- Latin American 0336
- Middle Eastern 0333
- United States 0337

History of Science 0585
Law 0398
Political Science
- General 0615
- International Law and Relations 0616
- Public Administration 0617

Recreation 0814
Social Work 0452
Sociology
- General 0626
- Criminology and Penology ... 0627
- Demography 0938
- Ethnic and Racial Studies 0631
- Individual and Family Studies 0628
- Industrial and Labor Relations 0629
- Public and Social Welfare 0630
- Social Structure and Development 0700
- Theory and Methods 0344

Transportation 0709
Urban and Regional Planning 0999
Women's Studies 0453

THE SCIENCES AND ENGINEERING

BIOLOGICAL SCIENCES
Agriculture
- General 0473
- Agronomy 0285
- Animal Culture and Nutrition 0475
- Animal Pathology 0476
- Food Science and Technology 0359
- Forestry and Wildlife 0478
- Plant Culture 0479
- Plant Pathology 0480
- Plant Physiology 0817
- Range Management 0777
- Wood Technology 0746

Biology
- General 0306
- Anatomy 0287
- Biostatistics 0308
- Botany 0309
- Cell 0379
- Ecology 0329
- Entomology 0353
- Genetics 0369
- Limnology 0793
- Microbiology 0410
- Molecular 0307
- Neuroscience 0317
- Oceanography 0416
- Physiology 0433
- Radiation 0821
- Veterinary Science 0778
- Zoology 0472

Biophysics
- General 0786
- Medical 0760

EARTH SCIENCES
Biogeochemistry 0425
Geochemistry 0996
Geodesy 0370
Geology 0372
Geophysics 0373
Hydrology 0388
Mineralogy 0411
Paleobotany 0345
Paleoecology 0426
Paleontology 0418
Paleozoology 0985
Palynology 0427
Physical Geography 0368
Physical Oceanography 0415

HEALTH AND ENVIRONMENTAL SCIENCES
Environmental Sciences 0768
Health Sciences
- General 0566
- Audiology 0300
- Chemotherapy 0992
- Dentistry 0567
- Education 0350
- Hospital Management 0769
- Human Development 0758
- Immunology 0982
- Medicine and Surgery 0564
- Mental Health 0347
- Nursing 0569
- Nutrition 0570
- Obstetrics and Gynecology .. 0380
- Occupational Health and Therapy 0354
- Ophthalmology 0381
- Pathology 0571
- Pharmacology 0419
- Pharmacy 0572
- Physical Therapy 0382
- Public Health 0573
- Radiology 0574
- Recreation 0575
- Speech Pathology 0460
- Toxicology 0383

Home Economics 0386

PHYSICAL SCIENCES
Pure Sciences
Chemistry
- General 0485
- Agricultural 0749
- Analytical 0486
- Biochemistry 0487
- Inorganic 0488
- Nuclear 0738
- Organic 0490
- Pharmaceutical 0491
- Physical 0494
- Polymer 0495
- Radiation 0754

Mathematics 0405
Physics
- General 0605
- Acoustics 0986
- Astronomy and Astrophysics 0606
- Atmospheric Science 0608
- Atomic 0748
- Electronics and Electricity 0607
- Elementary Particles and High Energy 0798
- Fluid and Plasma 0759
- Molecular 0609
- Nuclear 0610
- Optics 0752
- Radiation 0756
- Solid State 0611

Statistics 0463

Applied Sciences
Applied Mechanics 0346
Computer Science 0984
Engineering
- General 0537
- Aerospace 0538
- Agricultural 0539
- Automotive 0540
- Biomedical 0541
- Chemical 0542
- Civil 0543
- Electronics and Electrical 0544
- Heat and Thermodynamics ... 0348
- Hydraulic 0545
- Industrial 0546
- Marine 0547
- Materials Science 0794
- Mechanical 0548
- Metallurgy 0743
- Mining 0551
- Nuclear 0552
- Packaging 0549
- Petroleum 0765
- Sanitary and Municipal 0554
- System Science 0790

Geotechnology 0428
Operations Research 0796
Plastics Technology 0795
Textile Technology 0994

PSYCHOLOGY
General 0621
Behavioral 0384
Clinical 0622
Developmental 0620
Experimental 0623
Industrial 0624
Personality 0625
Physiological 0989
Psychobiology 0349
Psychometrics 0632
Social 0451

Nom _____

Dissertation Abstracts International est organisé en catégories de sujets. Veuillez s.v.p. choisir le sujet qui décrit le mieux votre thèse et inscrivez le code numérique approprié dans l'espace réservé ci-dessous.

_____ ☐☐☐ U·M·I

SUJET — CODE DE SUJET

Catégories par sujets

HUMANITÉS ET SCIENCES SOCIALES

COMMUNICATIONS ET LES ARTS
Architecture 0729
Beaux-arts 0357
Bibliothéconomie 0399
Cinéma 0900
Communication verbale 0459
Communications 0708
Danse 0378
Histoire de l'art 0377
Journalisme 0391
Musique 0413
Sciences de l'information 0723
Théâtre 0465

ÉDUCATION
Généralités 515
Administration 0514
Art 0273
Collèges communautaires 0275
Commerce 0688
Économie domestique 0278
Éducation permanente 0516
Éducation préscolaire 0518
Éducation sanitaire 0680
Enseignement agricole 0517
Enseignement bilingue et multiculturel 0282
Enseignement industriel 0521
Enseignement primaire. 0524
Enseignement professionnel 0747
Enseignement religieux 0527
Enseignement secondaire 0533
Enseignement spécial 0529
Enseignement supérieur 0745
Évaluation 0288
Finances 0277
Formation des enseignants 0530
Histoire de l'éducation 0520
Langues et littérature 0279
Lecture 0535
Mathématiques 0280
Musique 0522
Orientation et consultation 0519
Philosophie de l'éducation 0998
Physique 0523
Programmes d'études et enseignement 0727
Psychologie 0525
Sciences 0714
Sciences sociales 0534
Sociologie de l'éducation 0340
Technologie 0710

LANGUE, LITTÉRATURE ET LINGUISTIQUE
Langues
- Généralités 0679
- Anciennes 0289
- Linguistique 0290
- Modernes 0291

Littérature
- Généralités 0401
- Anciennes 0294
- Comparée 0295
- Médiévale 0297
- Moderne 0298
- Africaine 0316
- Américaine 0591
- Anglaise 0593
- Asiatique 0305
- Canadienne (Anglaise) 0352
- Canadienne (Française) 0355
- Germanique 0311
- Latino-américaine 0312
- Moyen-orientale 0315
- Romane 0313
- Slave et est-européenne 0314

PHILOSOPHIE, RELIGION ET THÉOLOGIE
Philosophie 0422
Religion
- Généralités 0318
- Clergé 0319
- Études bibliques 0321
- Histoire des religions 0320
- Philosophie de la religion 0322

Théologie 0469

SCIENCES SOCIALES
Anthropologie
- Archéologie 0324
- Culturelle 0326
- Physique 0327

Droit 0398
Économie
- Généralités 0501
- Commerce-Affaires 0505
- Économie agricole 0503
- Économie du travail 0510
- Finances 0508
- Histoire 0509
- Théorie 0511

Études américaines 0323
Études canadiennes 0385
Études féministes 0453
Folklore 0358
Géographie 0366
Gérontologie 0351
Gestion des affaires
- Généralités 0310
- Administration 0454
- Banques 0770
- Comptabilité 0272
- Marketing 0338

Histoire
- Histoire générale 0578
- Ancienne 0579
- Médiévale 0581
- Moderne 0582
- Histoire des noirs 0328
- Africaine 0331
- Canadienne 0334
- États-Unis 0337
- Européenne 0335
- Moyen-orientale 0333
- Latino-américaine 0336
- Asie, Australie et Océanie 0332

Histoire des sciences 0585
Loisirs 0814
Planification urbaine et régionale 0999
Science politique
- Généralités 0615
- Administration publique 0617
- Droit et relations internationales 0616

Sociologie
- Généralités 0626
- Aide et bien-être social 0630
- Criminologie et établissements pénitentiaires 0627
- Démographie 0938
- Études de l' individu et de la famille 0628
- Études des relations interethniques et des relations raciales 0631
- Structure et développement social 0700
- Théorie et méthodes. 0344
- Travail et relations industrielles 0629

Transports 0709
Travail social 0452

SCIENCES ET INGÉNIERIE

SCIENCES BIOLOGIQUES
Agriculture
- Généralités 0473
- Agronomie. 0285
- Alimentation et technologie alimentaire 0359
- Culture 0479
- Élevage et alimentation 0475
- Exploitation des pâturages 0777
- Pathologie animale 0476
- Pathologie végétale 0480
- Physiologie végétale 0817
- Sylviculture et faune 0478
- Technologie du bois 0746

Biologie
- Généralités 0306
- Anatomie 0287
- Biologie (Statistiques) 0308
- Biologie moléculaire 0307
- Botanique 0309
- Cellule 0379
- Écologie 0329
- Entomologie 0353
- Génétique 0369
- Limnologie 0793
- Microbiologie 0410
- Neurologie 0317
- Océanographie 0416
- Physiologie 0433
- Radiation 0821
- Science vétérinaire 0778
- Zoologie 0472

Biophysique
- Généralités 0786
- Medicale 0760

SCIENCES DE LA TERRE
Biogéochimie 0425
Géochimie 0996
Géodésie 0370
Géographie physique 0368
Géologie 0372
Géophysique 0373
Hydrologie 0388
Minéralogie 0411
Océanographie physique 0415
Paléobotanique 0345
Paléoécologie 0426
Paléontologie 0418
Paléozoologie 0985
Palynologie 0427

SCIENCES DE LA SANTÉ ET DE L'ENVIRONNEMENT
Économie domestique 0386
Sciences de l'environnement 0768
Sciences de la santé
- Généralités 0566
- Administration des hôpitaux 0769
- Alimentation et nutrition 0570
- Audiologie 0300
- Chimiothérapie 0992
- Dentisterie 0567
- Développement humain 0758
- Enseignement 0350
- Immunologie 0982
- Loisirs 0575
- Médecine du travail et thérapie 0354
- Médecine et chirurgie 0564
- Obstétrique et gynécologie 0380
- Ophtalmologie 0381
- Orthophonie 0460
- Pathologie 0571
- Pharmacie 0572
- Pharmacologie 0419
- Physiothérapie 0382
- Radiologie 0574
- Santé mentale 0347
- Santé publique 0573
- Soins infirmiers 0569
- Toxicologie 0383

SCIENCES PHYSIQUES
Sciences Pures
Chimie
- Généralités 0485
- Biochimie 487
- Chimie agricole 0749
- Chimie analytique 0486
- Chimie minérale 0488
- Chimie nucléaire 0738
- Chimie organique 0490
- Chimie pharmaceutique 0491
- Physique 0494
- PolymÈres 0495
- Radiation 0754

Mathématiques 0405
Physique
- Généralités 0605
- Acoustique 0986
- Astronomie et astrophysique 0606
- Électronique et électricité 0607
- Fluides et plasma 0759
- Météorologie 0608
- Optique 0752
- Particules (Physique nucléaire) 0798
- Physique atomique 0748
- Physique de l'état solide 0611
- Physique moléculaire 0609
- Physique nucléaire 0610
- Radiation 0756

Statistiques 0463

Sciences Appliqués Et Technologie
Informatique 0984
Ingénierie
- Généralités 0537
- Agricole 0539
- Automobile 0540
- Biomédicale 0541
- Chaleur et thermodynamique 0348
- Conditionnement (Emballage) 0549
- Génie aérospatial 0538
- Génie chimique 0542
- Génie civil 0543
- Génie électronique et électrique 0544
- Génie industriel 0546
- Génie mécanique 0548
- Génie nucléaire 0552
- Ingénierie des systèmes 0790
- Mécanique navale 0547
- Métallurgie 0743
- Science des matériaux 0794
- Technique du pétrole 0765
- Technique minière 0551
- Techniques sanitaires et municipales 0554
- Technologie hydraulique 0545

Mécanique appliquée 0346
Géotechnologie 0428
Matières plastiques (Technologie) 0795
Recherche opérationnelle 0796
Textiles et tissus (Technologie) 0794

PSYCHOLOGIE
Généralités 0621
Personnalité 0625
Psychobiologie 0349
Psychologie clinique 0622
Psychologie du comportement 0384
Psychologie du développement 0620
Psychologie expérimentale 0623
Psychologie industrielle 0624
Psychologie physiologique 0989
Psychologie sociale 0451
Psychométrie 0632

STRUCTURE AND STABILITY OF HYDROXY-Cr AND -Al INTERLAYERS IN MONTMORILLONITE

BY

WILLIAM E. DUBBIN

A Thesis submitted to the Faculty of Graduate Studies of the University of Manitoba in partial fulfillment of the requirements of the degree of

DOCTOR OF PHILOSOPHY

ACKNOWLEDGEMENTS

I offer my sincere gratitude to the following people who made this thesis possible. Firstly, I am grateful to Dr. Tee Boon Goh who gave this project direction then allowed me to follow my curiosity. Most importantly, though, I value his friendship, which made these four years a great pleasure. I am also grateful to the other members of my advisory committee, each of whom offered their expertise when needed: Dr. Dennis Oscarson, Dr. Chai Moo Cho, Dr. Frank Hawthorne, and Dr. Bill Last. I am also indepted to Dr. Geza Racz, Chair, Soil Science Department, who has provided support to this student in ways too numerous to count. I would also like to thank the many graduate students, staff, and summer students who made these four years very enjoyable and productive.

Financial assistance from the Natural Sciences and Engineering Research Council of Canada and the University of Manitoba in the form of several scholarships is also gratefully acknowledged.

Above all, I would like to thank my family for their love and support throughout a very enjoyable university career.

TABLE OF CONTENTS

LIST OF TABLES

LIST OF FIGURES

ABSTRACT

There is a lack of information concerning solid-phase Cr held in soils and sediments. This study was conducted to determine the structure and stability of hydroxy-Cr interlayers in montmorillonite, an abundant mineral in many soils and sediments. The hydroxy interlayers were prepared by adding varying amounts of $CrCl_3$ and $AlCl_3$ to separate montmorillonite suspensions. Each suspension was titrated with 0.1 *N* NaOH to give a $NaOH/M^{3+}$ molar ratio of 2.5 and then aged for 30 days.

X-ray photoelectron spectroscopic analysis of the solid-phase reaction products showed that all Cr which was detected was present as Cr(III). Montmorillonite was an effective sorbent for hydroxy-Cr species up to 1200 cmol(+)/kg. Above that concentration, sorption continued, though less efficiently. However, N_2-BET specific surfaces and cation exchange capacity measurements indicated that the montmorillonite could sorb significantly more than 1200 cmol(+)/kg. There was virtually no exchangeable Cr in any of the pure Cr clays, suggesting that this element was covalently bonded to the siloxane surface. Both infrared and nuclear magnetic resonance spectroscopy provided evidence in support of the inner-sphere complexation of Cr. Differential thermal analysis and thermogravimetric tracings showed that the rapid collapse of the pure Cr interlayers upon heating was due to a low-temperature loss of hydroxyls. Electron microscopy revealed that large amounts of sorbed hydrolyzed Cr induced the formation of montmorillonite microclusters. Due to

limitations in the instrumentation employed, however, it was not possible to identify all interlayer structures in the pure Cr clay.

As revealed by x-ray diffraction analysis, coprecipitated Al induced the formation of gibbsite-like polymers in each Cr clay. Data from cation exchanges, as well as from infrared and nuclear magnetic resonance spectroscopy, indicate that both Al and Cr were present within the same polymer. The presence of Cr reduced the exchangeability of the interlayers while Al increased the thermal stability.

In the presence of dilute NaOCl, the sorbed Cr(III) was oxidized rapidly. As the amount of Cr held by the pure Cr clays increased, the time required for complete interlayer dissolution decreased. Aluminum in the Al-Cr interlayers greatly decreased, but did not stop, the Cr(III) oxidation rate by forming a semi-permeable barrier around the Al-Cr polymers. The slow but sustained oxidation of Cr(III) from the Al-Cr clays was due to diffusion of Cr through the polymers. Despite modest protection offered by the Al, all sorbed Cr(III) was shown to be highly vulnerable to attack by powerful aqueous oxidants such as NaOCl.

Montmorillonite was shown to sorb large amounts of hydrolyzed Cr. The Cr was held strongly through covalent bonds with the siloxane surface and could not be displaced with simple cation exchange reactions. Under strongly oxidizing conditions, however, the sorbed Cr(III) was readily oxidized to the toxic Cr(VI) oxyanion. Therefore, although generally secure within the interlayers of montmorillonite, Cr presents a threat to ecosystem health when exposed to powerful aqueous oxidants.

1. INTRODUCTION

In recent years there has been a rapid accumulation of metals at the earth's surface due to the disposal of municipal and industrial wastes in landfill sites, as well as the application of sewage sludge to land (Lester 1987). Metals are also being added to soils and sediments either directly through agricultural practices or indirectly through atmospheric deposition of industrial pollutants and automobile emissions. The ultimate fate of these metals is of great concern due to their persistence and potential toxicity.

Chromium is among those metals which have caused the greatest concern, principally for two reasons. First, the human health risks posed by exposure to Cr(VI) are significant and have been well-founded in recent studies (Paustenbach et al. 1991; Sheehan et al. 1991). Second, Cr continues to be used widely in industry. Chromium is used mainly in the production of stainless steel and in electroplating. In addition, Cr is utilized in the tanning of leathers as well as the production of pigments, wood preservatives, and various oxidants (Hamilton and Wetterhahn 1988). In total, 10^6 to 10^7 tons of Cr are consumed globally each year. Thus, the potential anthropogenic input of Cr to the environment is high.

In the past, understanding the partitioning of Cr between the solid and liquid phases in soils and sediments was considered sufficient to evaluate the threat posed by this metal. Generally, solid-phase Cr was believed to occur simply as poorly-

soluble hydroxy polymers sorbed to colloids (Cary et al. 1977; Grove and Ellis 1980; James and Bartlett 1983). Only that Cr in solution was considered a threat to ecosystem health. As a consequence, all solid-phase Cr was considered equally non-toxic, despite a poor understanding of its various forms. The lack of information concerning the nature of solid-phase Cr prevented the development of a more comprehensive understanding of Cr behavior in soils and sediments. Only recently have efforts been directed toward elucidating the nature of this solid-phase component. Specifically, work has focussed on the sorption of Cr by Fe oxides (Charlet and Manceau 1992), Mn oxides (Manceau and Charlet 1992), and silica (Fendorf et al. 1994; Fendorf and Sparks 1994). Although these studies have provided significant new insights, there has not yet been any detailed work concerning the nature of hydroxy-Cr polymers sorbed to expandable layer silicates, which are major components of many soils and sediments.

Given the lack of information related to Cr held by expandable layer silicates, an investigation into the properties of hydroxy-Cr interlayers in these clays is well-justified. Montmorillonite is chosen as the parent clay due to its abundance in many soils and sediments as well as the ease with which it is intercalated. This investigation has two principal goals. The first objective is to determine the form of the sorbed hydroxy-Cr polymers. This goal encompasses both the gross structure of the hydroxy polymers as well as the mode of Cr complexation. The second aim is to determine the stability of the interlayered hydroxy-Cr polymers. More specifically, this entails

determining the exchangeability, thermal stability, and resistance to oxidative dissolution of the sorbed hydroxy-Cr polymers. In order to more closely mimic those interlayer materials which are likely to form in natural systems, hydroxy-Cr interlayers of several clay samples will be formed in the presence of Al. It is anticipated that all investigations will contribute to the fundamental understanding of Cr behavior in soils and sediments.

2. BACKGROUND

2.1 Structure and properties of expandable layer silicates

The basic structure of layer silicates has been presented elsewhere (Brindley and Brown 1980; Bailey 1988; Dixon and Weed 1989). Expandable layer silicates, that is those of the smectite and vermiculite groups, are characterized by a positive charge deficit arising from isomorphous substitution in the octahedral and/or tetrahedral sheets. Smectites are defined as those expandable layer silicates which have a charge deficit ranging from 0.5 to 1.2 per unit cell (Bailey 1980). In montmorillonite, which dominates the smectite group, the majority of this charge originates from the octahedral sheet. The need for electroneutrality results in the complexation of cations on the montmorillonite surface. The nature and concentration of these sorbed cations, as well as their mode of complexation, determine the distance between the individual 2:1 layers. The complexation of a simple hydroxy-metal polymer on montmorillonite is shown schematically in Figure 2.1. With specific surfaces that may exceed 800 m^2/g (van Olphen and Fripiat 1979) and interlayer distances as large as 30 Å (Rausell-Colom and Serratosa 1987), montmorillonite possesses a high capacity to sorb large amounts of counter-cations of diverse morphologies.

Functional groups in clay minerals may be defined as chemically reactive molecular units which are located at the particle margin (Sposito 1984). Phyllosilicates

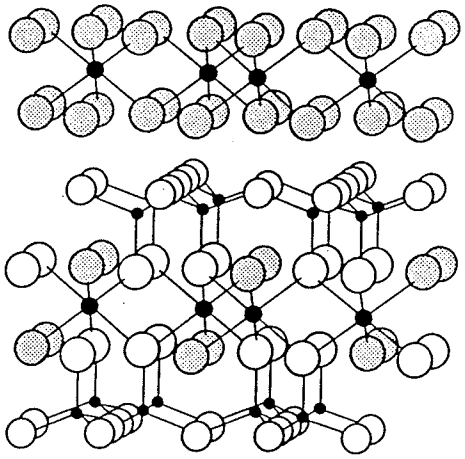

Figure 2.1. Ball and stick representation of a 2:1 layer with a hydroxide interlayer (From Sposito 1984).

possess two principal kinds of functional groups. The first type consists of the various hydroxyl groups at the edges of the octahedral and tetrahedral sheets. Of greater importance in studies concerning the intercalation of hydroxy-metal polymers are the functional groups on the basal surface of the tetrahedral sheets. The basal oxygen atoms of the silicon tetrahedra collectively comprise the siloxane surface. As a result of rotation of the silicon tetrahedra to fit the octahedral sheet, the siloxane oxygen atoms lie in two distinct planes which are separated by a distance of 0.2 Å. When viewed along the c-axis the siloxane oxygen appear to form hexagonal cavities but, because the oxygen atoms lie in two separate planes, the cavities are more accurately described as ditrigonal (Figure 2.2). In the absence of a positive charge deficit in the

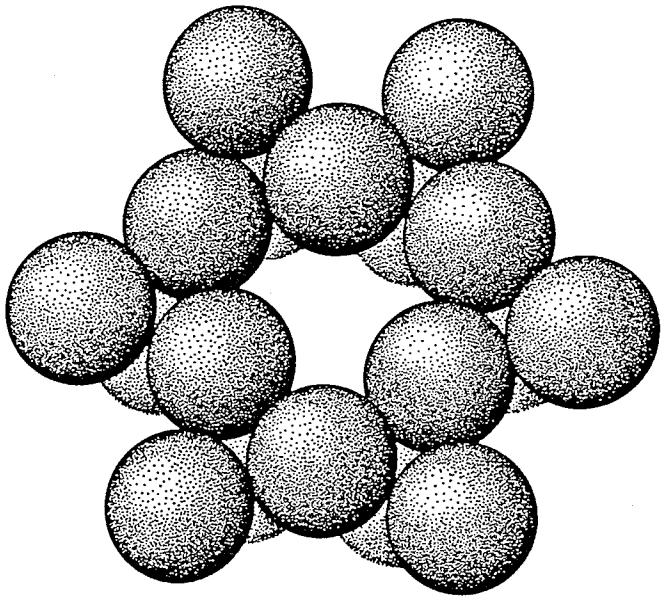

Figure 2.2. The siloxane ditrigonal cavity in a tetrahedral sheet of a layer silicate as viewed along the c-axis (From Sposito 1984).

2:1 layer, the ditrigonal cavities serve only as very soft Lewis bases. With isomorphous substitution, however, the ditrigonal cavities become increasingly stronger Lewis bases. The Lewis base character of the ditrigonal cavities is determined not only by the magnitude of the layer charge, but also by its location. If substitution occurs at a single site in the octahedral sheet, the resulting negative charge will be distributed mainly over 10 siloxane oxygen atoms (Sposito 1984). However, if the substitution occurs in the tetrahedral sheet, the excess negative charge will be distributed over only three oxygen atoms. Therefore, for an equivalent amount of substitution, charge originating from the tetrahedral sheet imparts a much greater

Lewis base character to the siloxane oxygen.

2.2 Formation of hydroxy-metal polymers

2.2.1 Cation hydrolysis

Cation hydrolysis is an important process in soils. The hydrolysis of metal cations, leading to their precipitation as hydroxides, decreases their solubility and, consequently, their bioavailability. Depending on the element, this may be deleterious or beneficial. Hydroxy polymers of metals, particularly Al and Fe, also play an important role in enhancing soil clay aggregation (El Swaify and Emerson 1975).

The ionic potential (IP) of a cation, defined as the cation's valence to radius ratio, may be used to identify those cations which hydrolyze extensively at pH 7. If the IP is 30 to 95 nm^{-1}, a cation is able to repel protons from a solvating water molecule strongly enough to form a hydrolytic species, but not so strongly that an oxyanion forms (Sposito 1994). The IP values of Al^{3+} and Cr(III) are 56 and 48 nm^{-1}, respectively, well within the range of hydrolyzing cations. Clearly, hydrolytic species of these two metals will be abundant at pH values normally encountered in soil.

The hydrolysis of Al^{3+} has been studied extensively (Hsu 1989). Hydrolysis begins with the loss of a proton from the hexaaqua Al complex and proceeds stepwise with the loss of additional protons:

$$Al(H_2O)_6^{3+} + H_2O \rightleftarrows Al(OH)(H_2O)_5^{2+} + H_3O^+ \qquad (1)$$

$$Al(OH)(H_2O)_5^{2+} + H_2O \rightleftarrows Al(OH)_2(H_2O)_4^{+} + H_3O^{+} \quad (2)$$

$$Al(OH)_2(H_2O)_4^{+} + H_2O \rightleftarrows Al(OH)_3(H_2O)_3^{0} + H_3O^{+} \quad (3)$$

The pK values for the first, second, and third hydrolysis reactions of Al^{3+} have been determined to be 5, 10, and 17, respectively (Nordstrom and May 1989). The hydrolysis of Cr(III) can likewise be described with a series of equilibrium reactions. The corresponding hydrolysis constants for Cr(III), while not known as precisely as those for Al^{3+}, are comparable (Baes and Mesmer 1976; Rai et al. 1987).

The kinetics of mononuclear hydrolysis are rapid for both Al^{3+} and Cr(III). The specific rate constant for the loss of a proton from $Al(H_2O)_6^{3+}$ was determined to be 1.1×10^5 s^{-1} (Fong and Grunwald 1969) while that for $Cr(H_2O)_6^{3+}$ was found to be 1.4×10^5 s^{-1} (Rich et al. 1969). With respect to the thermodynamics and kinetics of hydrolysis, therefore, Al^{3+} and Cr(III) behave similarly.

2.2.2 Cation polymerization

The rates of formation of polynuclear complexes of Al^{3+} and Cr(III) are significantly different. Polymers of Al form much more rapidly than those of Cr. The fundamental reason for this difference lies in the different rates of ligand substitution for these two metals. As shown in Figure 2.3, the exchange of coordinated water molecules with bulk water in a hexaaqua Al^{3+} complex is several orders of magnitude faster than the exchange in a Cr(III) complex. Similar exchanges are required for

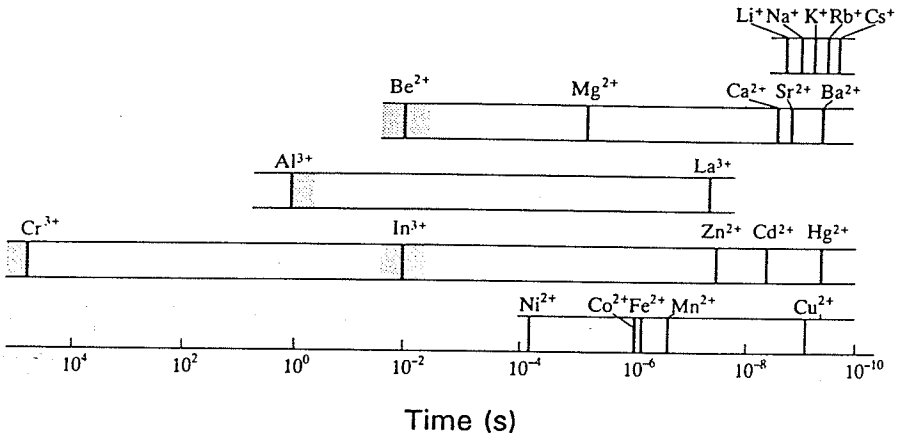

Figure 2.3. Typical lifetimes for the exchange of water molecules in hexaaqua complexes (From Shriver et al. 1990).

polymerization to occur. For example, during the dimerization process, each hydrolyzed cation must shed a single water molecule. The bound hydroxyls can then serve as bridging ligands. Because a water molecule is displaced, however, the hydrolyzed cation must temporarily adopt five-fold coordination. For metals with d^3 configuration, such as Cr(III), the energy required in going from octahedral to trigonal bipyramidal geometry is prohibitively high. This high energy barrier can be explained in terms of ligand field theory. In an octahedral field, the three d electrons of Cr(III) are in their ground state configuration (Figure 2.4). That is, all three electrons are unpaired and in the lower energy t_{2g} orbitals. Deviation from octahedral geometry forces electrons to be either spin-paired or promoted to higher energy orbitals.

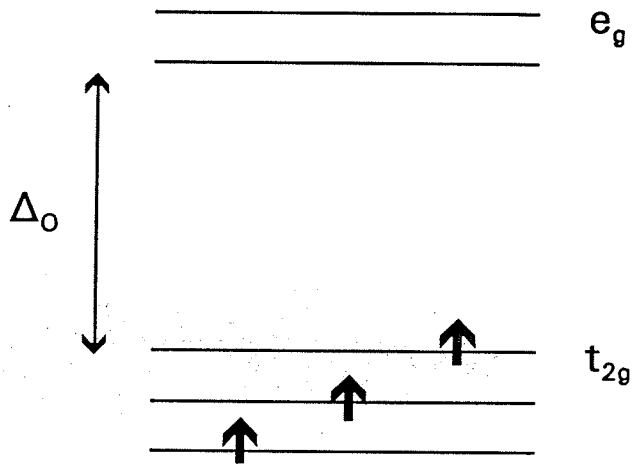

Figure 2.4. Orbital energy level diagram showing the ground state electron configuration of a d^3 octahedral complex.

Because both the ligand field splitting energy, Δ_o, and the pairing energy are high, the formation of a trigonal bipyramidal intermediate is highly unfavored. The end result of the slow ligand displacement around Cr(III) is that its polymerization is extremely slow. Unless the hydroxy-Cr polymers are allowed to age for months or years, they will remain small and poorly ordered.

2.3 Characteristics of hydroxy-interlayer materials

Hydroxy interlayers of many metals have been prepared in the laboratory or observed in natural environments. Specifically, hydroxy interlayers of Al (Keren

1980; Barnhisel and Bertsch 1989), Bi (Yamanaka et al. 1980), Cr (Brindley and Yamanaka 1979; Carr 1985), Cu (Bassett 1958), Fe (Herrera and Peech 1970), Mg (Brindley and Kao 1980), Ni (Yamanaka and Brindley 1978; Ghesquiere et al. 1982), Si (Sterte and Shabtai 1987; Lou and Huang 1988), and Zr (Yamanaka and Brindley 1979) have been reported. Of all the hydroxy polymers which have been studied, those of Al have received the most attention. The diverse and exhaustive studies of hydroxy-Al interlayers have been justified by the abundance and potential toxicity of Al, and have been made feasible by the ease with which these interlayers form.

The basic building block of the most widely accepted structure for hydroxy-Al interlayers is the hexamer, $[Al_6(OH)_{12}(H_2O)_{12}]^{6+}$ (Figure 2.5)(Hsu and Bates 1964).

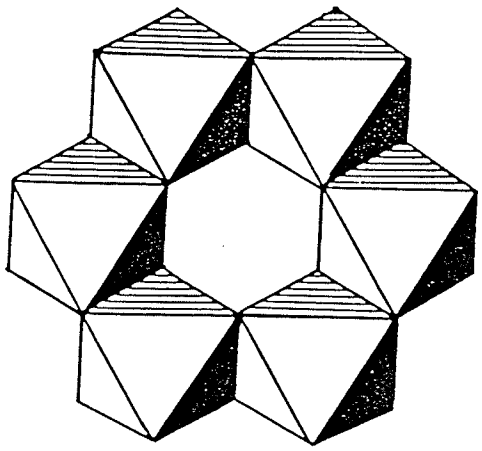

Figure 2.5. Illustration of the ring structure formed by the aluminum hexamer, $[Al_6(OH)_{12}(H_2O)_{12}]^{6+}$ (From Schutz et al. 1987).

Intercalation of layer silicates with these hexameric units yields a basal spacing of approximately 14 Å, similar to that of chlorite. Growth of the polymer is believed to be initiated by deprotonation of the edge-group water molecules. The polynuclear units can then coalesce as hydroxide bridges are formed. The growth of the hydroxy-Al polymers is depicted in Figure 2.6. It is clear from this sequence that as the polymers enlarge, the OH/Al ratio increases and the average charge per Al decreases.

Several workers have observed d(001) spacings of 18 to 19 Å for smectites intercalated with hydroxy-Al species (Brindley and Sempels 1977; Lahav and Shani 1978). Basal spacings of approximately 19 Å would arise if two hexameric Al polymers were stacked along the c-axis within the interlayer space. Alternatively, the hydroxy-Al species may be of the form depicted in Figure 2.7. This hydroxy polymer consists of a central tetrahedrally coordinated Al surrounded by four groups of three Al octahedra. The most commonly reported composition for this "Al_{13}" polynuclear species is $[AlO_4Al_{12}(OH)_{24}(H_2O)_{12}]^{7+}$ (Bertsch 1989). Intercalation of smectite with these Al_{13} polymers would also produce the observed 19 Å spacing. In fact, solid state ^{27}Al and ^{29}Si NMR studies have identified Al_{13} as the interlayer component of several clays (Plee et al. 1985; Schutz et al. 1987).

Hydroxy-Cr interlayers are not nearly as well understood as those of Al. The earliest investigations attempted to simply determine the molecular weight of the sorbed hydroxy-Cr polymers (Rengasamy and Oades 1978). In all cases, the hydroxy-Cr polymers were considerably smaller than their Al counterparts. Later, efforts were

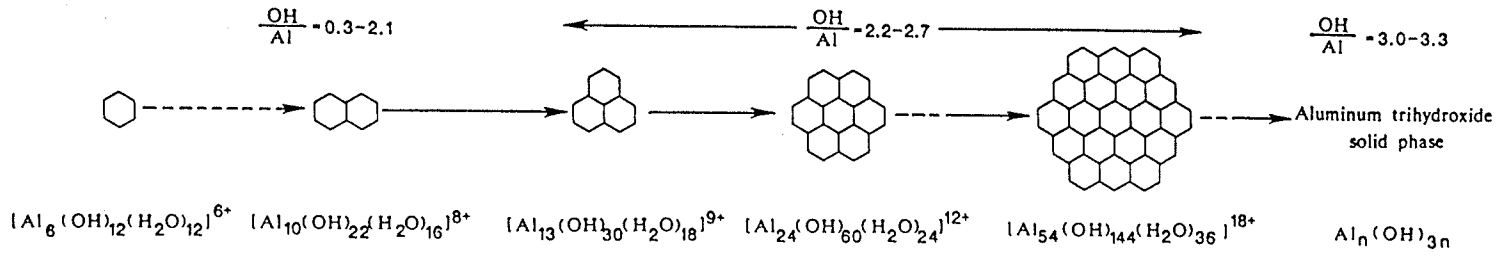

Figure 2.6. Depiction of aluminum polymerization as individual hexamers coalesce (From Bertsch 1989).

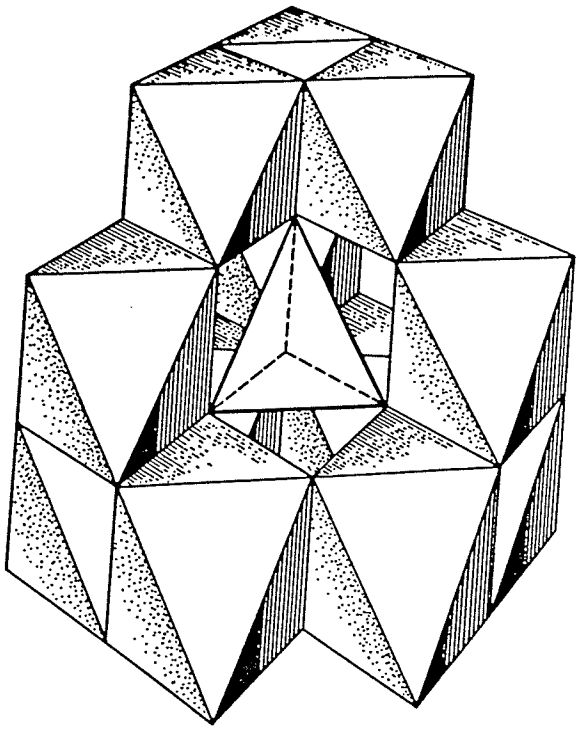

Figure 2.7. Representation of the $[AlO_4Al_{12}(OH)_{24}(H_2O)_{12}]^{7+}$ polynuclear species showing the central tetrahedrally coordinated Al surrounded by four sets of three Al octahedra (From Baes and Mesmer 1976).

directed at determining the composition of the interlayered polymeric species (Brindley and Yamanaka 1979; Carr 1985). These workers found that the interlayer material had $(OH+H_2O)/Cr$ molar ratios which were consistent with the polymers ranging in size from dimers to hexamers. The d(001) reflections of the interlayered montmorillonite ranged from 15 to 17 Å, considerably larger than for a chlorite. These reflections were also broad, indicating that the basal spacings were variable. The intercalation of montmorillonite with hydroxy-Cr oligomers of known size and structure yielded sharp basal reflections (Drljaca et al. 1992). After calculating the gallery height of the interlayered clay, these workers were then able to propose probable orientations for

the various oligomers. Because the calculated gallery heights of several of the clays were somewhat smaller than expected, the authors proposed that the oligomers were sorbed covalently to the montmorillonite. The formation of a covalent bond requires coordinated water to be released, thus reducing the effective size of the oligomers and also decreasing the gallery height.

There are significant differences in the nature of hydroxy interlayers formed in natural environments and those prepared in the laboratory. The most common basal spacing of all interlayered clays is approximately 14 Å. However, laboratory-synthesized clays can display basal spacings which deviate significantly from this value (Barnhisel and Bertsch 1989). The wide range of basal spacings in the laboratory-prepared clays reflects the diverse structures of the interlayer components, which may include the Al_{13} molecule. The conditions of formation may also govern the distribution of hydroxy polymers within the interlayer space. Two main arrangements have been proposed: (1) a uniform distribution and, (2) an "atoll" arrangement (Figure 2.8)(Dixon and Jackson 1962). A uniform distribution of polymers within the interlayer would provide greater support than an atoll arrangement against collapse upon heating. As revealed in Figure 2.8, a uniform distribution would also allow freer access to the exchange sites within the interior of the interlayer space. Given these differences, therefore, one must be cautious when assigning the properties of laboratory-prepared interlayers to those formed in natural environments.

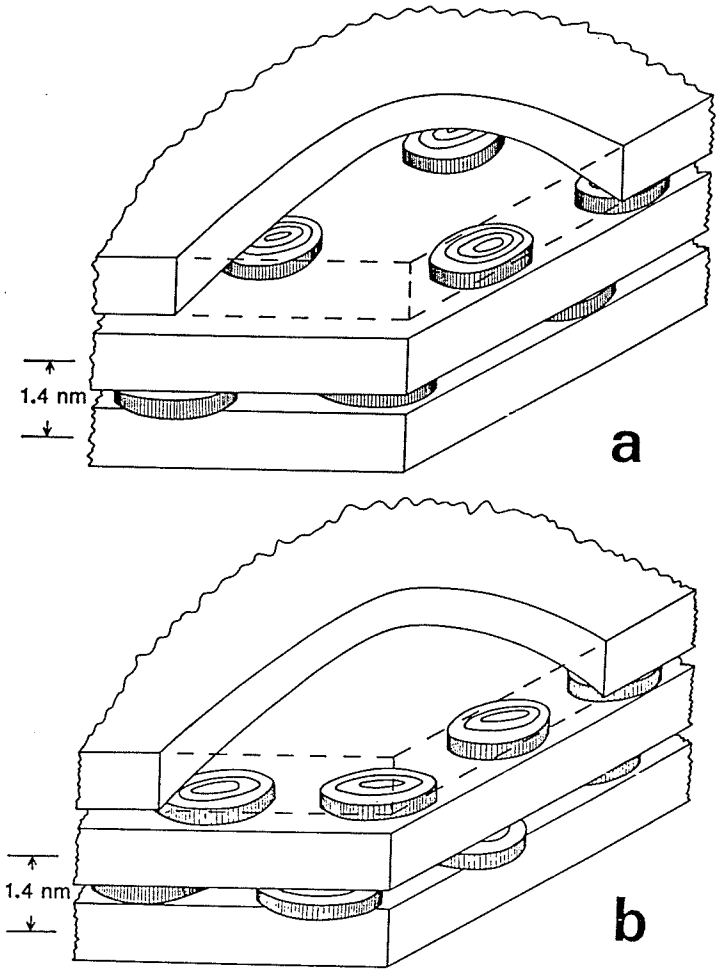

Figure 2.8. Illustration showing the distribution of hydroxy polymers in the interlayer space of 2:1 layer silicates: (a) uniform distribution; (b) an "atoll" arrangement (From Barnhisel and Bertsch 1989).

3. SORPTIVE CAPACITY OF MONTMORILLONITE FOR HYDROXY-Cr POLYMERS AND THE MODE OF Cr COMPLEXATION

3.1 Introduction

Expandable layer silicates have been proposed as sorbents for both organic and inorganic contaminants. In their native state, clays hold hydrated inorganic cations which give the clay surface a hydrophilic character. In this condition, the clays are ineffective sorbents for poorly water soluble organic contaminants. The native inorganic cations on the exchange sites must first be replaced with organic cations to form organo-clays that, unlike native clay, are effective sorbents for organic contaminants (Boyd et al. 1988; Jaynes and Boyd 1991).

Effective adsorption of inorganic cations, on the other hand, does not require any modification of the clay; the cations readily sorb to the unaltered colloid surfaces. The adsorption of various heavy metals by smectites has received considerable attention in the past. The adsorption of Cd (Egozy 1980; Inskeep and Baham 1983; van Bladel et al. 1993), Co (Egozy 1980), Cr (Rengasamy and Oades 1978; Brindley and Yamanaka 1979; Carr 1985; Dubbin et al. 1994), Cu (Inskeep and Baham 1983), Hg (Blatter 1973), Pb (Griffin and Au 1977), and Zn (Asher and Bar-Yosef 1982; van Bladel et al. 1993) are among those metals that have received the most attention. Most of the above-mentioned work, however, has focussed only on equilibrium studies or adsorption mechanisms. There has been relatively little effort to determine the sorptive capacity of smectites for these metals. Such studies are essential if one is to accurately

assess the potential role of smectites in the remediation of contaminated environments.

Among the aforementioned metals, Cr is of particular interest for several reasons. First, Cr is known to be toxic even at low concentrations when present as Cr(VI). Second, Cr-rich effluents are released from many industries world-wide (Lester 1987). Also, because much of the positive charge from Cr is eliminated in hydroxy polymers, the sorptive capacity of smectites is greater for Cr than for metals which do not hydrolyze or do not hydrolyze as extensively as Cr. Finally, previous work indicated that Cr may be strongly sorbed by montmorillonite (Drljaca et al. 1992). These reasons suggest that the removal of Cr from polluted environments may be particularly effective via sorption by smectites.

The effectiveness of smectites in ameliorating environments polluted with Cr depends on both the sorptive capacity of the clay for Cr as well as the strength of Cr complexation. The author is not aware of any reports in the literature concerning the sorptive capacity of montmorillonite for hydrolyzed Cr species. Neither is there conclusive evidence concerning the mode of Cr complexation. Although some workers have proposed that Cr forms inner-sphere complexes with the basal siloxane oxygen (Drljaca et al. 1992), others were unsure of its mode of complexation (Cheslock-Fitzgerald 1990). It must be concluded, therefore, that the mode of Cr complexation remains uncertain. In view of this lack of information concerning the adsorption of Cr by smectites, this study was conducted with two goals in mind. The primary goal was to determine the mode of Cr complexation. An additional goal was to determine

the sorptive capacity of montmorillonite for hydroxy-Cr polymers. Information obtained from these investigations would assist in the evaluation of smectites as possible ameliorants in Cr contaminated environments.

3.2 Materials and Methods

3.2.1 Clay synthesis

The montmorillonite (SWy-1, Crook County, Wyoming) was obtained from the Source Clays Repository of The Clay Minerals Society. Prior to fractionation, the clay was Na-saturated by washing five times with 1 *N* NaCl then washed free of Cl^- as determined by the $AgNO_3$ test. Five grams of the <2 μm fraction were suspended in 2 L of deionized water. Preweighed amounts of $CrCl_3$ were added to separate clay suspensions to give seven Cr(III) concentrations (200, 300, 400, 600, 1200, 1800, and 2400 cmol(+)/kg clay). The seven clay-cation suspensions were stirred vigorously and titrated at 1 mL/min with 0.1 *N* NaOH until a final $NaOH/Cr^{3+}$ molar ratio of 2.5 was reached. An eighth clay suspension containing 5 g of the <2 μm fraction, which did not have any Cr or NaOH added, served as the control. After all eight suspensions were brought to final volumes of 3 L the initial pH was determined and then they were transferred to capped bottles. The suspensions were aged at 23 $\pm$ 0.5°C for 30 days and were agitated daily. After aging, the final pH was measured. Each suspension was then separated into its filtrate and solid phase by ultrafiltration through a Millipore filter of 0.025 μm pore size. The solid phase of each sample was washed

free of Cl^- as determined by the $AgNO_3$ test.

3.2.2 Analysis of solid phase reaction products

Cation exchange capacity (CEC) of each whole solid phase reaction product was determined by first saturating the clay with Ca using 1 *N* $CaCl_2$ and then displacing the Ca with Mg using 1 *N* $MgCl_2$ (Rich 1961). The displaced Ca was measured by atomic absorption spectroscopy (AAS). Exchangeable Cr was determined by washing 100 mg clay subsamples five times (9 mL each) with 1 *N* KCl. Separate 100 mg subsamples were washed using 1 *N* $CaCl_2$. Chromium in the extracts was determined by AAS. Specific surfaces of the clays were determined by two methods: (1) adsorption of ethylene glycol monoethyl ether (EGME) as described by Carter et al. (1986) and (2) from N_2-BET sorption data obtained using an Autosorb-1 surface area analyser (Quantachrome Corporation). X-ray powder diffraction (XRD) analyses of oriented specimens were carried out with a Philips PW 1710 diffractometer using Cu Kα radiation. For infrared (IR) analysis, KBr wafers were prepared (1.5% w/w) and scanned from 1400 to 600 cm^{-1} in a Perkin Elmer 881 spectrometer. The spectra were digitally modified to enhance the Si-O vibrational region.

3.3 Results

3.3.1 Chemical analyses

The control clay suspension had an initial pH of 7.29 (Table 3.1). There was no significant change in this pH value during the aging period. The initial pH values of the Cr-clay suspensions were different for each suspension, despite a constant $NaOH/Cr^{3+}$ ratio for each. Generally, the initial pH of the suspension was inversely related to the amount of added Cr. As the amount of added Cr increased, the pH decreased. This same trend between added Cr and pH was also observed for the final pH values. These trends can be explained in terms of the hydroxy-Cr oligomer concentrations. Because the volumes of all suspensions were equal, samples treated with greater amounts of Cr contained greater concentrations of the hydroxy-Cr oligomers. At higher concentrations, the hydroxy-Cr oligomers would collide more frequently with each other. The greater number of collisions increased the probability that two oligomers would collide with the proper orientation for polymerization to occur. Therefore, a decrease in pH with increasing Cr content can be explained by more extensive hydrolytic polymerization of the Cr.

The pH values of all Cr-clay suspensions decreased not only with increasing Cr content, but also during the aging period. This indicates that hydrolytic polymerization occurred during the 30 days. Clays treated with 200, 300, 400, and 600 cmol(+)/kg clay displayed pH reductions of approximately one-half of a pH unit. Clay suspensions treated with 1200, 1800, and 2400 cmol(+)/kg clay, however, had

Table 3.1. Selected properties of the eight pure Cr clays.

Supernatant Cr conc.(cmol(+)/kg)		pH			CEC	Exchangeable Cr		Specific Surface	
						1*N* KCl	1*N* $CaCl_2$	EGME	N_2-BET
Initial	Final	Initial	Final	ΔpH	cmol(+)/kg			m^2/g	
0 (Control)	0	7.29	7.34	0.05	95.1	0	0	795	33
200	0	8.53	7.91	0.62	53.0	0	0	747	44
300	0	7.97	7.34	0.63	45.8	0	0	731	62
400	0	7.86	7.23	0.63	36.8	0	0	710	85
600	4	6.41	5.97	0.44	38.7	0	0	668	91
1200	197	5.72	4.20	1.52	15.5	1	1	617	122
1800	736	5.68	4.12	1.56	16.3	1	1	528	111
2400	1151	5.69	4.40	1.29	14.1	1	1	594	103

pH reductions of about one and one-half pH units. This greater decrease in pH for clays treated with larger amounts of Cr further emphasizes the importance of Cr concentration in determining the extent of Cr polymerization.

The amount of Cr sorbed increased with the amount added (Table 3.1). At the end of the aging period there was no Cr detected in the supernatant of clays treated with 200, 300, or 400 cmol(+)/kg clay. There were only minor amounts of Cr present in the supernatant of the clay treated with 600 cmol(+)/kg clay. At Cr concentrations greater than 600 cmol(+)/kg clay, however, large amounts of Cr remained in solution even after 30 days. Although amounts of sorbed Cr continued to increase with added Cr, the effectiveness of montmorillonite as a sorbent for hydroxy-Cr polymers decreased markedly at Cr concentrations greater than 1200 cmol(+)/kg clay. Of the 2400 cmol(+)/kg clay added to the most Cr-rich suspension, approximately one-half of the Cr remained in the supernatant at the end of the aging period.

The control clay had a CEC of 95.1 cmol(+)/kg (Table 3.1). All clays treated with Cr displayed reductions in CEC, indicating that the sorbed hydroxy polymers were largely nonexchangeable. Generally, the clays that sorbed the greatest amount of Cr had the greatest reductions in CEC. However, clays treated with 1200, 1800, and 2400 cmol(+)/kg retained substantial CEC, despite an abundance of Cr in the supernatant. This observation may be explained by considering the distribution of polymers within the interlayer space. The initial polymers to be sorbed within the

interlayer region were likely distributed in such a way that the resulting pore geometry restricted the entry of larger polymers remaining in solution. With such an arrangement, only Ca and Mg would be sufficiently small to navigate the porous structure of the interlayer region and access the remote exchange sites within the interior. Therefore, despite an abundance of hydroxy polymers in solution, a significant portion of the clay's surface remained free to participate in cation exchange. An alternate explanation for residual CEC in the 1200, 1800, and 2400 clays is that the smallest hydroxy polymers were displaced by Ca during CEC determination, thereby liberating exchange sites that subsequently participated in cation exchange.

Neither K nor Ca displaced any Cr from clays treated with the four lowest amounts of Cr (Table 3.1). Only trace amounts of Cr were displaced from clays treated with 1200, 1800, and 2400 cmol(+)/kg. The difficulty in displacing Cr indicates that this element was strongly sorbed by the montmorillonite. Because Cr was so strongly sorbed, the first explanation for the residual CEC of the 1200, 1800, and 2400 clays given above is likely correct. The alternate explanation, that the smallest polymers were displaced during CEC determination, thereby liberating exchange sites, must be wrong.

3.3.2 Specific surfaces

The specific surface of the control, as determined by the EGME technique,

was 795 m^2/g (Table 3.1). All clays treated with Cr displayed reductions in this specific surface, indicating that the interlayer region was partially occupied by hydroxy polymers. Generally, as the amount of sorbed Cr increased, the EGME-determined specific surface decreased. However, the clay treated with 2400 cmol(+)/kg showed an increase in specific surface although it sorbed the largest amount of Cr.

The N_2-BET method showed the control to have a specific surface of 33 m^2/g. In contrast to the EGME technique, which measures both internal and external surfaces, the N_2-BET method measures only the external surface area. Consequently, the N_2-BET specific surfaces are smaller than the EGME-determined surfaces. The N_2-BET specific surface increased with increases in sorbed Cr because the interlayered hydroxy polymers created a porous framework for the N_2 molecules to penetrate. The diameter of these pores must be larger than the N_2 molecule, which is known to be about 0.315 nm (Weast 1976). Because the N_2-BET specific surface increased steadily to a maximum of 122 m^2/g for the 1200 clay, the interlayer pore space must also have increased steadily. The decrease in N_2-BET specific surface at Cr concentrations greater than 1200 cmol(+)/kg indicates that the amount of pore space decreased as more hydroxy polymers were sorbed.

3.3.3 X-ray powder diffraction

X-ray diffraction analyses showed all Cr clays to have basal spacings greater

than the 9.7 Å of the control (Figure 3.1), indicating that the hydroxy polymers were located within the interlayer spaces. The basal spacings increased with the amount of added Cr. Clay treated with 200 cmol(+)/kg gave very broad d(001) reflections with the most intense peaks occurring at 12 to 13 Å. Clays treated with 1200, 1800, and 2400 cmol(+)/kg, however, displayed somewhat sharper d(001) reflections at 17 to 18 Å. These sharper peaks indicate that the intercalated hydroxy-Cr species became more highly ordered as the Cr content increased. A 4.58 Å peak was not present in any of the diffractograms, indicating that there was no crystalline $Cr(OH)_3$ phase present in any clay sample.

The interlayer spaces began to collapse upon heating (Figures 3.2, 3.3). Because all clays collapsed with similar ease, the more crystalline polymers present in the most Cr-rich clays did not significantly increase thermal stability. After heating at 300°C for 4 hours, most clays gave d(001) reflections at approximately 10 Å (Figure 3.3), similar to that of non-interlayered smectite. The 1800 and 2400 clays, however, did not yield any dominant peaks, indicating that the interlayer spaces were filled largely with highly disordered polymers.

With glycerol solvation the basal spacing of all clays increased approximately 5 Å (Figure 3.4). The d(001) peak intensity was greatest for clays which contained the least amount of Cr. Because the hydroxy polymers occupied only a small portion of the interlayer region in these low-Cr clays, most of the interlayer was allowed to expand freely. In the most Cr-rich clays, however, much of the internal surface was

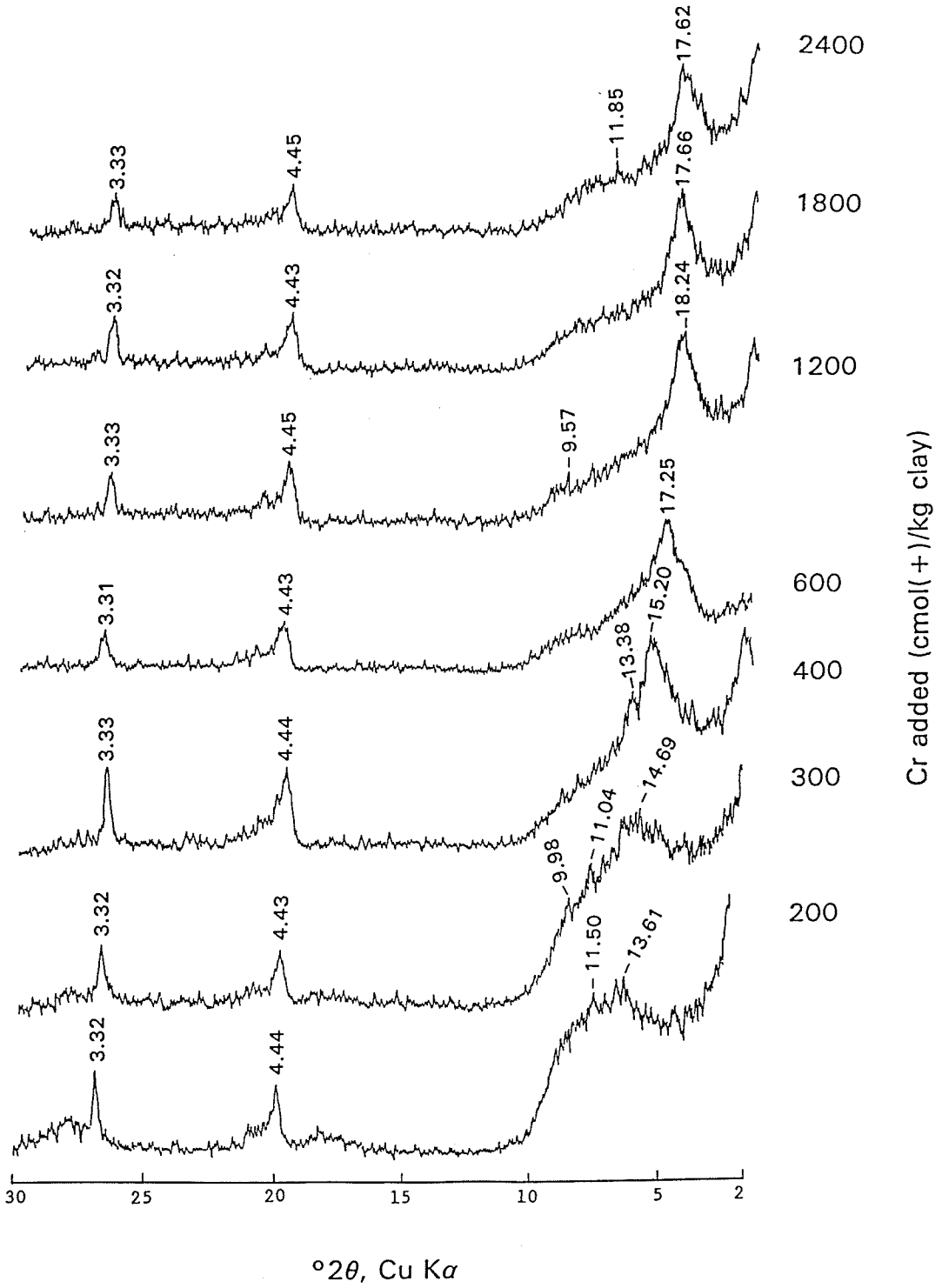

Figure 3.1. X-ray diffractograms of Cr clays under ambient temperature and 54 % relative humidity (spacings are in Å).

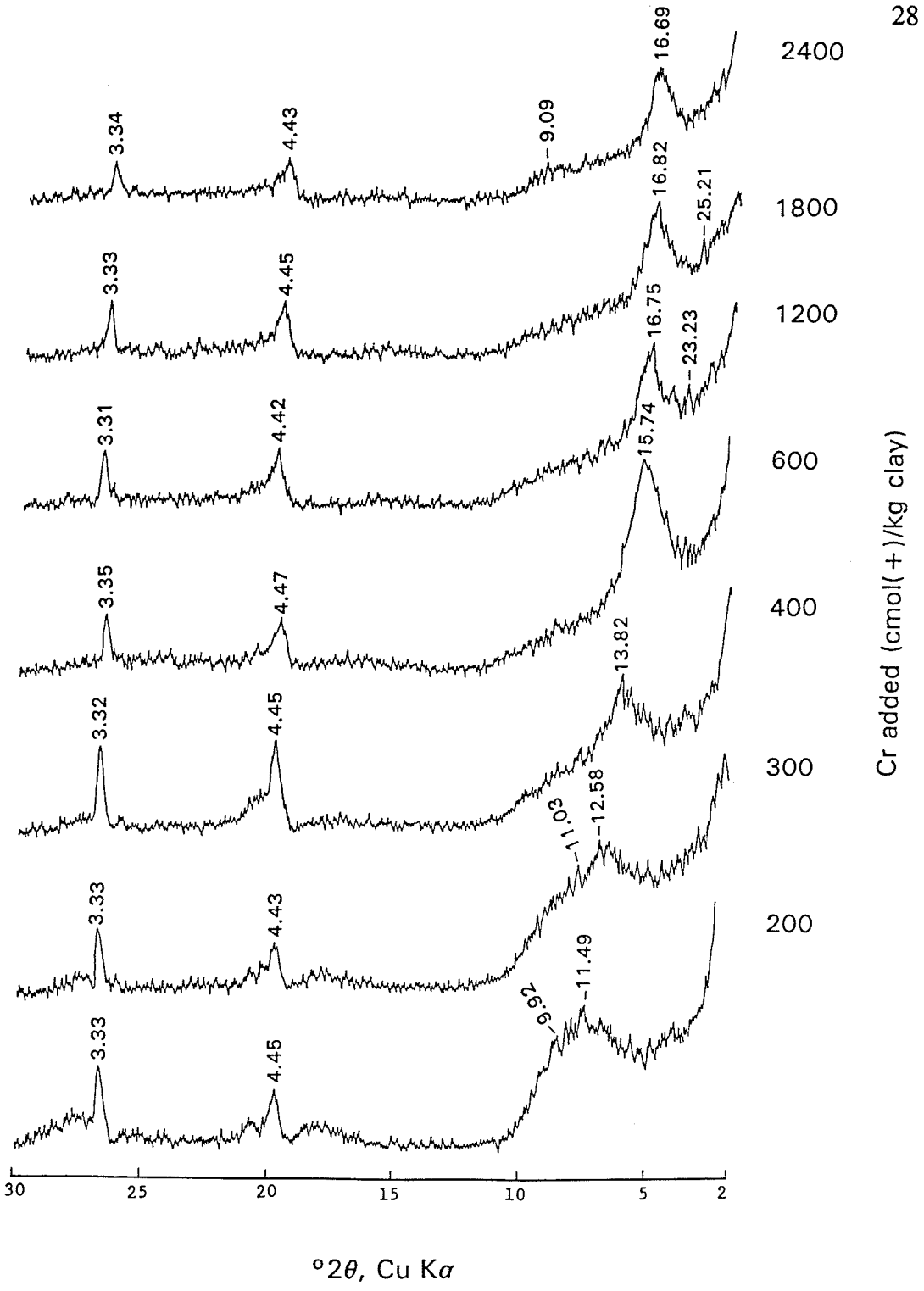

Figure 3.2. X-ray diffractograms of Cr clays after heating at 100 °C for four hours (spacings are in Å).

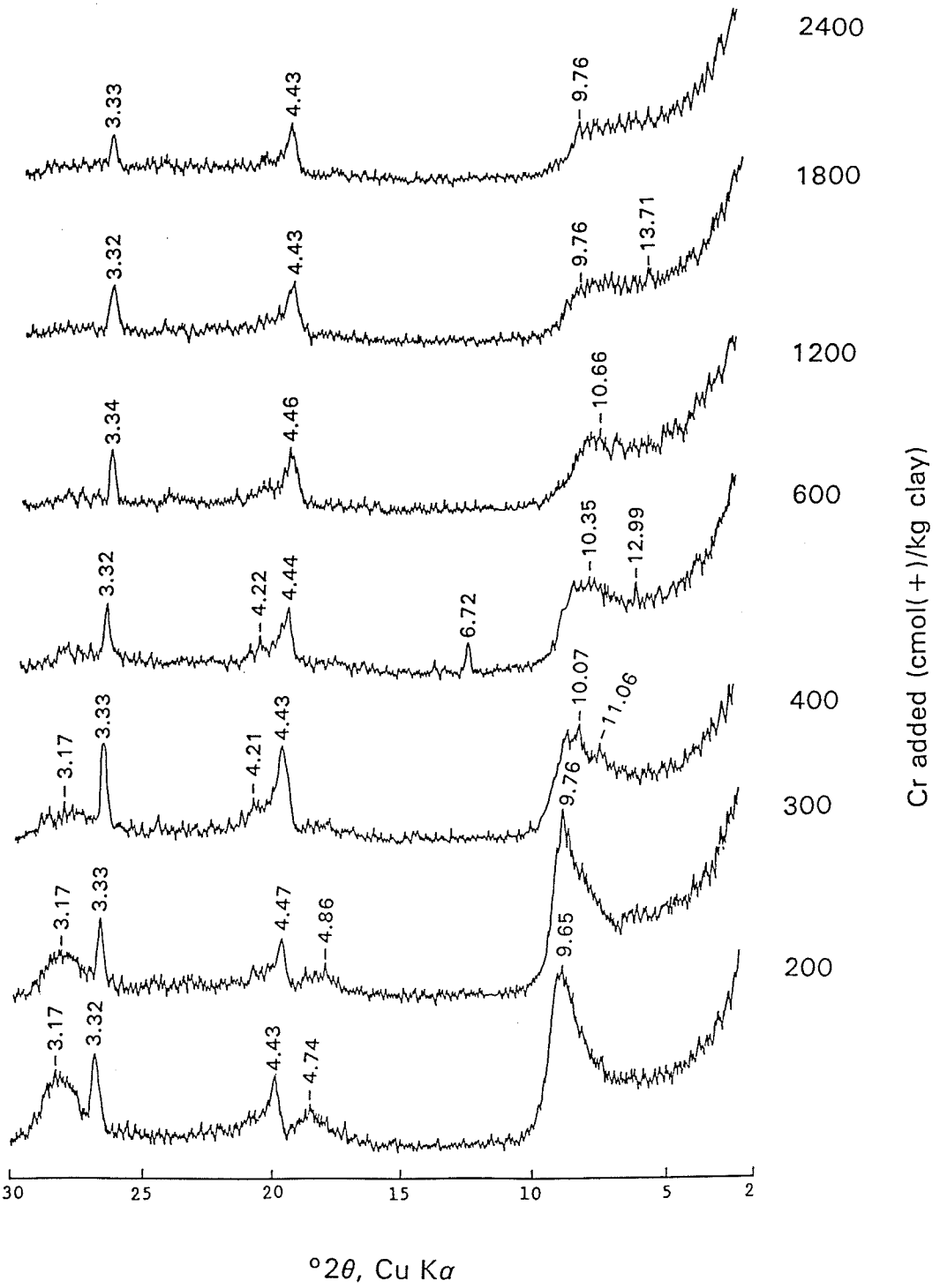

Figure 3.3. X-ray diffractograms of Cr clays after heating at 300°C for four hours (spacings are in Å).

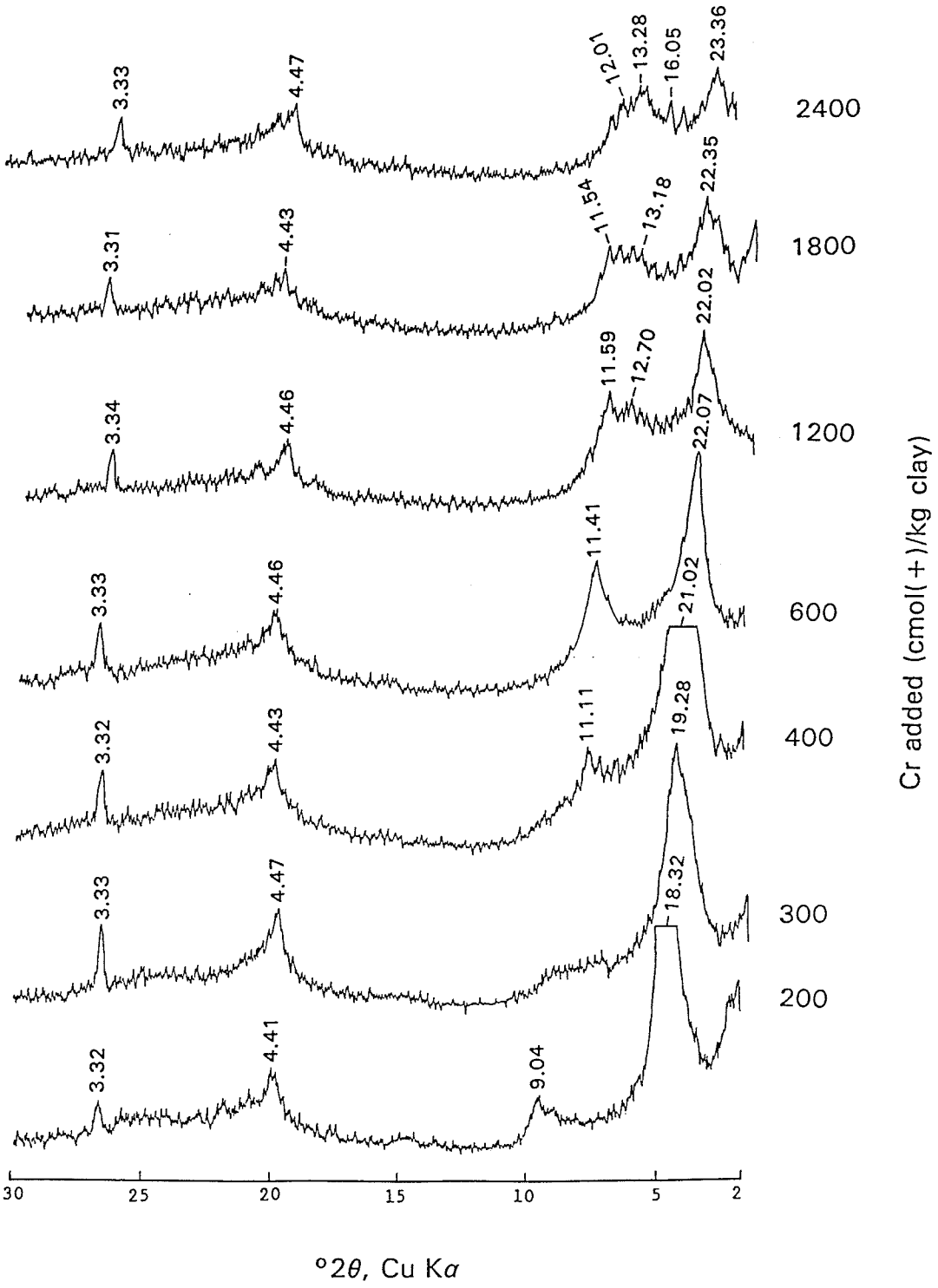

Figure 3.4. X-ray diffractograms of Cr clays after glycerol solvation (spacings are in Å).

covered with hydroxy polymers. The d(001) reflection of these clays, therefore, is very weak because only small regions of the interlayer could expand freely. Glycerol solvation showed that the sorbed hydroxy polymers hindered the free expansion of the interlayer region in all clays.

3.3.4 Infrared spectroscopy

The infrared absorption spectra of the control and two Cr-clays are given in Figure 3.5. Absorption bands near 1100 cm^{-1} are due to Si-O vibrations perpendicular to the 2:1 layer. Using the notation of Farmer (1974), these stretches correspond to the a_1^1 vibrations of pyrophyllite. The greatest absorption occurred in the 970-1070 cm^{-1} range and was due to in-plane Si-O-Si stretching vibrations, corresponding to e_1^1. A band not found in the control occurred in the Cr-clays at 1015-1020 cm^{-1}. The origin of this band is believed to be an attenuation of the a_1^1 vibration caused by inner-sphere complexation of the interlayer Cr with the siloxane oxygen. Though diminished in intensity, the original band near 1100 cm^{-1} is still present because many Si-O bonds have not been affected by complexation. Another possible origin of this new band in the Cr-clays is a weakening of the e_1^1 vibrations. However, this second explanation is less satisfactory than the first. The a_1^1 vibrations, because they are perpendicular to the 2:1 layer, would be much more sensitive to the effects of complexation than the in-plane vibrations of e_1^1.

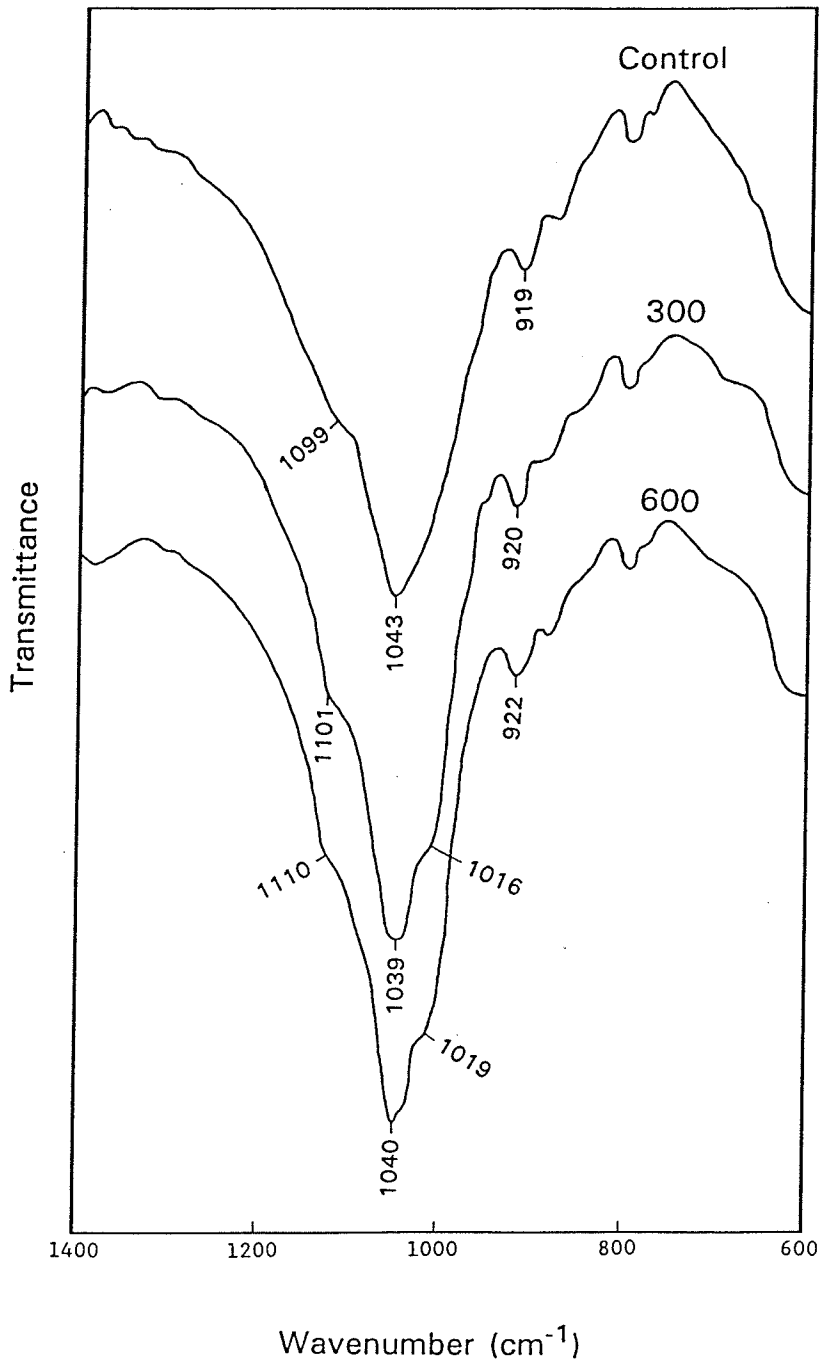

Figure 3.5. Infrared spectra showing the Si-O vibrational region of the control and two Cr clays.

3.4 Discussion

3.4.1 Mode of Cr complexation

Theoretical considerations indicate that Cr is likely to form inner-sphere complexes with the siloxane oxygen of smectites. The principle of hard and soft Lewis acids and bases (HSAB) predicts that, in general, hard acids complex with hard bases and soft acids complex with soft bases (Jensen 1978). The siloxane oxygen atoms of smectite are relatively soft Lewis bases (Sposito 1984). The relative softness of Cr(III) was determined with the Misono softness parameter (Misono et al. 1967) and found to be 2.80, which is considered borderline soft. According to the HSAB principle, therefore, the inner-sphere complexation of Cr(III) with the siloxane oxygen is not unexpected.

The difficulty in displacing Cr from smectite further indicates that the Cr is bonded specifically. If Cr was held through outer-sphere complexes, the smallest hydroxy polymers would be readily displaced by Ca. In fact, there was no Cr extracted from any of the four lowest-Cr clays (Table 3.1). Similar observations were made by Drljaca et al. (1992). These workers found that, while the montmorillonite was still wet, the adsorbed Cr could be exchanged with other cations very easily. Upon drying, however, the Cr became virtually non-exchangeable. These authors suggested that, as the interlayer region collapsed due to loss of water, the Cr came in more intimate contact with the siloxane surface, allowing inner-sphere complexes to form.

Additional evidence for the inner-sphere complexation of Cr is found in the work of Carr (1985), which revealed the surface-catalyzed polymerization of intercalated hydroxy-Cr oligomers. Hydrolytic polymerization of Cr(III) requires the replacement of H_2O with OH^- within the coordination sphere of Cr(III). Because transition metals of the d^3 type must overcome a large energy barrier in the formation of intermediates, ligand displacement reactions of Cr(III) complexes are extremely slow (Cotton and Wilkinson 1988). However, once the first ligand exchange has occurred, subsequent exchanges are more rapid. The inner-sphere complexation of Cr with the siloxane oxygen of montmorillonite (i.e. exchange of $O^{\delta-}$ for H_2O) would provide this first ligand exchange and allow for the enhanced polymerization observed by Carr (1985).

The most direct evidence for the inner-sphere complexation of Cr is provided by the infrared spectra (Figure 3.5). In the non-interlayered montmorillonite, the perpendicular Si-O vibrations occur freely and result in an absorption band at about 1100 cm^{-1}. These vibrations are shown schematically in Figure 3.6a. The formation of a Cr-O-Si linkage in the interlayered clay results in a redistribution of electrons at the clay-water interface. Electron requirements of Cr(III) cause a shift in the electron density from the Si-O bond toward the newly-formed Cr-O bond. Consequently, the Si-O bond weakens, lengthens, and its vibration frequency decreases (Figure 3.6b). This weakened Si-O bond now vibrates at 1015-1020 cm^{-1}.

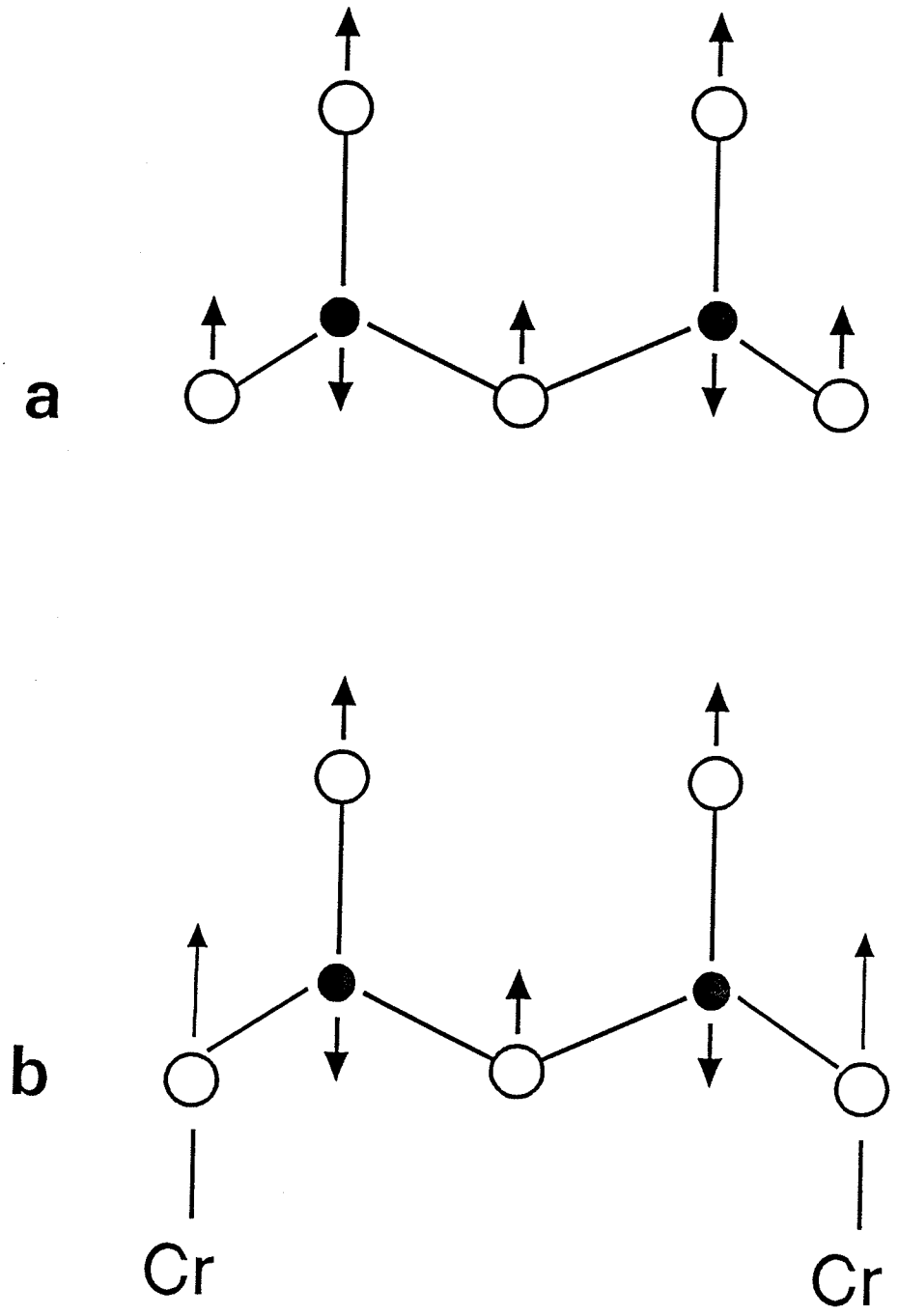

Figure 3.6. Schematic representation of Si-O vibrations in: a) control clay; b) interlayered clay where a covalent Cr-O bond has formed (open circle - oxygen; solid circle - silicon).

3.4.2 Sorptive capacity

X-ray powder diffraction data indicate that the interlayered hydroxy-Cr polymers are poorly ordered (Figure 3.1). Hence, they would not be packed efficiently within the interlayer region. In contrast to the well-ordered, and often complete, octahedral sheet of interlayer Al, the hydroxy-Cr interlayer is fragmented and often characterized by abundant pore spaces. However, this porous network allows for the sorption of large amounts of hydrolyzed Cr.

A plot of sorbed versus added Cr shows that, although sorption continued to increase at all Cr concentrations, there was an obvious decrease in the affinity of montmorillonite for hydroxy-Cr polymers at concentrations greater than 1200 cmol(+)/kg (note the decreasing slope in Figure 3.7). Once the montmorillonite had sorbed 1200 cmol(+)/kg, much of the internal surface would be complexed with the hydroxy-Cr species. Only the smallest and most remote exchange sites would remain available for sorption. At concentrations greater than 1200 cmol(+)/kg, therefore, Cr could sorb through only two mechanisms. First, those polymers in solution which are sufficiently small would be able to navigate the porous network of the interlayer and access the remote exchange sites within the interior. In this first mechanism, Cr from the small polymers would complex directly with the siloxane surface. The second mechanism involves the addition of Cr to those polymers which are already sorbed. If the subsequent polymer growth occurred along the a or b axes, pore space would decrease. Polymer growth along the c-axis, however, would increase the gallery

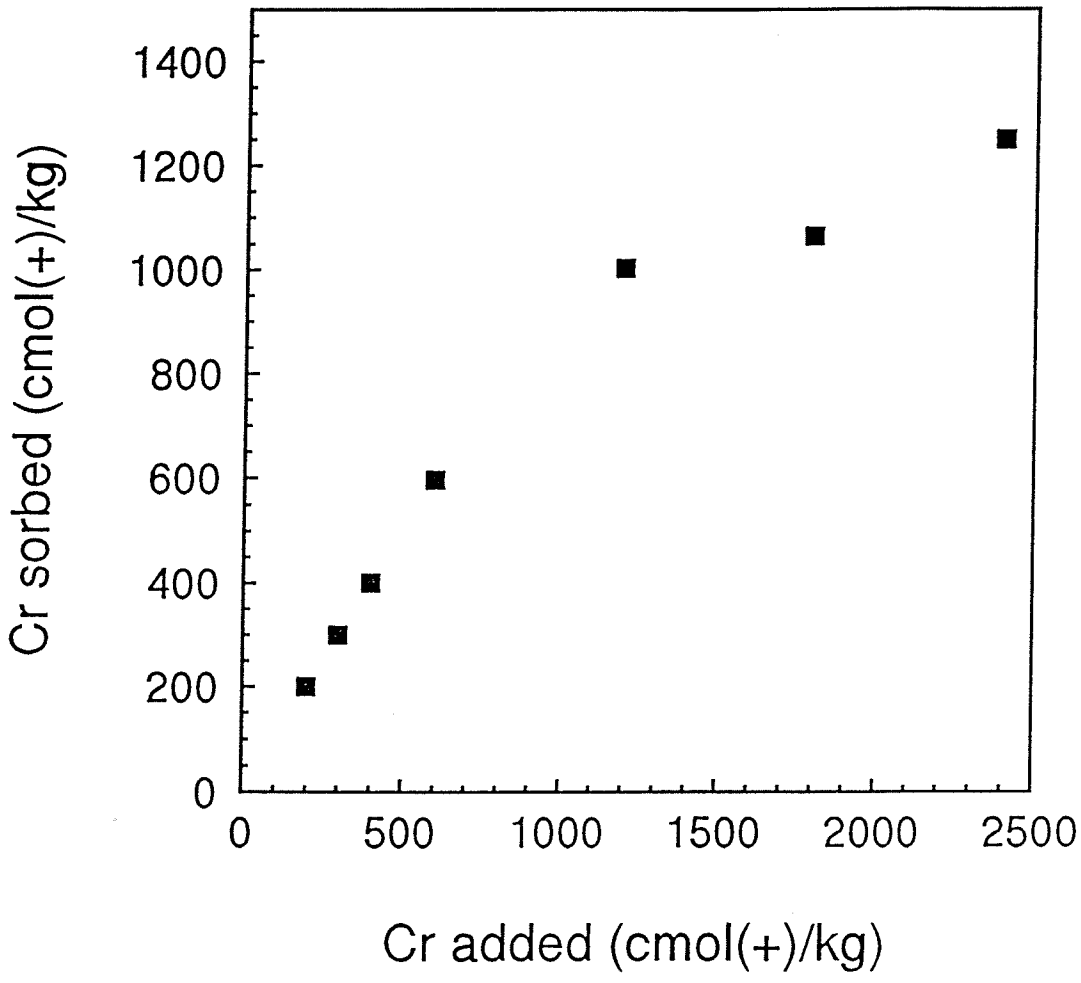

Figure 3.7. Plot of sorbed versus added Cr. Sorbed Cr is considered to be the difference in supernatant Cr concentration before and after aging.

height, thereby increasing the pore space and, consequently, also the sorptive capacity of the montmorillonite.

In this study, the sorptive capacity of montmorillonite was approached but not reached. As indicated by the decrease in N_2-BET specific surfaces, pore space was reduced as the supernatant Cr concentration increased from 1200 to 2400 cmol(+)/kg. This decrease in pore space was caused by the newly-sorbed Cr. However, even at 2400 cmol(+)/kg, there was sufficient pore space and negative colloid charge remaining for substantial amounts of Cr to be sorbed. The amount of Cr sorbed was limited, not by the montmorillonite, but rather by the small pore diameters of the interlayer material and the slow kinetics of Cr polymerization.

3.5 Conclusions

Both the sorptive capacity of the montmorillonite and the mode of Cr complexation indicate that this mineral is an effective sorbent for hydrolyzed Cr species. Chromium is readily sorbed by montmorillonite in amounts up to about 1000 cmol(+)/kg. At greater amounts, Cr continues to be sorbed, albeit less efficiently. The inner-sphere complexation of Cr by the siloxane surface of montmorillonite is supported by both theoretical considerations and experimental observations. Because Cr is held strongly through covalent bonds, its displacement is extremely difficult via simple exchange reactions. Under most conditions to which the clay would be exposed, therefore, the integrity of the hydroxy-Cr interlayers would be maintained.

However, the potential for Cr(III) to be oxidized to the more toxic hexavalent form is of some concern. Further work is needed, therefore, to determine the stability of these interlayered hydroxy-Cr polymers under strongly oxidizing conditions.

4. ELECTRON MICROSCOPE OBSERVATIONS OF CHROMIUM HYDROXIDE-INDUCED MONTMORILLONITE MICROCLUSTERS

4.1 Introduction

The adsorption of hydroxy-Cr polymers by smectites has received considerable attention in recent years. Most work has focussed on the intercalation of smectites with hydroxy polymers of Cr alone (Pinnavaia et al. 1985) or of Cr along with Al (Carrado et al. 1986; Skoularikis et al. 1988). These clays are then heated to produce fixed oxide pillars which give the clay catalytic properties. Other workers have intercalated smectite simply to elucidate the structure of the unheated hydroxy-Cr polymers (Carr 1985; Drljaca et al. 1992; Dubbin et al. 1994). Despite advances in understanding the nature of these hydroxy-Cr polymers, little is known of their effect on the arrangement of individual smectite tactoids. Variations in this arrangement could greatly influence access to the interlayer region by reactant molecules.

Tactoid thickness is a function of the type of adsorbed cation (Schramm and Kwak 1982). Multivalent cations increase tactoid thickness due largely to greater electrostatic forces. The adsorption of hydroxy-metal polymers further increases tactoid thickness (Barnhisel and Bertsch 1989). The effectiveness of a hydroxide as a cementing agent increases with decreasing crystallinity (Hsu 1989). Iron hydroxides have been shown to be less effective cementing agents than Al hydroxides, due to greater crystallinity of the former (Frenkel and Shainberg 1980). Chromium

hydroxides, as they are less crystalline than either Al or Fe hydroxides, would be expected to be the most effective cementing agents. The superior cementing ability of hydroxy-Cr polymers would reveal itself not only in the presence of thicker tactoids, but likely also in the formation of unique structures. Within this chapter is reported, for the first time, the formation of microclusters of montmorillonite tactoids induced by adsorbed hydroxy-Cr polymers.

4.2 Experimental

Prior to fractionation, the montmorillonite (SWy-1, Crook County, Wyoming) was Na-saturated by washing five times with 1 *N* NaCl then washed free of Cl^- as determined by the $AgNO_3$ test. Five grams of the <2 μm fraction were suspended in 2 L deionized water. Aluminum chloride and $CrCl_3$ were added to separate clay suspensions to give each suspension a total trivalent cation (M^{3+}) concentration of 400 cmol(M^{3+})/kg clay. The two clay-cation suspensions were stirred vigorously and titrated at 1 mL/min with 0.1 *N* NaOH until a final NaOH/M^{3+} molar ratio of 2.5 was reached (Dubbin et al. 1994). A third clay suspension containing 5 g of the <2 μm fraction, which did not have any Al, Cr, or NaOH added, served as the control. All three suspensions were brought to final volumes of 3 L and then transferred to capped bottles. The suspensions were aged at 23 $\pm$ 0.5°C for 30 days and were agitated daily. After aging, the solid phase was isolated by ultrafiltration through a Millipore filter of 0.025 μm pore size and then washed free of Cl^- as determined by the $AgNO_3$

test. Aluminum and Cr in the supernatant were quantified by atomic absorption spectroscopy. All clays were allowed to dry by evaporation under ambient conditions.

In preparation for scanning electron microscopy (SEM), the gently-powdered clay samples were mounted on aluminum stubs with carbon paint then sputter-coated with gold in a vacuum evaporator. The SEM images were obtained with a Cambridge Stereoscan 120 microscope operating at 20 kV. Image enhancement and storage was carried out with an IBAS 20 image analyser. Samples for transmission electron microscopy (TEM) were prepared by evaporating a dilute clay suspension onto carbon-coated Formvar films supported by copper grids. Analysis was conducted with a Philips EM 420 microscope operating at 100 kV.

4.3 Results and Discussion

The pH of the Cr-clay suspension decreased from 5.7 to 4.2 during the aging period. This decrease indicated that the Cr had undergone hydrolysis and polymerization. Of the 400 cmol Cr/kg clay added to the suspension, only 66 cmol Cr/kg clay remained in the supernatant after 30 days. Therefore, most of the hydroxy-Cr polymers were sorbed to the montmorillonite surface at the end of the aging period. Previous analyses with X-ray photoelectron spectroscopy found all the Cr in these sorbed hydroxy polymers to be Cr(III) (Dubbin et al. 1994).

Arrows indicate nearly spherical clusters of montmorillonite tactoids, approximately 1 μm in diameter, on the surface of a large montmorillonite

microaggregate (Figure 4.1). As these clusters of montmorillonite were not present in either the untreated clay or the Al-clay, the adsorbed hydroxy-Cr polymers were shown to be a requirement for cluster formation. At a higher magnification, a single microcluster can be seen on a base of flat montmorillonite flakes (Figure 4.2). The outer shell of the cluster appears to be composed of several montmorillonite flakes enveloping a central core. Magnification of the microcluster approximately 75,000 times allowed for a rare, direct observation of individual montmorillonite tactoids (Figure 4.3). By assigning a basal spacing of 18 Å for this interlayered clay (Dubbin and Goh 1995a), each tactoid is shown to consist of 20 to 30 lamellae. This increased tactoid thickness is consistent with the expected cementing properties of Cr hydroxide. At this higher magnification, one can also see that several tactoids are not adhering fully to the cluster. These tactoids may be recent additions that have not yet fully complexed with the central core of the cluster.

Transmission electron microscopy revealed the presence of Cr hydroxide polymers, 5 to 10 nm in diameter, sorbed to the external surface of the montmorillonite (Figure 4.4). The strong contrast between these polymers and the montmorillonite grain indicated that the polymers had a substantial thickness along the c-axis. Residual positive charge on these polymers would provide an effective means for binding adjacent tactoids.

Microcluster formation is believed to involve several steps. First, evaporative drying causes the montmorillonite flakes at the surface to curl. A single

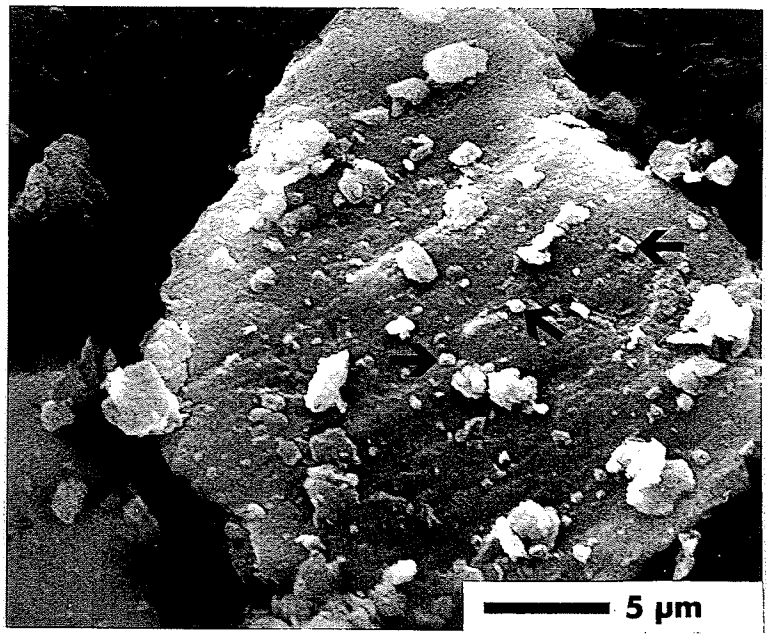

Figure 4.1. SEM image of a large montmorillonite microaggregate. Arrows indicate microclusters (approximately 1 μm in diameter) on the surface.

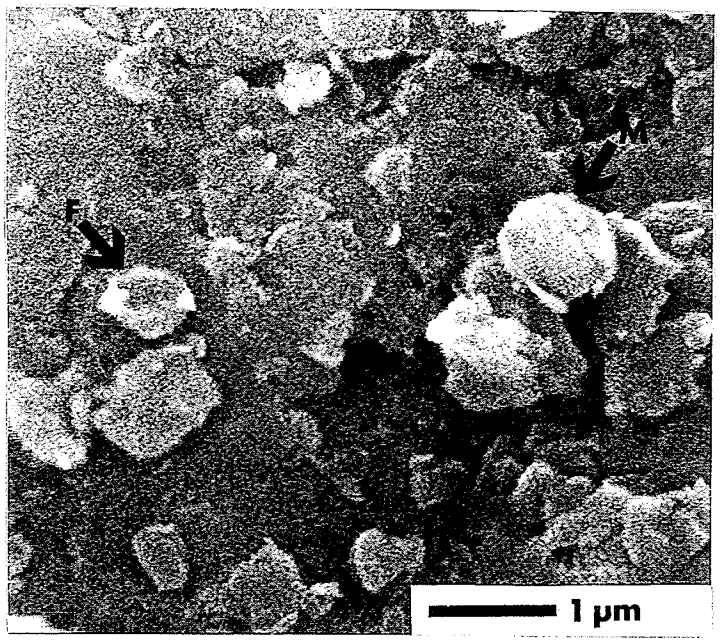

Figure 4.2. SEM image showing a single microcluster (M) at right. A curled montmorillonite flake (F) is visible at left. Several other flakes display raised edges.

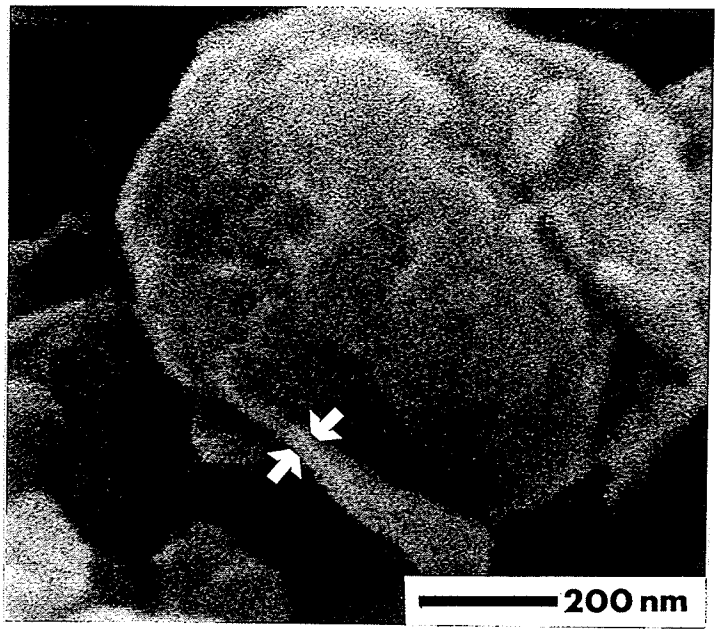

Figure 4.3. High magnification (approximately 75,000 times) SEM image of the microcluster (M) in Figure 4.2. Individual tactoids, 20 to 30 lamellae thick, are visible (arrows).

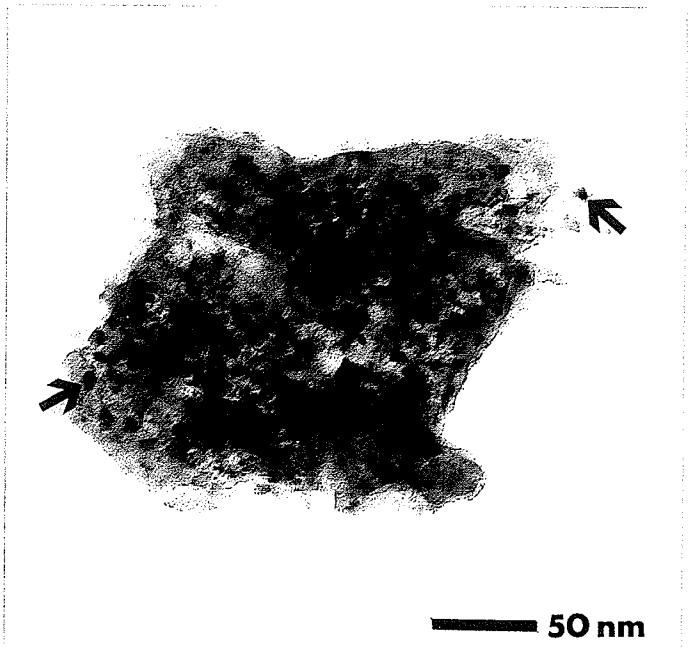

Figure 4.4. TEM image with arrows showing hydroxy-Cr polymers (5 to 10 nm in diameter) distributed on the external surface of a montmorillonite flake.

montmorillonite grain in this first stage of cluster formation is visible in Figure 4.2. Several other grains in this image display raised edges. As adjacent flakes encounter each other they would adopt a quasi-spherical arrangement which, for curled particles, would be the most stable conformation. As much of the water from the clay surface is lost on drying, the tactoids are able to come into intimate contact with each other. This close contact allows adjacent tactoids to be bridged through the hydroxy-Cr polymers. The resultant microclusters would be highly resistant to mechanical disruption because, as noted, Cr likely forms stable inner-sphere complexes with the oxygen of the siloxane surface (Drljaca et al. 1992). Chemical destruction, however, would be easily achieved through either proton dissolution of the polymers or oxidation of the Cr(III). As Figure 4.5 reveals, microcluster growth occurs simply through the incorporation of additional montmorillonite flakes. Growth would continue as long as dried montmorillonite flakes of appropriate size are available.

Only a small portion of the total montmorillonite was present as clusters. Evaporative drying, which was used in this study, does not favor the formation of these spherical aggregates (Xiang et al. 1992). However, the population of clusters would be greatly increased through the use of a spray-drying technique similar to that employed by Tsvetkov et al. (1990). The cluster population, therefore, may be altered to suit the intended use of the clay. If one wishes to increase the accessibility of the interlayer region, then the cluster population should be reduced or eliminated. This reduction can be achieved either by modifying the method of drying or by decreasing

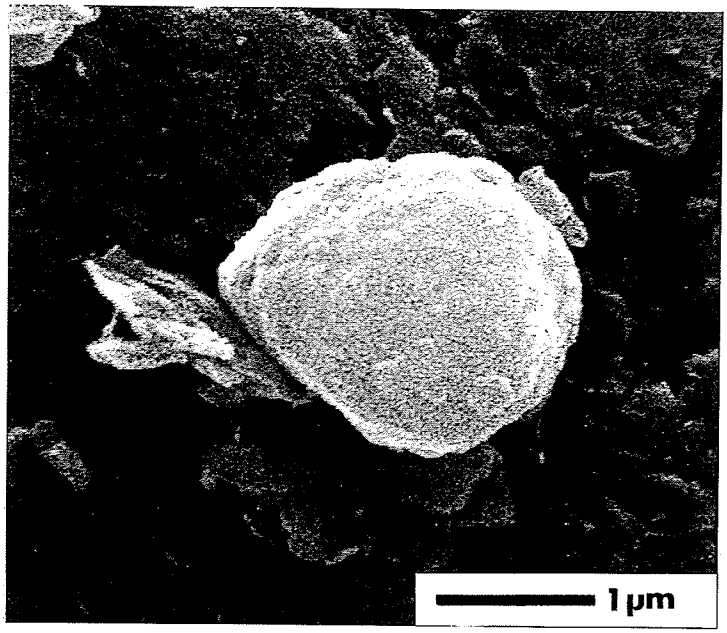

Figure 4.5. SEM image depicting the proposed mode of cluster growth. A single montmorillonite flake is shown to envelope the central core from left to right.

the number of hydroxy-Cr polymers on the external surface of the clay. If, however, the clusters are shown to have some application, their numbers could be deliberately increased.

5. PROPERTIES OF COPRECIPITATED HYDROXY-Cr AND -Al INTERLAYERS IN MONTMORILLONITE

5.1 Introduction

Intercalation of hydroxy-Al polymers in expandable layer silicates is a well-known natural process. Laboratory studies have also been successful in producing hydroxy interlayers of Al (Rich 1968; Goh and Huang 1986; Barnhisel and Bertsch 1989), Fe (Carstea et al. 1970; Martin-Luengo et al. 1989), Zr (Yamanaka and Brindley 1979), Ni (Yamanaka and Brindley 1978), and Cr (Brindley and Yamanaka 1979; Carr 1985). The hydroxy-Cr interlayered montmorillonite prepared by Brindley and Yamanaka (1979) displayed a basal spacing near 16.8 Å, considerably larger than the 14.4 Å spacing of chlorite. As the first observed diffraction peak was broad and higher orders were weak or absent, the authors suggested that the basal spacings were probably variable. These workers were unable to determine the structure of the hydroxy-Cr polymers. While studying hydration states of interlamellar Cr in montmorillonite, Carr (1985) observed that the interlayer region catalyzed the formation of larger hydroxy-Cr polymers. The first-order reflections of the interlayered clays varied from 10 to 15 Å and tended to be broad, indicating variable basal spacings. As the exact composition of the hydroxy-Cr polymers was not known, the structures of the interlayered species were not determined.

Hydroxy-aluminochromium interlayers have been synthesized by those

interested in the petrochemical applications of clays (Carrado et al. 1986). Upon calcination, the hydroxy polymers convert to fixed oxide pillars which give the clay catalytic properties. Although the properties of the oxide pillars have received much attention, the nature of unheated hydroxy-aluminochromium species remains unclear. In environments contaminated with Cr, the interlayers of expandable layer silicates may serve as sinks for Cr, which can be toxic when in solution (Bartlett and Kimble 1976). The structure and stability of the hydroxy-aluminochromium polymers, therefore, merit attention.

In this study, hydroxy interlayers were formed with five different Al/(Al+Cr) molar ratios in montmorillonite. The structure and stability of the interlayer material were examined to determine the possible interactions between Al and Cr.

5.2 Materials and Methods

The montmorillonite (SWy-1, Crook County, Wyoming) was obtained from the Source Clays Repository of The Clay Minerals Society. Prior to fractionation, the clay was Na-saturated by washing five times with 1 *N* NaCl then washed free of Cl^- as determined by the $AgNO_3$ test. Five grams of the <2 μm fraction were suspended in 2 L deionized water. Preweighed amounts of $AlCl_3$ and $CrCl_3$ were added to separate clay suspensions to give five Al/(Al+Cr) molar ratios (1.0, 0.67, 0.5, 0.33, 0). The total trivalent cation (M^{3+}) concentration in each suspension was 600 cmol(+)/kg clay. The five clay-cation suspensions were stirred vigorously and titrated

at 1 mL/min with 0.1 *N* NaOH until a final $NaOH/M^{3+}$ molar ratio of 2.5 was reached. A sixth clay suspension containing 5 g of the <2 μm fraction, which did not have any Al, Cr, or NaOH added, served as the control. All six suspensions were brought to final volumes of 3 L and then transferred to capped bottles. The suspensions were aged at 23 $\pm$ 0.5°C for 30 days and were agitated daily. After aging, each suspension was separated into its filtrate and solid phase by ultrafiltration through a Millipore filter of 0.025 μm pore size. The solid phase of each sample was washed free of Cl^- as determined by the $AgNO_3$ test.

Cation exchange capacity (CEC) of each whole solid phase reaction product was determined by first saturating the clay with Ca using 1 *N* $CaCl_2$ and then displacing the Ca with 1 *N* $MgCl_2$ (Rich 1961). The displaced Ca was measured by atomic absorption spectroscopy (AAS). Exchangeable Al and Cr were determined by washing 100 mg clay subsamples five times (9 mL each) with 1 *N* KCl. Separate 100 mg subsamples were washed using 1 *N* $CaCl_2$. Aluminum and Cr in the extracts were determined by AAS. Specific surfaces of the clays were determined by adsorption of ethylene glycol monoethyl ether (EGME) as described by Carter et al. (1986). X-ray powder diffraction (XRD) analysis of oriented specimens was carried out with a Philips PW 1710 diffractometer using Cu Kα radiation. For infrared (IR) analysis, KBr wafers were prepared (1.5% w/w) and scanned from 4000 to 600 cm^{-1} in a Perkin Elmer 881 spectrometer. Differential thermal analysis (DTA) and thermogravimetric (TG) tracings were obtained by heating the clays from ambient to

1000°C at 10°/min in an argon atmosphere (PL Thermal Sciences, model PL-STA 1500). X-ray photoelectron spectroscopy (XPS) was carried out using a Perkin Elmer PHI-5300 ESCA spectrometer; the spectra were produced using Mg Kα radiation.

5.3 Results and Discussion

5.3.1 Chemical analysis and surface area

The pH values of all clay suspensions except the control decreased over the aging period (Table 5.1). The final pH values of the suspensions reflect the relative amounts of Al and Cr. Specifically, those with more Al had lower pH values, indicating the greater hydrolyzing power of Al (Baes and Mesmer 1976). At the end of the aging period, there was no Al or Cr detected in the supernatant (data not shown). The treated clays displayed varying amounts of CEC reduction. Generally, the trend in CEC values mimicked the trend in final pH values. Smaller hydroxy polymers are known to predominate at lower pH values (Hsu 1989). Smaller polymers, as they have a greater positive charge per cation than larger polymers, are more effective at reducing CEC. The greatest CEC reductions, therefore, were observed for samples which had the lowest final pH values. However, one can not rely entirely on final solution pH to predict relative CEC values. Variation in CEC was also due to the formation of external phase hydroxy polymers. As the Al in external phase hydroxy polymers does not contribute to CEC reduction, the CEC would be higher than if all Al were interlayered. The Al end-member, therefore,

Table 5.1. Selected properties of the non-interlayered montmorillonite, pure end-members, and three Al-Cr clays.

Al/(Al+Cr) molar ratio	pH			CEC	KCl Extraction		$CaCl_2$ Extraction		Specific Surface*
	Initial	Final	ΔpH	cmol (+)/kg	Al	Cr	Al	Cr	(m^2/g)
Control	7.36	7.43	0.07	95.1	0	0	0	0	781
1.0	5.31	4.62	0.69	34.4	21.0	0	27.3	0	403
0.67	5.59	4.90	0.69	30.4	12.7	3.6	15.3	2.7	383
0.5	5.82	5.24	0.58	27.6	6.3	2.6	9.8	1.8	388
0.33	5.97	5.48	0.49	25.5	3.9	1.8	6.6	1.0	385
0	6.63	6.31	0.32	45.2	0	0	0	0	652

* EGME method

which contained external phase hydroxy polymers, had a higher CEC than what one would have predicted from pH alone.

The amounts of Al and Cr extracted from the five samples are shown in Table 5.1. The interlayer that was the most difficult to displace was the Cr end-member (Al/(Al+Cr) = 0). Neither KCl nor $CaCl_2$ displaced any Cr from this clay. The presence of Al, however, increased the extractability of the Cr by interfering with the complexation of Cr with the siloxane surface of montmorillonite. In all samples there was less extractable Cr than Al, even where the interlayer material contained more Cr. The major reason for this difference is that Cr is more strongly sorbed than Al on the 2:1 layer surface (Mengel and Kirkby 1987; Drljaca et al. 1992; Dubbin and Goh 1995a).

All interlayered clays had lower specific surfaces than the control (Table 5.1). The specific surface of the Al end-member (Al/(Al+Cr) = 1.0) was 403 m^2/g. The clays of intergradient composition had even smaller specific surfaces. Their smaller specific surfaces may be explained by the presence of smaller interlayer polymers. The presence of both Al and Cr in the interlayer may have induced the formation of smaller polymers. Clays that contained smaller polymers must also have contained a greater number of those polymers. A larger number of polymers would have caused the packing of the ethylene glycol molecules to be interrupted more frequently, thereby resulting in less efficient packing. The result would be a lower measured specific surface. The Cr end-member had a specific surface of 652 m^2/g. As the XRD

data indicated the interlayer had a spacing of 7-8 Å before addition of EGME (Figure 5.1), the ethylene glycol molecules could have formed a bilayer similar to that found in non-interlayered smectites without any further expansion of the interlayer. Upon addition of EGME, further expansion would have allowed even greater amounts of ethylene glycol to be adsorbed, resulting in the relatively high measured specific surface.

5.3.2 X-ray powder diffraction

The basal spacing of the control prior to heating was 11 Å (Figure 5.1). Interlayering of the montmorillonite with a gibbsite-like sheet was indicated by the nearly 14 Å spacings observed for samples with Al/(Al+Cr) molar ratios = 1.0, 0.67, 0.5, 0.33 (Figure 5.1). A basal spacing of 16.7 Å was observed for the Cr end-member, which is similar to the 16.8 Å spacing reported by Brindley and Yamanaka (1979). As the basal reflection of the Cr end-member was broad, the basal spacings were shown to be variable. A secondary basal spacing of 19.2 Å was also present. This spacing would arise if Keggin molecules were present in the interlayer (Pinnavaia et al. 1984; Plee et al. 1985; Schutz et al. 1987; Fripiat 1988). The Keggin molecule, which consists of a central tetrahedron surrounded by four sets of three octahedra, is approximately 9 Å in size and can accommodate many different types of cations (Cotton and Wilkinson 1988). Although two gibbsite-like sheets stacked in the c-direction would also yield a spacing of approximately 19 Å, such gibbsite-like structures are unlikely in the Cr end-member because even a 14 Å spacing was

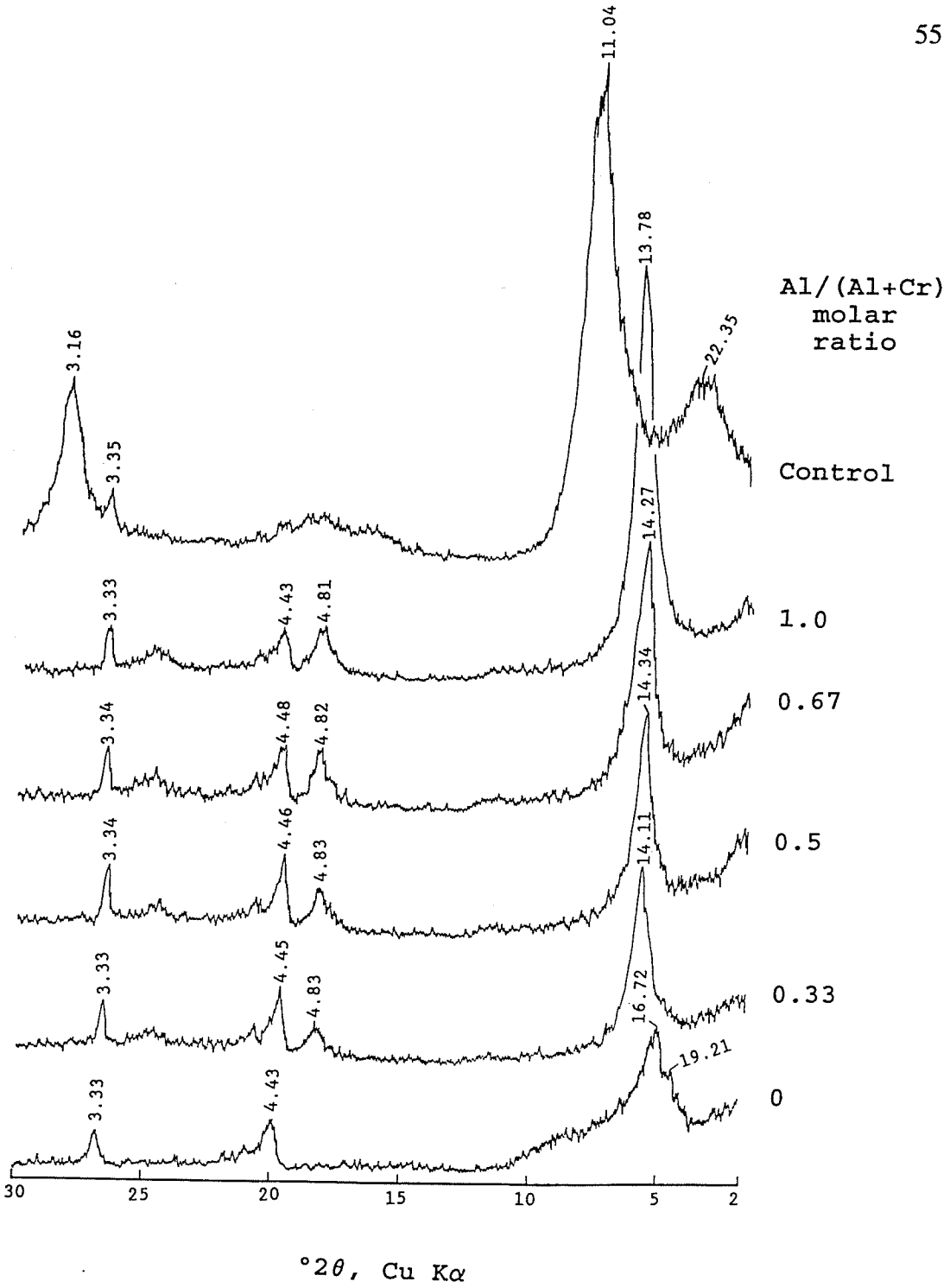

Figure 5.1. X-ray diffractograms of the control, two end-members, and three Al-Cr clays under ambient conditions. All clays were analyzed at 54% relative humidity (spacings are in Å).

not observed. A basal spacing of approximately 19 Å would also arise from the intercalation of hydrolytic trimers where the three octahedra are arranged linearly. Dimensions of individual Cr(III) hydrolytic oligomers were determined by Drljaca et al. (1992). Based on the dimensions these workers calculated for a dimer, a linear hydrolytic trimer would be 9.5-10 Å along the longest axis. Intercalation of these trimers with their long axes oriented parallel to the c-axis would give the observed 19 Å basal spacing.

The clays of intergradient composition and the Al end-member displayed basal spacings of about 14 Å, which indicated the formation of a similar gibbsite-like structure in each (Figure 5.1). It is likely that Cr substituted for Al in the hydroxy polymers. If there were separate hydroxy-Cr polymers, one would expect basal spacings of about 16.7 Å as well as the 14 Å spacings due to the gibbsite-like interlayers. In a system containing both Al and Cr, therefore, the data indicate that Al determines the structure which will form. Diffraction peaks at about 4.83 Å showed that all clays treated with Al also contained minor amounts of external phase Al hydroxide. As these diffraction peaks were broad, one can not easily attribute them to either gibbsite or nordstrandite. Whether gibbsite or nordstrandite, however, the broad diffraction peaks showed the Al hydroxide to be poorly crystalline.

The intensity of the basal reflections decreased as Cr content increased (Figure 5.1). This indicated that Cr increased the disorder of the interlayer material. As the clays were heated to increasingly higher temperatures, the interlayers began to

collapse (Figure 5.2). The least heat-stable interlayer was the Cr end-member. At 300°C the interlayer collapsed so that there were no discernible peaks. At 400°C, however, the montmorillonite basal spacing of 9.7 Å appeared. The other hydroxy polymers displayed greater heat-stability. The basal spacings of these other four clays decreased gradually to 11-12 Å at 550°C. The presence of Al increased heat-stability, possibly by promoting the formation of gibbsite-like "islands" which prop open the interlayer.

Glycerol solvation increased the basal spacings of all samples (Figure 5.2). The basal spacings of most interlayered clays increased only slightly (about 1 Å). The basal spacing of the Cr end-member, however, increased by about 5 Å. This indicates that the hydroxy-Cr polymers may be distributed mainly around the margin of the interlayer. Such an arrangement would allow for easier expansion of the interior of the interlayer space.

5.3.3 Infrared spectroscopy

The OH-stretching absorption band of the control sample was 3635 cm^{-1} (Figure 5.3). This is nearly identical to the 3632 cm^{-1} band observed in montmorillonite by Farmer and Russell (1967). The hydroxy-Al interlayered clay gave a high frequency shoulder at 3700 cm^{-1}. Other workers have found similar high frequency absorption bands in hydroxy-Al interlayered montmorillonite and assigned them to the gibbsite-like interlayer (Weismiller et al. 1967; Ahlrichs 1968; Occelli and Tindwa 1983). The pure hydroxy-Cr clay gave an OH-stretching frequency of 3656

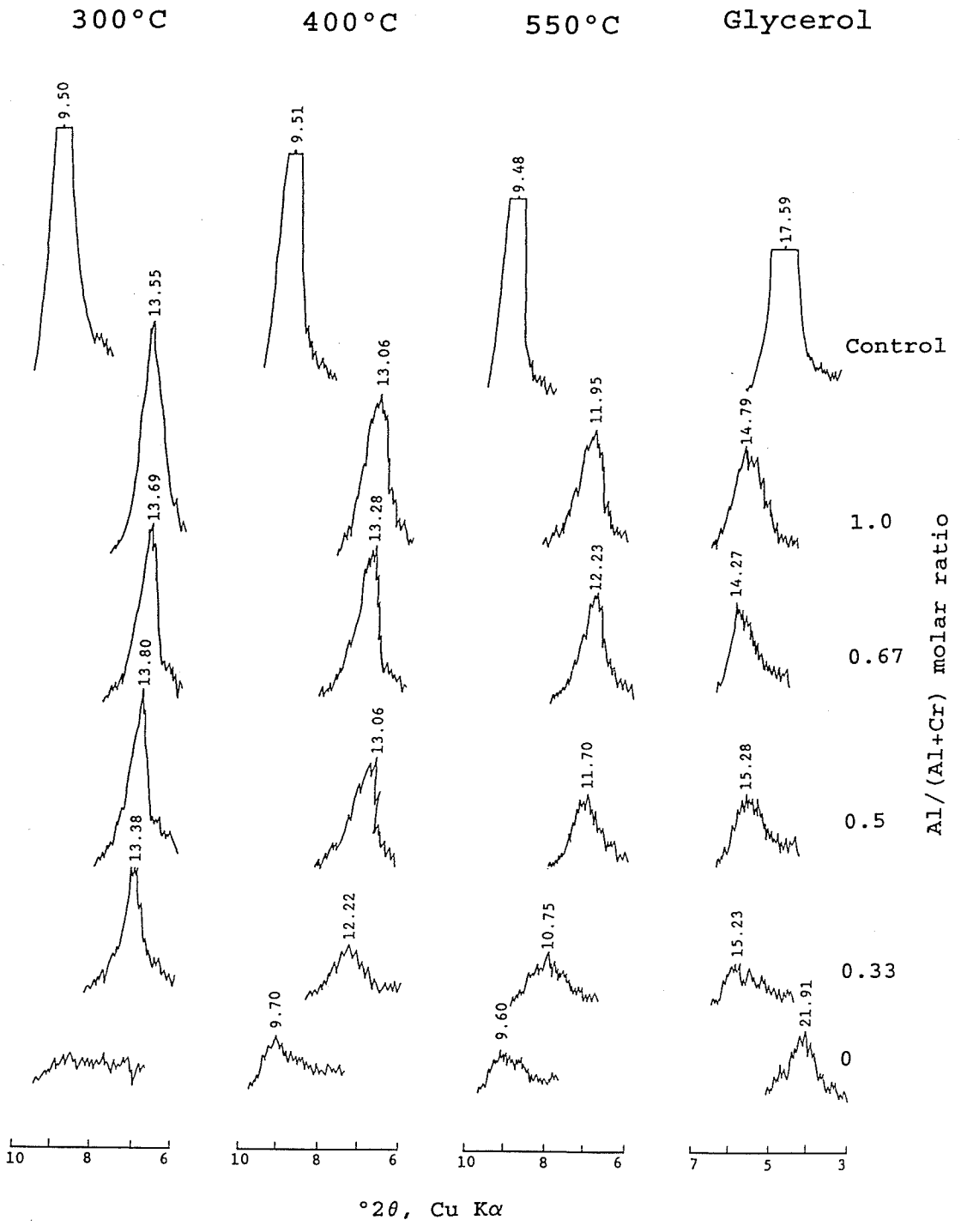

Figure 5.2. Basal reflections of the control, two end-members, and three Al-Cr clays after each of four pretreatments. (spacings are in Å).

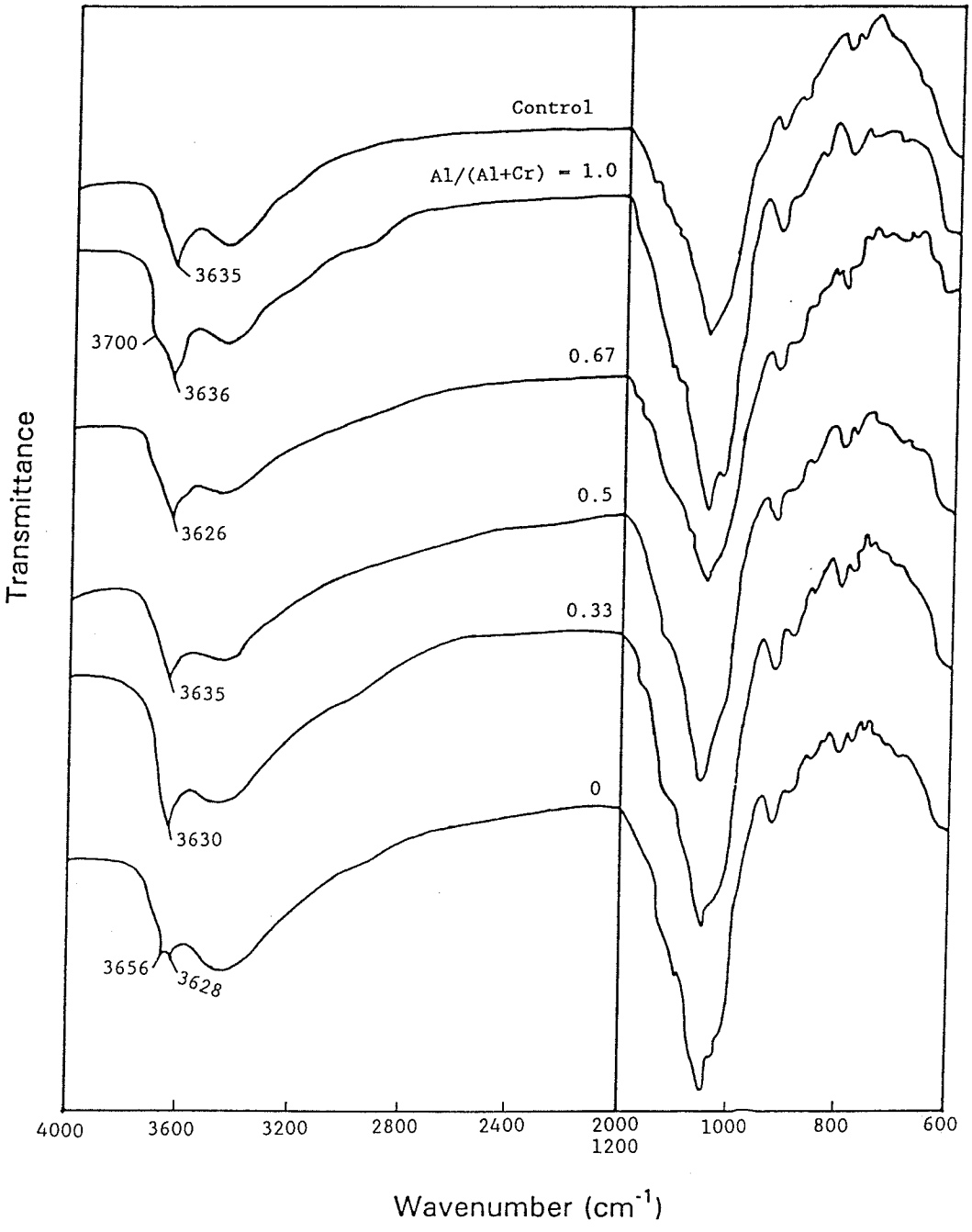

Figure 5.3. Infrared spectra of the control, two end-members, and three Al-Cr clays.

cm^{-1}, lower than that for the pure hydroxy-Al clay. The greater atomic mass of Cr contributed to the decreased frequency in the pure hydroxy-Cr clay.

Hydroxyl stretching frequencies of the clays with intergradient interlayer compositions were similar to OH-stretching frequencies of the control clay. In fact, OH-stretching frequencies of the interlayer material were so close to those of the 2:1 silicate layer that only one absorption band could be discerned. As only one OH-stretching frequency was observed for the intergrades, their interlayers would not contain separate hydroxy-Cr and -Al polymers. If there were separate polymers, the IR spectra of the intergrades would be a composite of the end-members.

5.3.4 Thermal analysis

As the thermal analysis tracings of all clays with intergradient compositions were similar, only one (Al/(Al+Cr) = 0.5) is shown (Figure 5.4c). Differential thermal analysis of all clays except the Cr end-member showed endotherms at about 75°C (Figure 5.4). These endotherms were attributed to the loss of adsorbed water (Tan et al. 1986) and represent 5-7% of the total clay weight. The corresponding endotherm for the Cr end-member occurred at 90°C and represented 12% of the clay weight. The greater weight loss from the Cr end-member as compared to the clay of intergradient composition is shown clearly by the thermogravimetric tracings (Figure 5.5). This higher temperature and greater weight loss for the Cr end-member was due to loss of structural water from the interlayer hydroxy-Cr polymers (Carr 1985). The endotherm at 347°C for the Al end-member was attributed to a discrete $Al(OH)_3$ phase

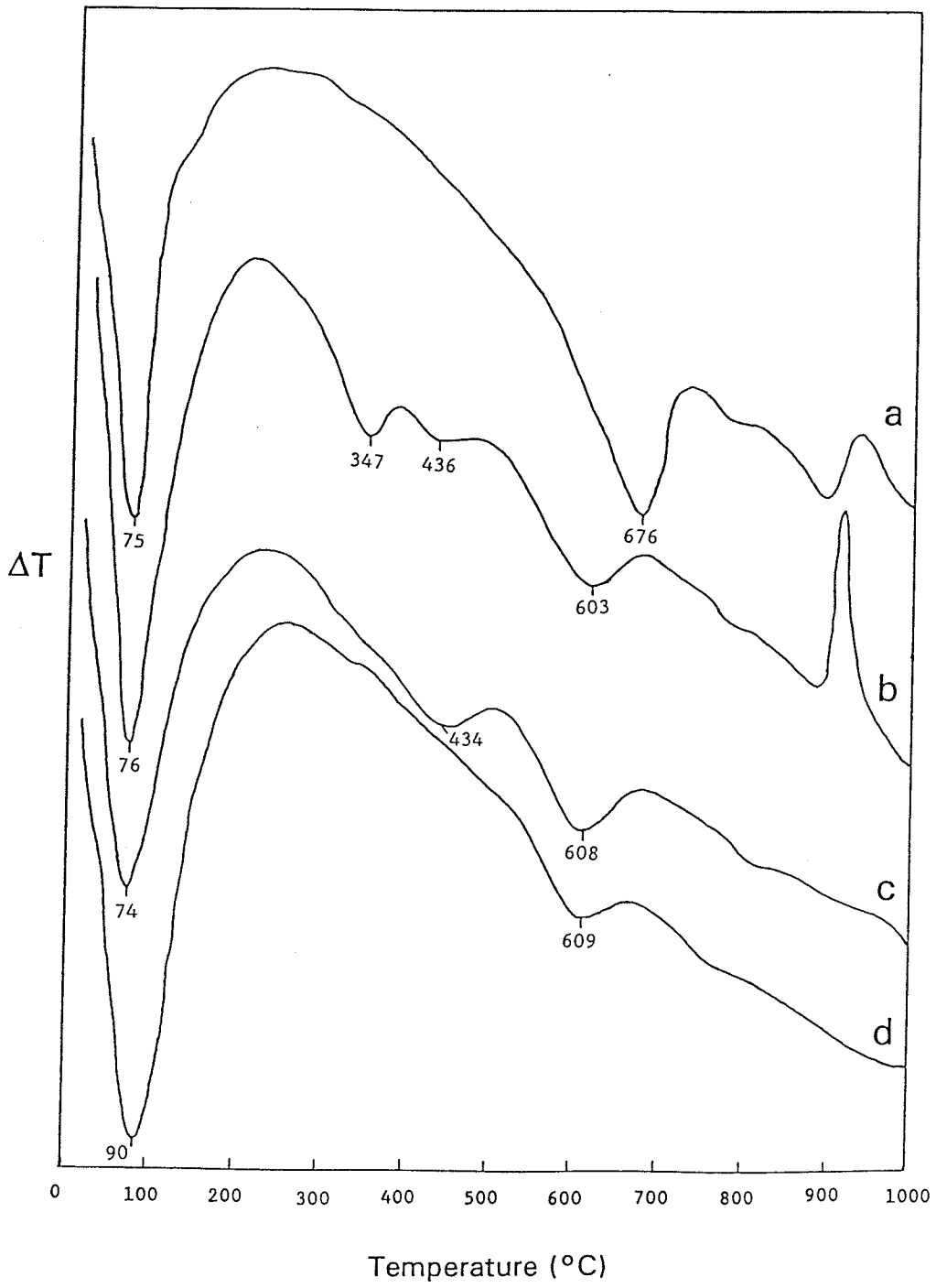

Figure 5.4. DTA tracings of the control, (a); interlayered clay where the Al/(Al+Cr) molar ratio = 1.0, (b); 0.5, (c); and 0, (d).

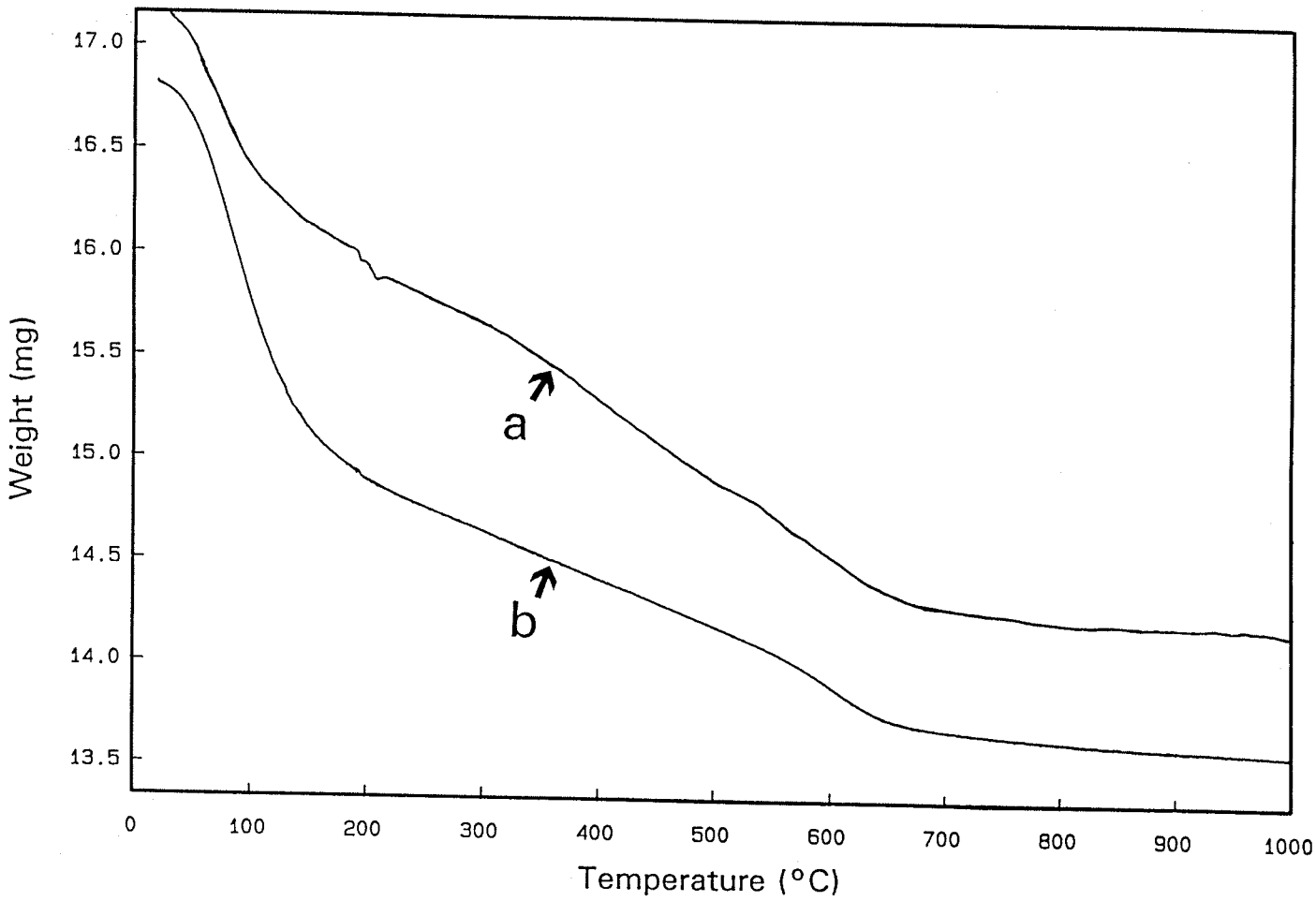

Figure 5.5. TG tracings of the interlayered clay where the Al/(Al+Cr) molar ratio = 0.5, (a); and 0, (b).

(Hsu 1989). There were no corresponding peaks for the clays containing Cr. Endotherms at 430-440°C from the Al end-member and the intergrades represented loss of hydroxyls from the interlayer (Glenn and Nash 1964; Barnhisel and Bertsch 1989). The absence of a corresponding endotherm for the Cr end-member supports the idea of a low-temperature loss of structural water from the hydroxy interlayer. Dehydroxylation of the control occurred at 676°C and that of the 2:1 portion in the interlayered clays occurred at 603-609°C. This decrease of the dehydroxylation temperature has been attributed to the expanded interlayer (Rich 1968).

5.3.5 XPS analysis

Survey XPS spectra of $CrCl_3 \cdot 6H_2O$ and two interlayered clays are shown in Figure 5.6. The wide-scan spectra give information concerning the elements associated with both the samples and the supporting Cu coupon. The observed features of the spectra and their assignments are summarized in Table 5.2. Detailed spectra of the Cr 2p region of the three samples are given in Figure 5.7. Binding energies for the Cr $2p_{1/2}$ and Cr $2p_{3/2}$ peaks for $CrCl_3 \cdot 6H_2O$ were 587.0 and 577.5 eV, respectively, while the corresponding peaks for the Cr end-member were 587.5 and 577.5 eV. As the binding energies of Cr in the clay and the $CrCl_3 \cdot 6H_2O$ standard were essentially the same, the Cr in the clay detected by XPS was present as Cr(III). The Cr 2p peaks for the two clays were somewhat broader than for the $CrCl_3 \cdot 6H_2O$. This indicates that not all the Cr(III) sorbed by the clay has the same chemical environment (Sunder et al. 1995). The sorbed Cr(III) atoms may differ with respect to the number and type of

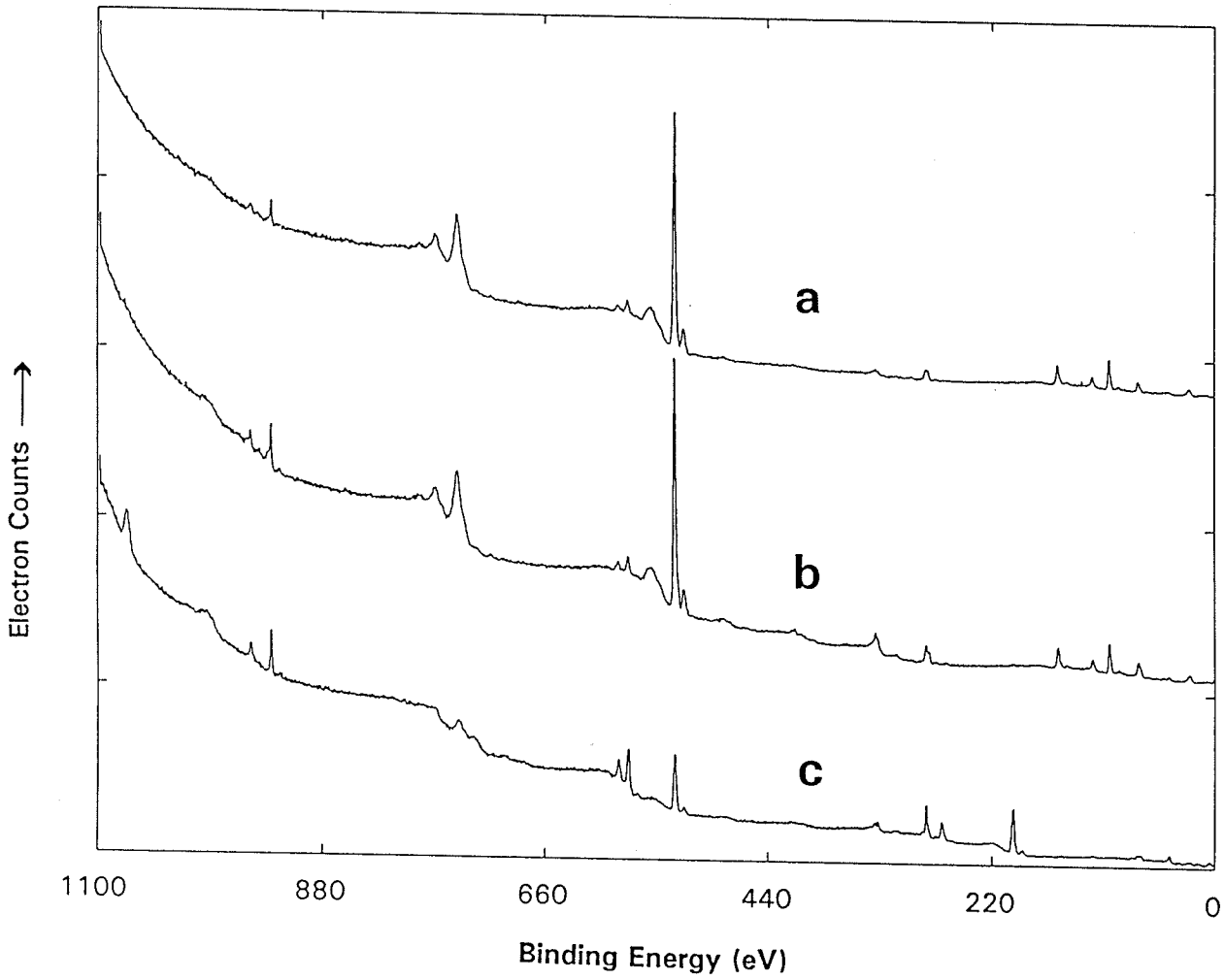

Figure 5.6. Survey XPS spectra of the interlayered clay where the Al/(Al+Cr) molar ratio = 0, (a); and 0.33, (b). The spectrum for $CrCl_3 \cdot 6H_2O$ is given in (c) (From Sunder et al. 1995).

Table 5.2. Features of the XPS survey spectra for: clays with Al/(Al+Cr) molar ratios = 0, 0.33; the $CrCl_3 \cdot 6H_2O$ (binding energies are in eV). (Data compiled by Sunder et al. 1995).

Al/(Al+Cr) molar ratio			
0	0.33	$CrCl_3 \cdot 6H_2O$	Assignment
		1071.0 s	Cl Auger
989.5 vw		993.0 m	C Auger
950.5 m	950.0 w	950.0 s	Cu $2p_{1/2}$
930.0 s	930.0 m	930.0 s	Cu $2p_{3/2}$
783.5 w	783.0 w		O Auger
767.5 m	767.0 m	768.0 w	O Auger/Cr Auger
746.0 s	746.0 s	744.0 m	O Auger
		729.5 w	Cr Auger
		700.5 w	Cr 2s
587.5 m	587.5 w	587.0 s	Cr $2p_{1/2}$
577.5 m	578.0 m	577.5 s	Cr $2p_{3/2}$
		569.0 w	Cr sat
532.5 s	532.0 s	532.0 s	O 1s
524.0 m	524.0 m	524.0 w	O 1s sat
485.0 w	484.0 w	485.0 vw	Cu Auger
413.5 w	413.0 vw	416.0 vw	Cu Auger
334.5 m	334.5 w	335.5 m	Cu Auger
		332.5 m	Na Auger
315.0 w	313.5 vw	316.5 w	Cu Auger
	300.0 vw		Mg Auger
285.0 m	285.0 m	285.0 s	C 1s
276.0 vw	275.5 vw	276.5 w	C 1s sat
		269.5 m	Cl 2s
	198.0 vw	198.5 s	Cl 2p
		190.0 m	Cl 2p sat
154.0 m	154.0 m		Si 2s
145.5 vw	145.0 w		Si 2s sat
	137.0 vw		Cu 3s
120.0 m	119.5 m		Al 2s
	110.5 vw		Al 2s sat
103.0 m	102.5 s		Si 2p
94.0 w	93.5 w		Si 2p sat/Mg 2s
75.0 m	74.5 m	75.5 w	Cr 3s/Al 2p
65.5 vw	64.5 vw		Na 2s
50.0 vw	49.5 vw		Mg 2p
45.0 w	44.5 w	44.5 w	Cr 3p
		35.5 vw	Cr 3p sat
24.5 m	24.5 w	24.5 vw	O 2s
		16.0 vw	Cl 3s
7.0 vw	7-10 vw	5.0 vw	O 2p

s, m, w and vw represent strong, medium, weak and very weak, respectively.
sat represents X-ray satellites.

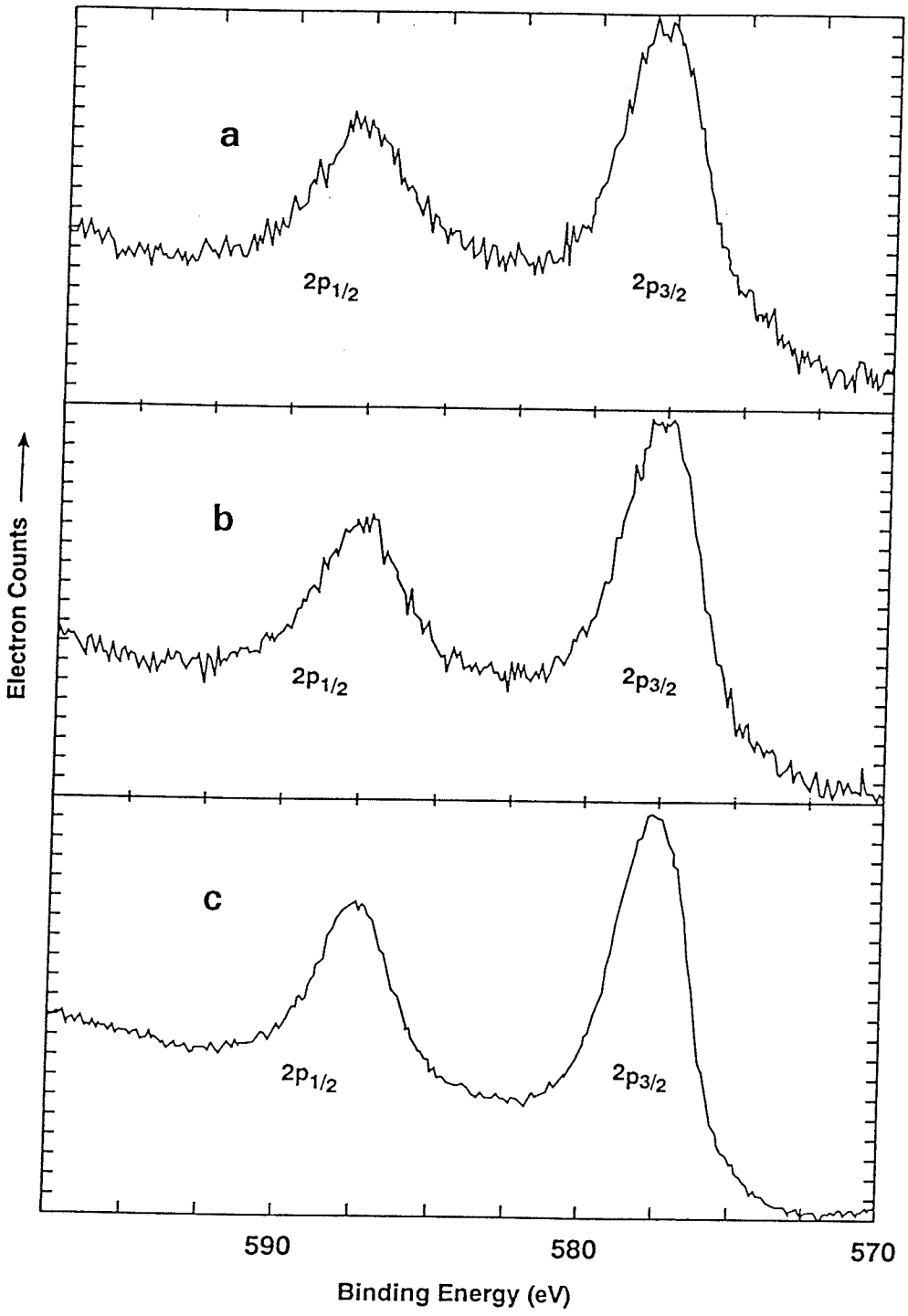

Figure 5.7. XPS spectra of the Cr 2p region of the interlayered clay where the Al/(Al+Cr) molar ratio = 0, (a); and 0.33, (b). The corresponding spectrum for $CrCl_3 \cdot 6H_2O$ is given in (c) (From Sunder et al. 1995).

ligands they are coordinated with.

Previously, the presence of the Keggin structure was invoked to explain the 19.2 Å spacing of the Cr end-member. However, the central cation in the Keggin molecule is tetrahedrally coordinated to four O. As only higher oxidation states of Cr can be tetrahedrally coordinated to O, the presence of the Keggin structure must be dismissed. One must conclude, therefore, that the 19.2 Å basal spacing was caused by the intercalation of linear hydrolytic trimers. It is important to note, however, that XPS analyzes to a depth of only 10-50 Å (Hochella 1988). If the Keggin molecules were located only within the interior of the clay particle, the higher oxidation states of Cr would not be detected by XPS.

5.4 Conclusions

All interlayer materials which contain Al have formed similar gibbsite-like polymers. Substitution of Cr for Al in these polymers was supported by XRD and IR data. Data indicate, therefore, that Al may have served as a template in the formation of the gibbsite-like polymers. It was not possible to determine the structures of all the pure hydroxy-Cr interlayer components. Based on XRD data, however, a simple octahedral sheet arrangement was an unlikely structure. Data from XPS, meanwhile, tended to rule out the presence of the Keggin molecule. Only intercalated linear hydrolytic trimers would give the clay properties which are consistent with the data.

Chromium increased the resistance of the interlayer to displacement. As Cr

content increased, displacement of Cr by both K and Ca became more difficult. Aluminum, however, increased the thermal stability of the interlayer. As Al content increased, the interlayer became more resistant to collapse upon heating. The presence of both Cr and Al in the hydroxy polymers resulted in chemical and physical properties which seem to be contradictory. The most heat-stable interlayers (those with the most Al) were also the least resistant to displacement. Meanwhile, the least heat-stable interlayers (those with the most Cr) were the most resistant to displacement. A possible explanation for this apparent contradiction is that, while the hydroxy-Cr polymers were poorly crystalline, the Cr may have formed strong inner-sphere complexes with the siloxane surface. Despite uncertainties concerning the structure of the interlayer material, however, one may conclude that expandable layer silicates serve as effective sinks for Cr.

6. SOLID STATE ^{27}Al and ^{29}Si NMR ANALYSIS OF HYDROXY-Cr AND -Al INTERLAYERED MONTMORILLONITE

6.1 Introduction

Magic-angle spinning nuclear magnetic resonance (MAS NMR) spectroscopy has provided important information concerning the ordering and local chemical environment of atoms in solids (Kirkpatrick 1988). Chief among those nuclides which have been studied are ^{27}Al and ^{29}Si. Aluminum coordination is easily determined with MAS NMR because peaks representing tetrahedral (Al^{IV}) and octahedral (Al^{VI}) sites are easily resolved in the ^{27}Al spectra (Goodman and Stucki 1984; Wilson et al. 1984; Morris et al. 1990). As with ^{27}Al, the largest influence on the ^{29}Si chemical shift is the nearest-neighbor structural environment. Therefore, as with ^{27}Al, tetrahedral and octahedral sites for ^{29}Si are easily distinguished. The ^{29}Si chemical shift is also sensitive to the type of cations in adjoining polyhedra. This sensitivity has been exploited by those attempting to determine Al and Si distributions in the tetrahedral sheets of layer silicates (Herrero et al. 1985; 1987). The chemical shift of ^{29}Si is also responsive to the mode of complexation and the nature of interlayer cations (Sanz and Serratosa 1984; Plee et al. 1985; Liang and Sherriff 1993; Malla and Komarneni 1993). It is in this last respect that ^{29}Si MAS NMR will be employed in this study.

In light of the known hazards of Cr(VI), considerable work has been directed toward understanding the fate of Cr in soils and sediments. Most Cr(III) in soils and

sediments is held as poorly-soluble hydroxy polymers on colloid surfaces (Shewry and Peterson 1976; Cary et al. 1977; Grove and Ellis 1980). Before one can accurately assess the potential of this Cr(III) to be oxidized to Cr(VI), one must first determine both the mode of complexation of the Cr(III) and the chemical environment in which it exists. In previous studies, hydroxy polymers of this potentially-toxic metal were sorbed onto montmorillonite alone (Carr 1985; Drljaca et al. 1992; Dubbin and Goh 1995a) and in conjunction with Al (Dubbin et al. 1994). Attempts were then made, with moderate success, to elucidate the mode of complexation and chemical environment of the sorbed Cr(III). In the present study, a technique more definitive than those previously used, MAS NMR of ^{27}Al and ^{29}Si, will be employed in order to determine: (1), the coordination of interlayer Al; (2), the relative positions of Al and Cr within the interlayered hydroxy polymers; and (3), the mode of Cr complexation.

6.2 Experimental

Intercalation of montmorillonite (SWy-1, Clay Minerals Society Source Clays Repository) with hydroxy polymers of Al, Cr, and coprecipitated Al-Cr, has been described in earlier work (Dubbin et al. 1994; Dubbin and Goh 1995a,b). After aging, the intercalated clays were first isolated by means of filtration through a Millipore filter of 25 nm pore size, air dried, then gently-powdered in preparation for NMR analyses. The non-interlayered clay, pure Al-clay, and coprecipitated Al-Cr clays

(Al/(Al+Cr) molar ratios of 0.5 and 0.33) were each analyzed with ^{27}Al MAS NMR. The non-interlayered clay, two pure Cr-clays (200 and 355 cmol Cr^{3+} sorbed/kg), and a coprecipitated Al-Cr clay (Al/(Al + Cr) molar ratio of 0.33) were each analyzed with ^{29}Si MAS NMR.

High-resolution spectra were collected using a Bruker AMX-500 console and 11.7 Tesla magnet. The samples were spun at 5.0 to 7.5 kHz in a Doty high-speed MAS probe at an angle of 54.7° to the magnetic field. Spectra were observed at different spinning speeds in order to distinguish true peaks from spinning sidebands (SSB's). The ^{27}Al spectra were recorded at 130.3 MHz while those for ^{29}Si were recorded at 99.3 MHz. ^{27}Al peak positions were measured with reference to 1 *M* aqueous $AlCl_3$, while those for ^{29}Si were measured with reference to tetramethylsilane.

6.3 Results

6.3.1 ^{27}Al Spectra

The ^{27}Al MAS NMR spectrum of the non-interlayered montmorillonite gave an intense peak near 3 ppm, indicating the presence of Al^{VI} (Figure 6.1). The spinning frequency employed for this scan caused a SSB to occupy a region of the spectrum in which a peak for Al^{IV} would normally appear (Goodman and Stucki 1984; Wilson et al. 1984; Morris et al. 1990). Therefore, for a subsequent scan, the spinning frequency was decreased to 5.0 kHz. This second scan did not detect any Al^{IV}. However, based on chemical analyses, previous work has shown that 1.5 to 3 % of

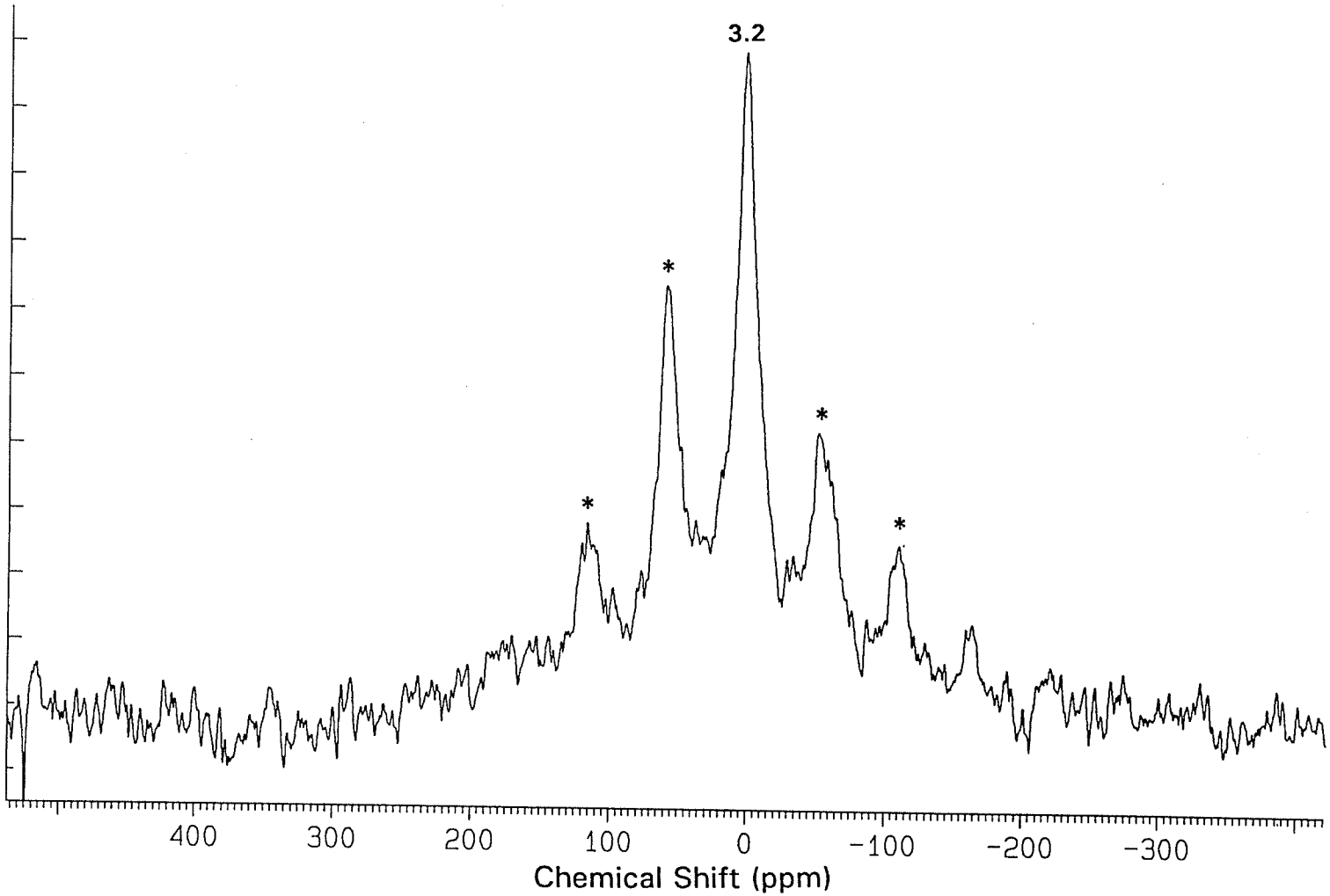

Figure 6.1. ^{27}Al MAS NMR spectrum of the non-interlayered montmorillonite. Asterisks indicate SSB's.

the tetrahedral sites in SWy-1 montmorillonite are occupied by Al (Weaver and Pollard 1973; Woessner 1989). Other workers were also unable to detect any Al^{IV} in this clay using MAS NMR, despite chemical analyses which indicated that several percent of the tetrahedral sites were occupied by Al (Kinsey et al. 1985). Apparently, ^{27}Al MAS NMR is not sensitive enough to detect minor amounts of Al^{IV} above the background noise.

Similar to the non-interlayered clay, the montmorillonite which contained the pure hydroxy-Al interlayers gave only a single peak near 4 ppm, indicating the presence of a single environment for Al^{VI} (Figure 6.2). Interpretation of ^{27}Al spectra for clays which held coprecipitated hydroxy-Al and -Cr interlayers was somewhat more difficult. The paramagnetic nature of Cr(III) increased the intensity of the SSB's and broadened the central peak (Figures 6.3 and 6.4). However, the shape of the central peak in Figures 6.1 and 6.2 is clearly different from that in Figures 6.3 and 6.4. The peak in each of the latter two spectra has been split, with the two sub-peaks differing by approximately 3 ppm. This difference in peak shape becomes more apparent when one examines the juxtaposed detailed spectra of the control, Al montmorillonite, and Al-Cr montmorillonite (Figure 6.5). For the Al-Cr clay, a peak near 3 ppm represents Al^{VI} in the 2:1 layer. An additional peak at 0.2 ppm represents interlayer Al^{VI}. One may conclude, therefore, that the presence of sorbed Cr has created a second, slightly more shielded environment for interlayer Al^{VI}.

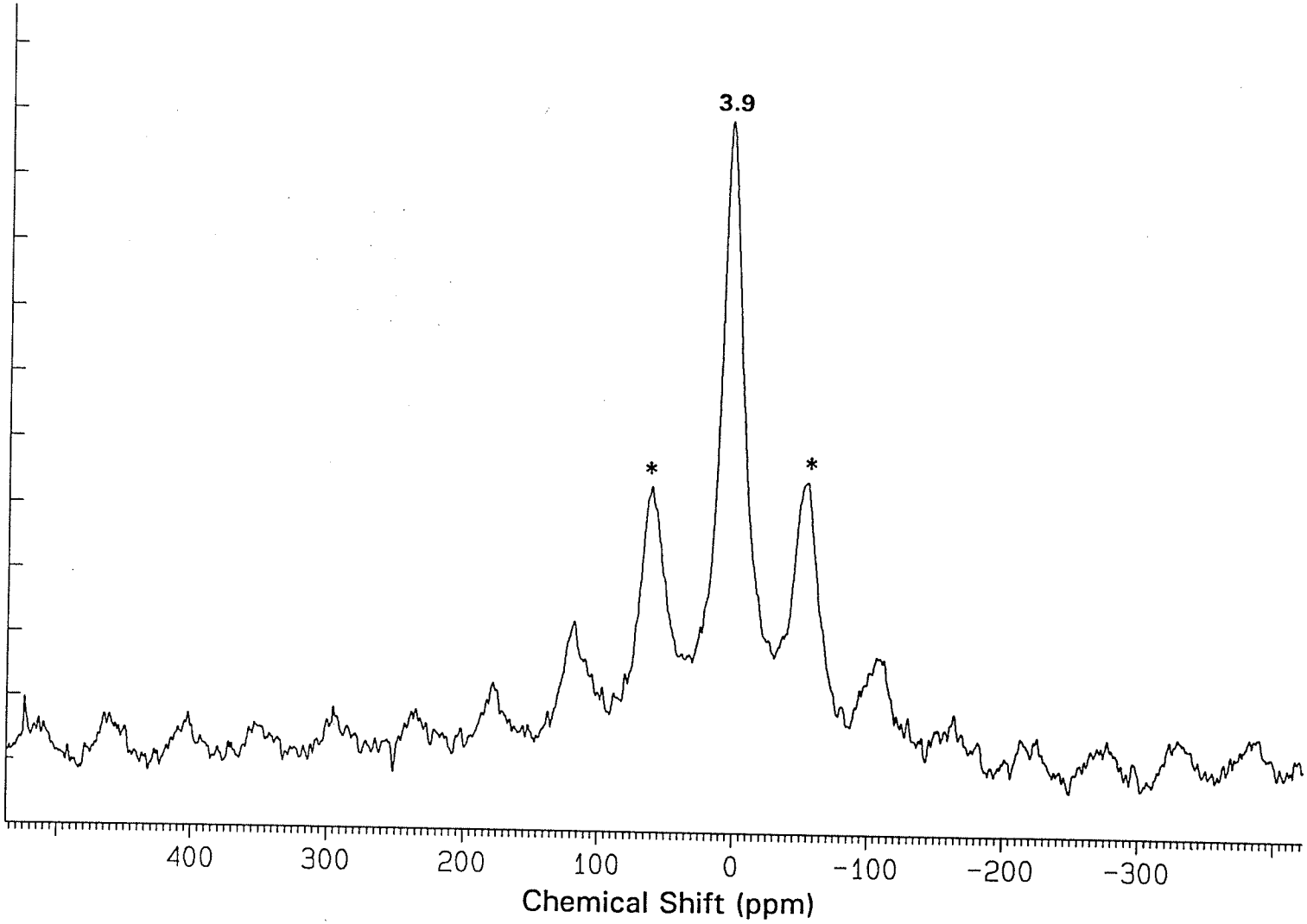

Figure 6.2. ^{27}Al MAS NMR spectrum of the pure hydroxy-Al interlayered montmorillonite. Asterisks indicate SSB's.

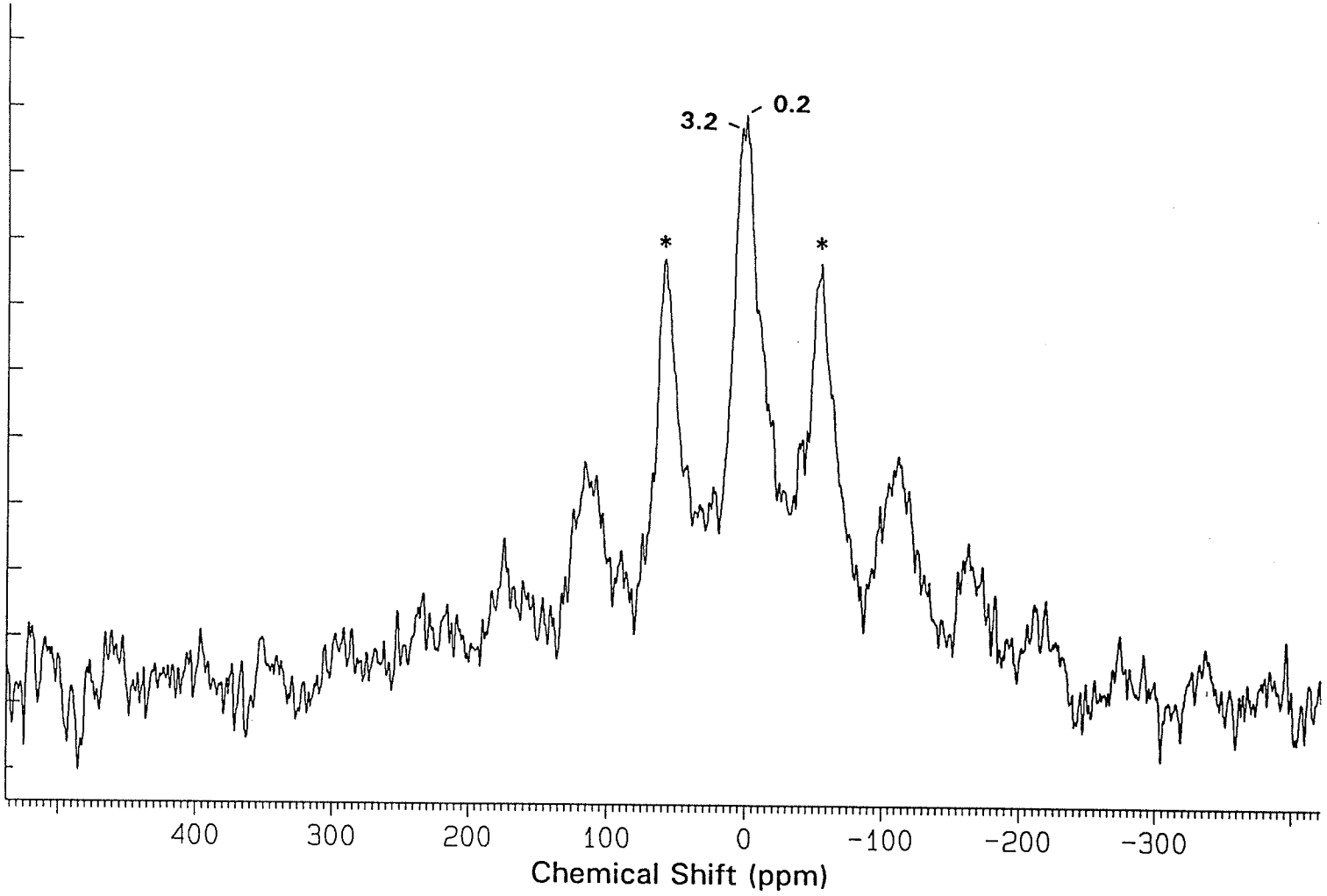

Figure 6.3. ^{27}Al MAS NMR spectrum of a coprecipitated Al-Cr clay (Al/(Al+Cr) molar ratio = 0.5). Asterisks indicate SSB's.

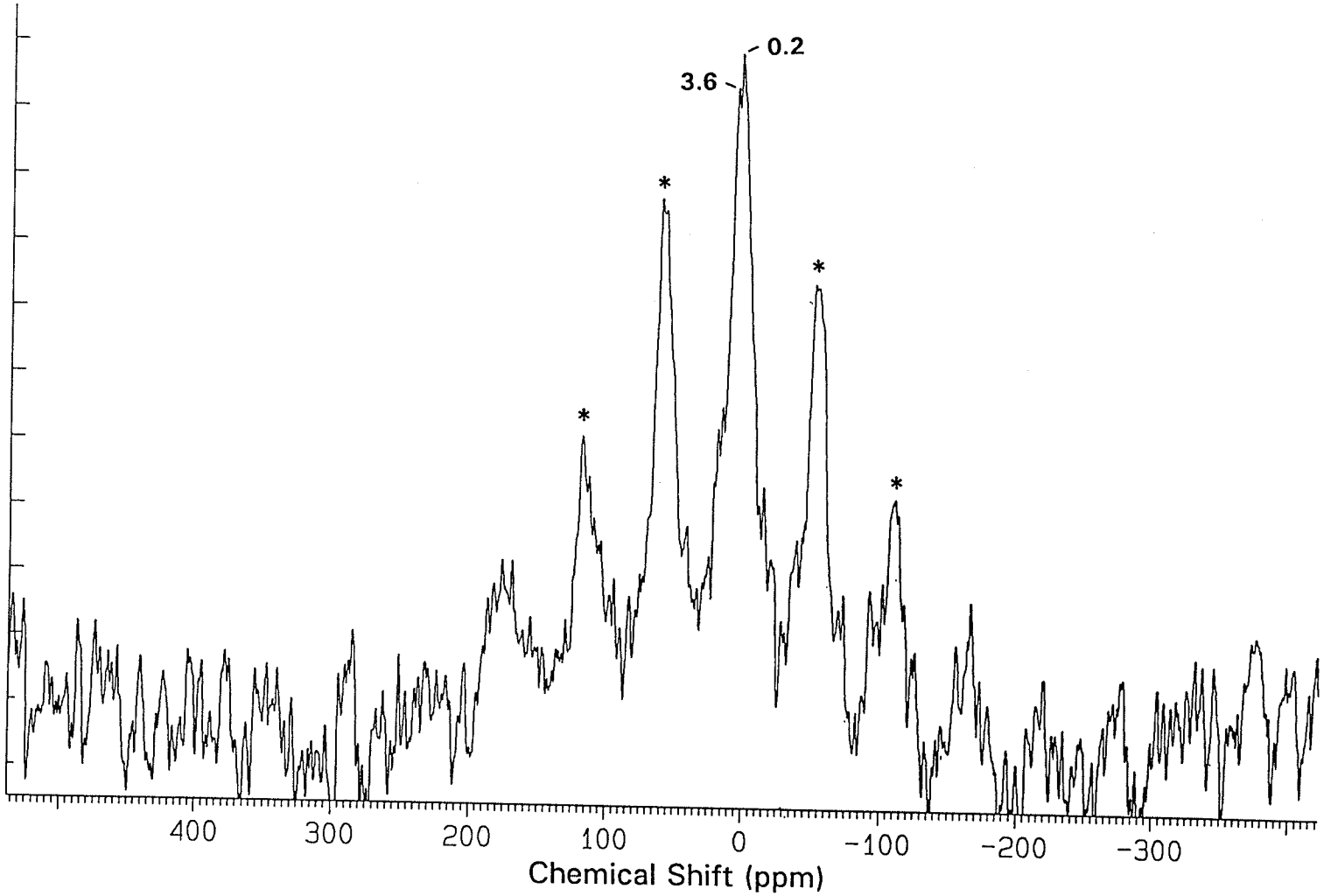

Figure 6.4. ^{27}Al MAS NMR spectrum of a coprecipitated Al-Cr clay (Al/(Al+Cr) molar ratio = 0.33). Asterisks indicate SSB's.

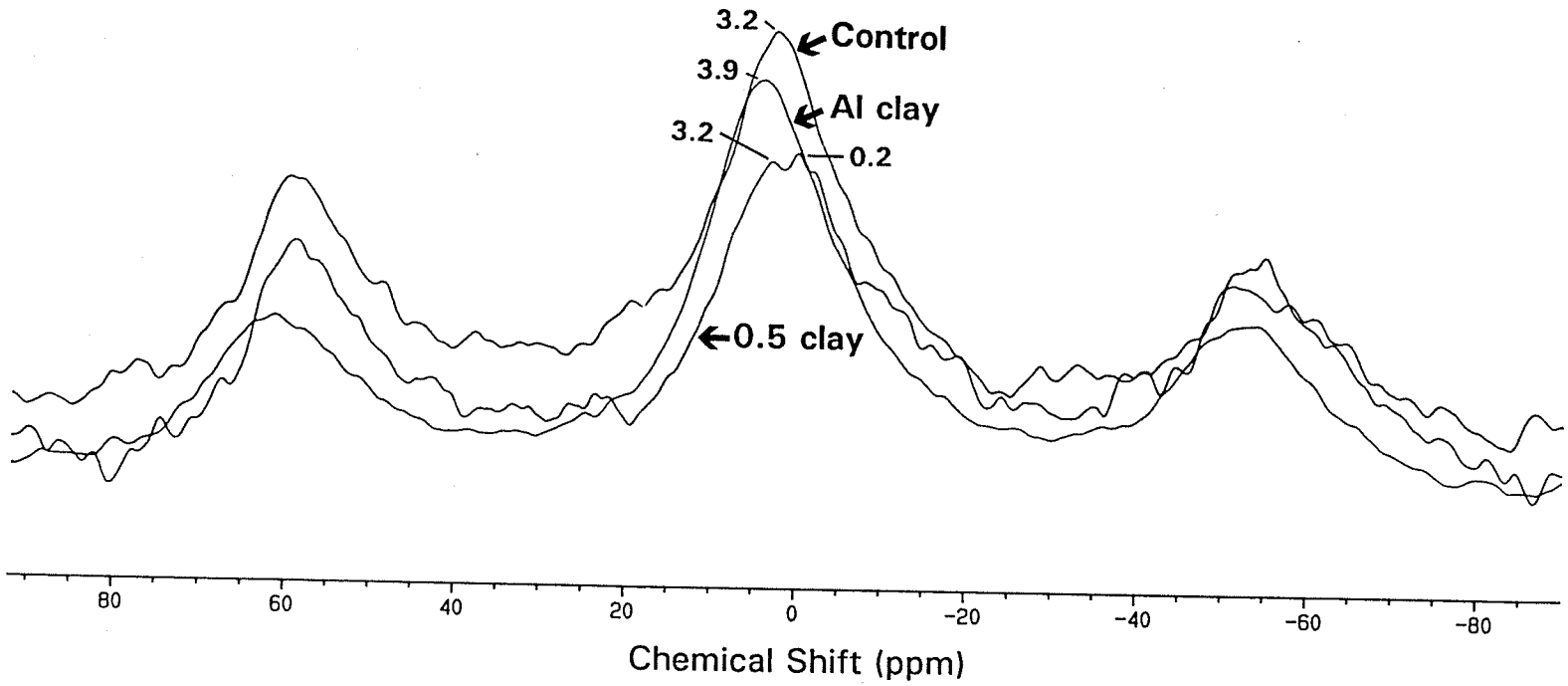

Figure 6.5. Detailed ^{27}Al MAS NMR spectra of the non-interlayered (control) clay, pure hydroxy-Al clay, and Al-Cr clay where the Al/(Al+Cr) molar ratio = 0.5.

6.3.2 ^{29}Si Spectra

The non-interlayered montmorillonite gave major peaks at -94 and -108 ppm (Figure 6.6). The peak at -94 ppm corresponds to the Si(0Al) environment of Si in the tetrahedral sheet. Although small amounts of Al were present in the tetrahedral sheets of this montmorillonite, the Si(1Al) environment for Si was not sufficiently abundant to give the corresponding peak near -90 ppm. Montmorillonite samples similar to that used in this investigation have been analyzed previously with ^{29}Si MAS NMR (Kinsey et al. 1985; Liang and Sherriff 1993; Malla and Komarneni 1993). In each of these previous studies, the montmorillonite also yielded a major peak near -94 ppm.

The peak at -108 ppm is attributed to Si from quartz, which is known to occur in small amounts as an impurity in SWy-1 montmorillonite (van Olphen and Fripiat 1979). The ^{29}Si chemical shift for tetrahedral sites in pure crystalline silicates ranges from -100 to -120 ppm, with that for crystalline quartz occuring near -107 ppm (Oestrike et al. 1987). The considerable area of the -108 ppm peak suggests that the quartz is present in quantities greater than the minor amounts reported by van Olphen and Fripiat (1979). However, a previous investigation found that about one-half of the quartz ^{29}Si peak width could be attributed to instrumental factors (Oestrike et al. 1987). Therefore, the area of the -108 ppm peak observed in the present study probably over-represents the true abundance of Si from quartz.

A small peak at -101 ppm was detected in the spectra of the Al-Cr clay (Figure 6.7). The intensity of this peak increased as the amount of sorbed Cr increased

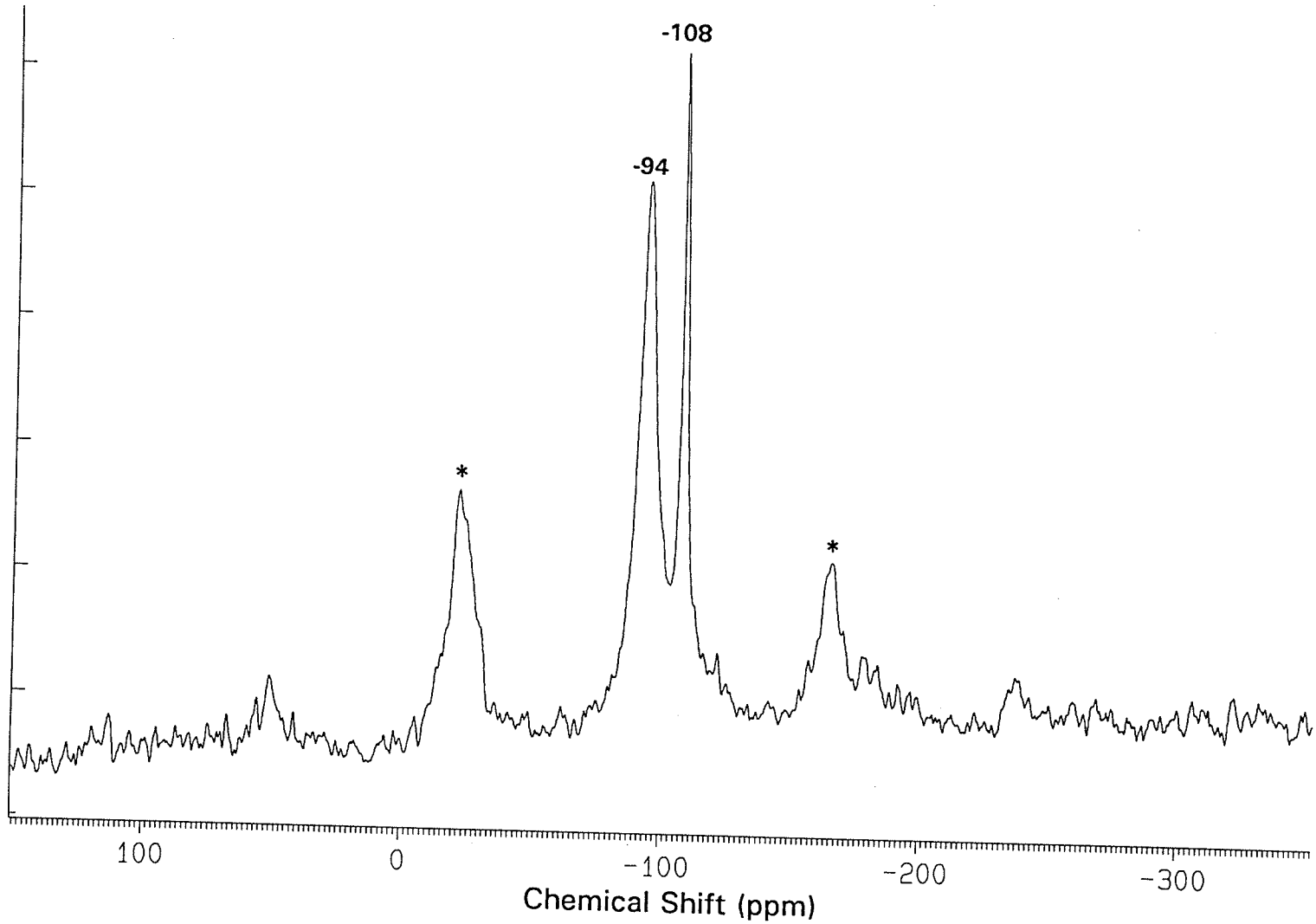

Figure 6.6. ^{29}Si MAS NMR spectrum of the non-interlayered montmorillonite. Asterisks indicate SSB's.

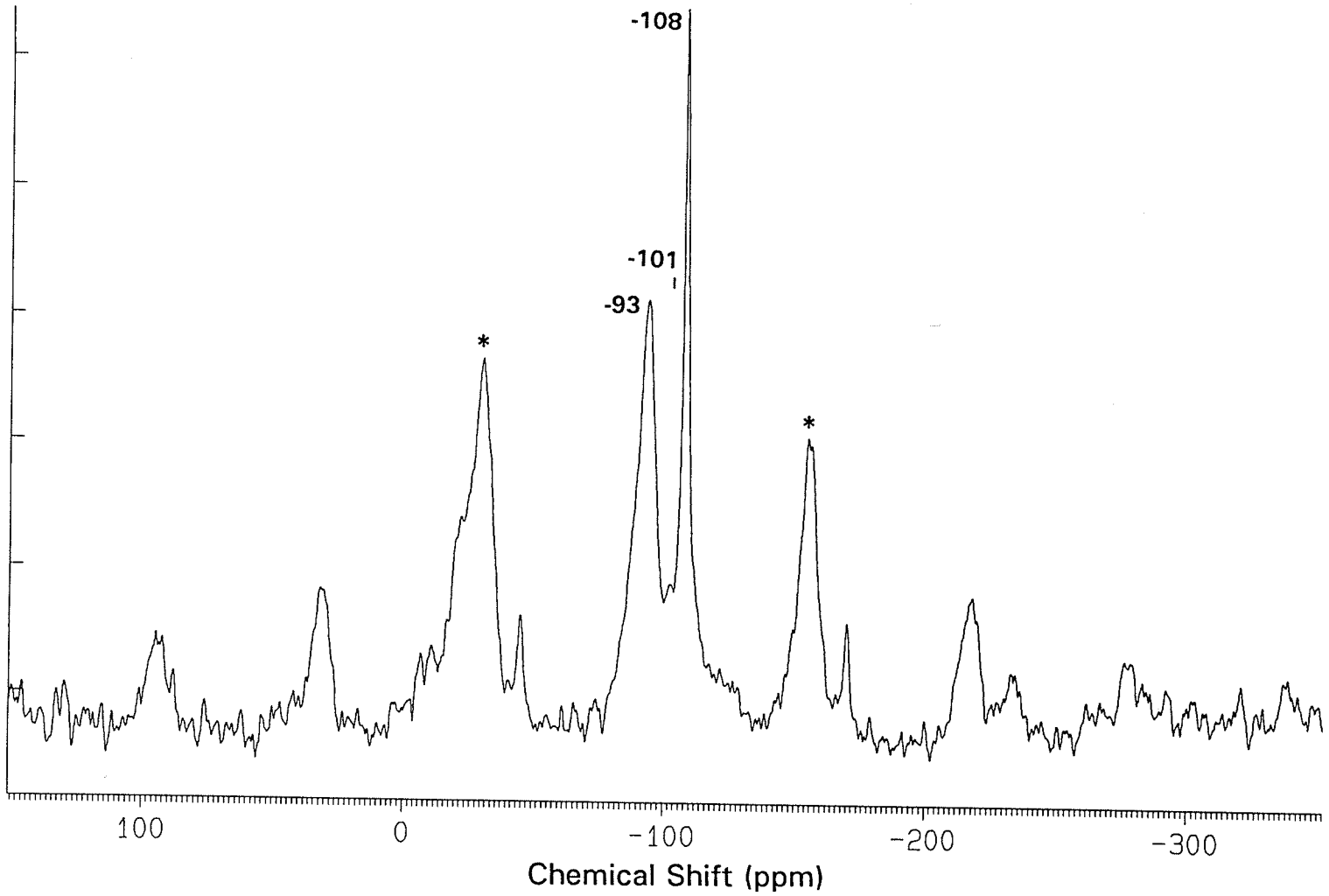

Figure 6.7. ^{29}Si MAS NMR spectrum of a coprecipitated Al-Cr clay (Al/(Al+Cr) molar ratio = 0.33). Asterisks indicate SSB's.

(Figures 6.8 and 6.9). Even at its greatest intensity, however, this peak is very small and may be mistaken for background noise. Its identity as a true peak is revealed by the constancy of its position; peaks representing background noise are transient and change their positions with each scan. This peak at -101 ppm is attributed to the effect of interlayer Cr on the shielding of Si in the 2:1 layer.

6.4 Discussion

6.4.1 Chemical environment of Al

Results of the ^{27}Al MAS NMR analyses indicate that all of the Al which was detected was present in an octahedral environment. This observation is consistent with previous work which found that the intercalated hydroxy-Al polymers, whether existing alone or coprecipitated with Cr, occur as simple octahedral sheets or fragments thereof (Dubbin et al. 1994). As revealed in Figure 6.5, the sorbed Cr created an environment for interlayer Al^{VI} which was slightly more shielded than that for Al^{VI} in the 2:1 layer. The Cr altered the environment of interlayer Al^{VI} by acting through the oxygen shared with the adjoining Al octahedra. Therefore, the slightly less positive chemical shift for interlayer Al^{VI} in Al-Cr clays is evidence for the presence of Al-O-Cr linkages. The detailed spectrum of the Al-Cr clay reveals that the two sub-peaks have nearly the same intensity. Although peak area is a more accurate measure of the abundance of a particular environment, the strong intensity of the 0.2 ppm peak indicates that the Al-O-Cr linkages are quite abundant. It is

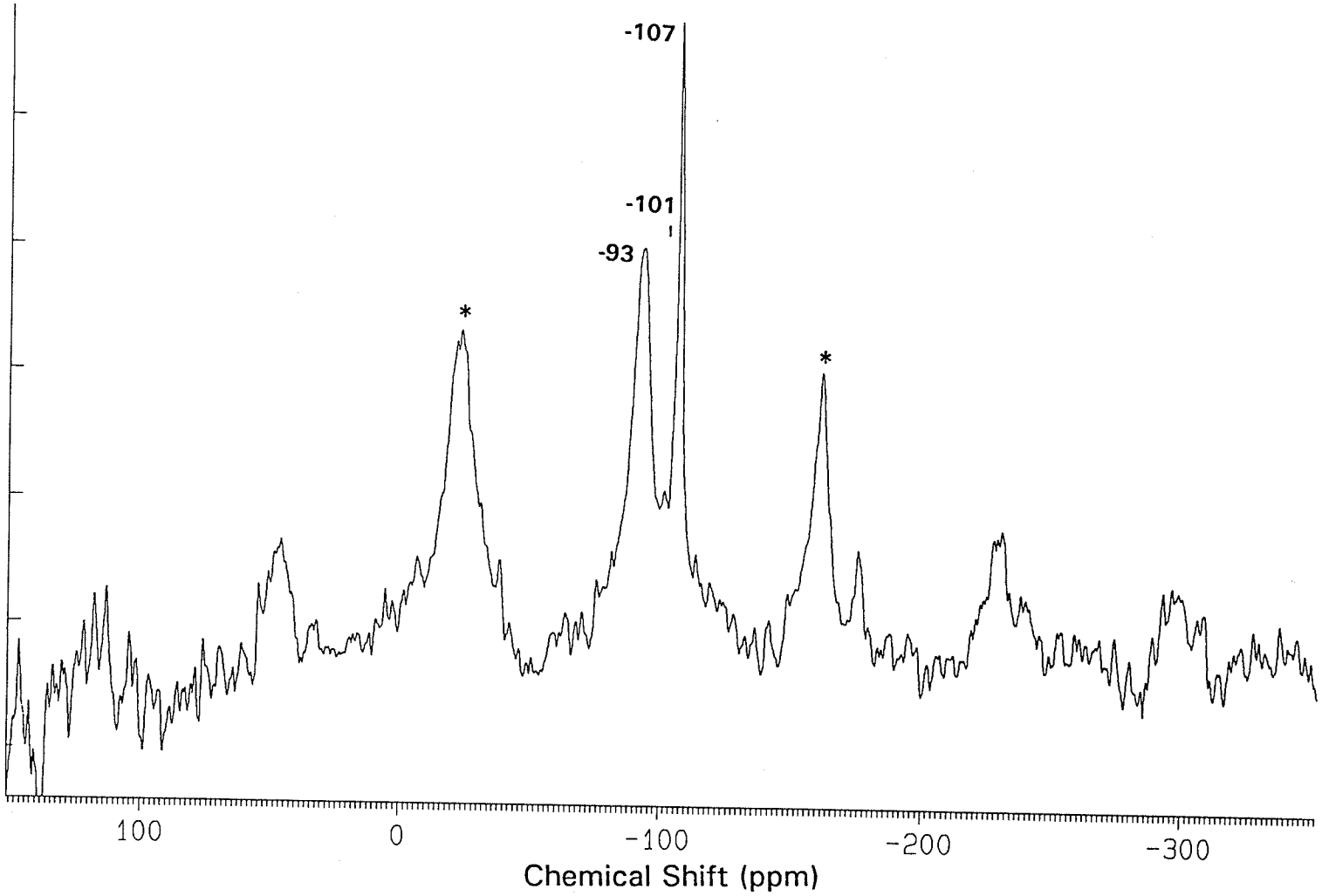

Figure 6.8. ^{29}Si MAS NMR spectrum of a pure hydroxy-Cr interlayered montmorillonite (200 cmol Cr^{3+} sorbed/kg). Asterisks indicate SSB's.

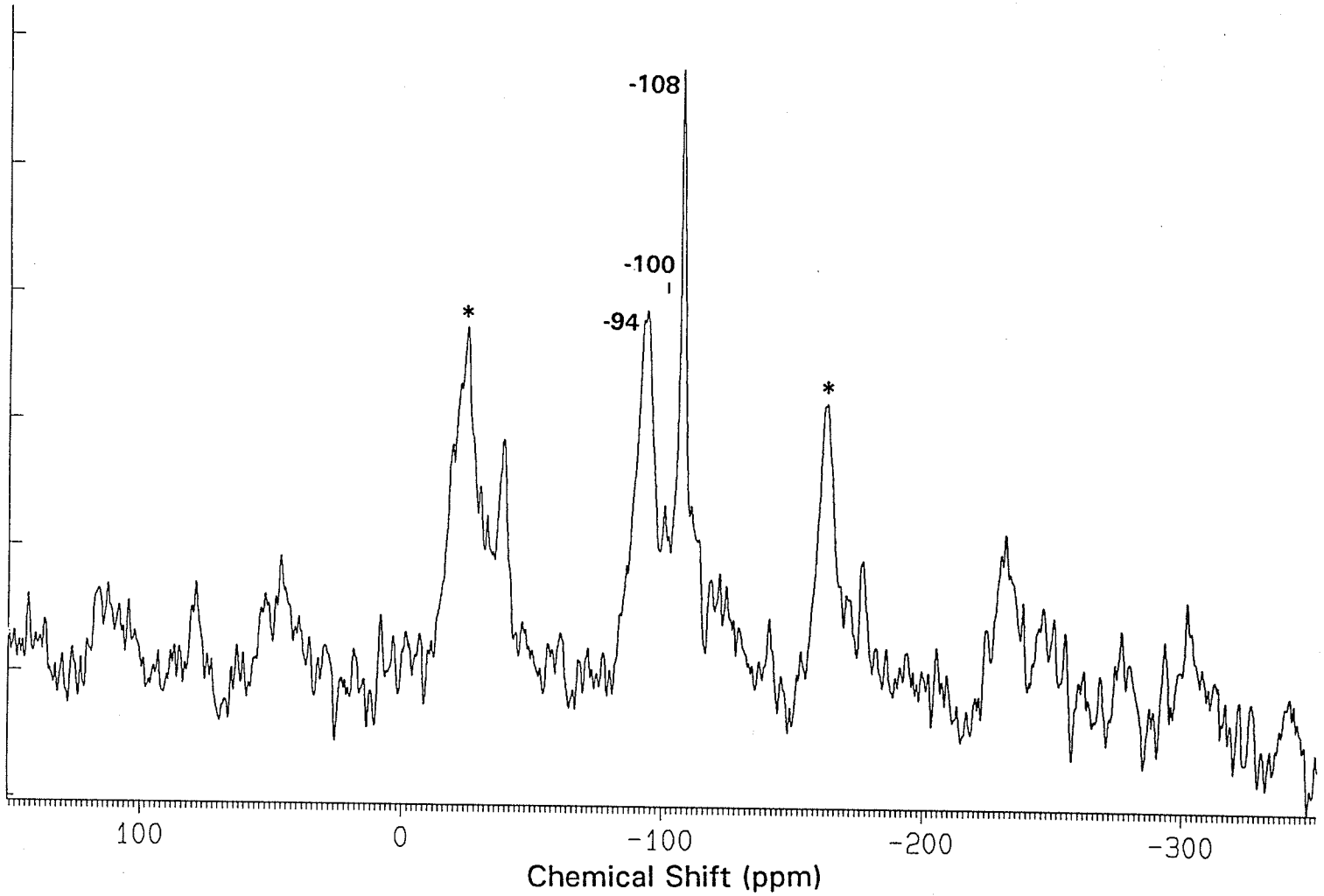

Figure 6.9. ^{29}Si MAS NMR spectrum of a pure hydroxy-Cr interlayered montmorillonite (355 cmol Cr^{3+} sorbed/kg). Asterisks indicate SSB's.

proposed, therefore, that Al and Cr are distributed fairly uniformly within the hydroxy polymers. This arrangement would provide a greater number of Al-O-Cr linkages than if Al and Cr were segregated.

The underlying cause of the ^{27}Al chemical shift in the Al-Cr clays is not known for certain. However, because both Al and Cr have the same valence, differences in ionic charge can be disregarded. These two elements also have comparable electronegativities; the small difference which does exist would not be expected to contribute significantly to the chemical shift. Aluminum and Cr(III) do, however, possess substantially different ionic radii. The radius of Al^{3+} (0.68 Å) is significantly smaller than that of Cr(III) (0.76 Å). The presence of the larger Cr(III) ion in the octahedral sheet would distort adjacent Al octahedra. This distortion, in turn, would result in a redistribution of electrons around the Al nucleus, producing the observed chemical shift.

6.4.2 Mode of Cr complexation

The ^{29}Si chemical shift of layer silicates is sensitive to the nature of interlayer cations. Sorbed cations alter the distribution of electrons at the siloxane surface, thereby changing the chemical environment of Si. It is, however, difficult to predict whether interlayer cations will increase or decrease the shielding of tetrahedral Si. Intercalation of montmorillonite with positively charged SiO_2-TiO_2 particles has been shown to decrease the shielding of Si and, consequently, move the ^{29}Si peak to slightly

less negative values (Malla and Komarneni 1993). By determining the position of the ^{29}Si chemical shift for talc-phlogopite and pyrophyllite-muscovite pairs, interlayer K^+ was also shown to decrease the shielding of Si (Sanz and Serratosa 1984). However, because micas hold K^+ through inner-sphere complexes, the redistribution of electrons at the siloxane surface was greater than would occur through outer-sphere complexes. Consequently, the change in chemical shift induced by K^+ (5 ppm) was greater than that induced by the SiO_2-TiO_2 particles, which were held through only electrostatic forces. In contrast to the above findings, other work has indicated that interlayer cations increase the shielding of tetrahedral Si. The sorption of both hydroxy-Al polymers (Plee et al. 1985) and Pb(II) (Liang and Sherriff 1993) onto layer silicates was shown to move the ^{29}Si peak to more negative values. Of all the Pb(II)-exchanged clays examined by Liang and Sherriff (1993), however, a shift in the ^{29}Si peak position was observed only for vermiculite, presumably because only the vermiculite had a charge that was large enough to induce an interaction with the Pb(II) which was sufficiently strong to alter the Si environment.

Despite difficulty in predicting whether interlayer cations will increase or decrease the shielding of Si, it is apparent from the previous discussion that the magnitude of change in chemical shift is directly related to the strength of the cation-siloxane oxygen complex. Cations held covalently have a greater effect on the electron density of siloxane O than those held simply through coulombic forces. As shown in Figures 6.7 through 6.9, the two principal environments of Si in the tetrahedral sheet

differ by about 8 ppm. This large difference can be accounted for only by the presence of Si-O-Cr linkages. Formation of a covalent bond between Cr and siloxane O would decrease the electron density of the Si-O bond. Adopting the explanation Kirkpatrick (1988) proposed to explain a similar chemical shift, this decrease in electron density would decrease the paramagnetic deshielding of Si and cause the observed change to a more negative chemical shift. Therefore, the creation of a second environment for Si in the tetrahedral sheet, significantly more shielded than the first, provides the most definitive evidence yet to support the idea of inner-sphere complexation of Cr.

6.4.3 Cr arrangement on the siloxane surface

The Cr atoms would not be sorbed randomly on the siloxane surface. As indicated previously, the -94 ppm peak represents a single, relatively broad environment for Si in the tetrahedral sheet (ie. Si(0Al)). Within this major environment, however, the Si atoms will experience slightly different sub-environments, depending on their proximity to substitution sites (ie. Mg^{2+} for Al^{3+}) in the octahedral sheet. These sub-environments contribute to peak broadening. Of all the siloxane O available for complexation, one would expect Cr to preferentially complex with those which carry the greatest charge; that is, those closest to octahedral substitution sites. Therefore, Cr would alter the environment of Si atoms which occupy a fairly narrow range of environments. Consequently, the peak representing

the newly-created Si environment would be narrower than the -94 ppm peak, reflecting the greater uniformity of the new environment. The apex of the -100 ppm peak appears to be sharper than that of the -94 ppm peak, thereby supporting this proposal (Figure 6.9). However, an accurate comparison of peak widths is difficult due to the small size of the -100 ppm peak.

Geometric constraints dictate that a single Cr(III) atom can complex with only one O from the same Si tetrahedron. The O-O interatomic distance on the basal surface of a Si tetrahedron is approximately 2.6 Å whereas the O-O distance for a $Cr^{3+}(H_2O)_6$ octahedron is near 2.9 Å (Grim 1968). Clearly, the differing bond lengths preclude the possibility of bidentate complexation to a single tetrahedron. For the simplest case, that of a single Cr(III) in octahedral coordination with H_2O and OH, one can envisage an arrangement depicted in Figure 6.10. In this scenario the Cr(III) is held through a monodentate complex at each surface and is, therefore, bidentate overall. The potential for Cr(III) to be sorbed through a bidentate complex on a single surface will depend on the distance between O of different tetrahedra, which depends primarily on the amount of rotation of the tetrahedra.

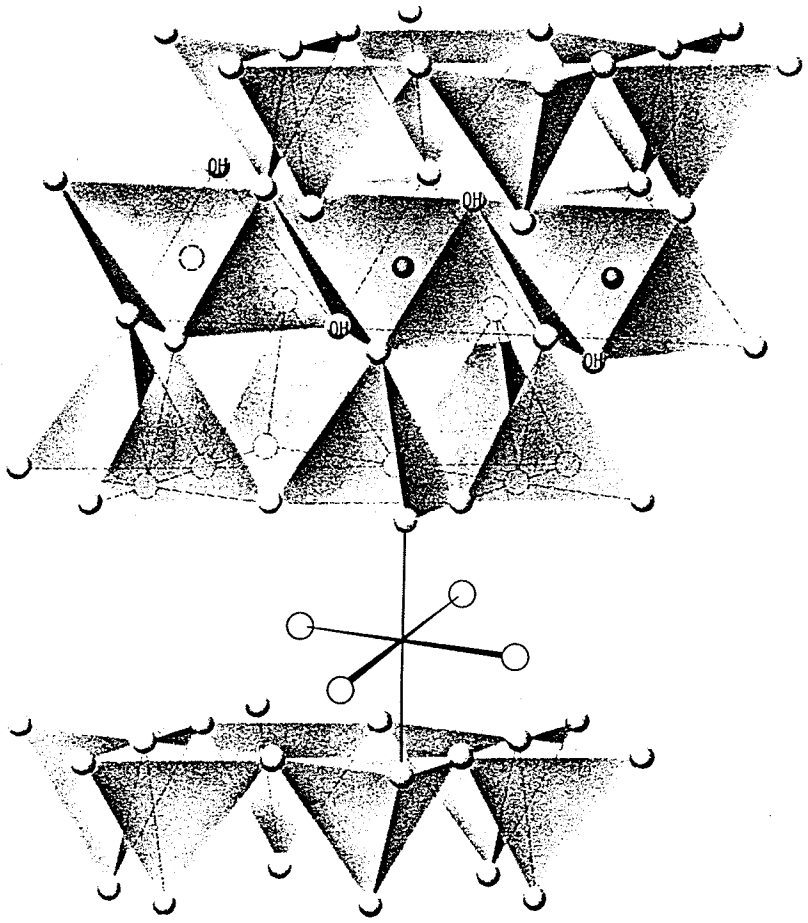

Figure 6.10. Depiction of octahedrally coordinated Cr(III) adsorbed through an inner-sphere complex at each siloxane surface (modified from Klein and Hurlbut 1985).

6.5 Conclusions

All of the Al detected by ^{27}Al MAS NMR was present in an octahedral environment. The environment of Al^{VI} in the interlayer region was altered slightly by the sorbed Cr, indicating the presence of Al-O-Cr linkages. Both of these observations are consistent with the results of previous investigations and further support the idea of a uniform distribution of Al and Cr within the interlayered octahedral hydroxy polymers.

A major goal of this study was to elucidate the mode of Cr complexation. Earlier studies proposed, but did not confirm, an inner-sphere adsorption mechanism. In this study, ^{29}Si MAS NMR revealed a second environment for Si in the tetrahedral sheet of the Cr-clays. Such an environment could be created only by the covalent bonding of Cr with siloxane O. Therefore, ^{29}Si MAS NMR has provided the most definitive evidence yet in support of the inner-sphere mechanism of Cr adsorption.

7. OXIDATIVE DISSOLUTION OF HYDROXY-Cr INTERLAYERS IN MONTMORILLONITE

7.1 Introduction

In soils and sediments, chromium may be present in two thermodynamically stable oxidation states, Cr(III) and Cr(VI) (Bartlett and Kimble 1976). Chromium(VI) is known to pose a significant health hazard and the US EPA has, therefore, established a limit of 1.7 ppm for Cr(VI) in effluent water (U.S. Environmental Protection Agency 1977). Chromium(III), however, presents only a low health risk. The only significant threat from Cr(III) is its potential oxidation to Cr(VI). In light of the known hazards of Cr(VI), considerable effort has been directed toward understanding the oxidative behavior of Cr(III).

In natural systems the only common oxidants of Cr(III) are Mn oxides and, at pH values greater than 9, molecular oxygen. The oxidation of Cr(III) by Mn oxides has been examined extensively in recent years (Eary and Rai 1987; Johnson and Xyla 1991; Fendorf et al. 1992; Fendorf and Zasoski 1992; Fendorf et al. 1993). All of this work, however, has examined the oxidation of aqueous Cr(III) to Cr(VI) by reaction with solid phase Mn. It is well known, though, that most Cr(III) in soils and sediments occurs, not in solution, but rather as highly insoluble hydroxy polymers sorbed to colloid surfaces (Shewry and Peterson 1976; Cary et al. 1977; Grove and Ellis 1980). Of the total Cr(III) pool, only a small fraction is present in solution.

Therefore, solid phase Cr(III) poses a much greater potential risk to ecosystem health than aqueous Cr(III).

Expandable layer silicates such as montmorillonite are often major constituents of soils and sediments and have been shown to have a high sorptive capacity for hydrolyzed Cr (Dubbin and Goh 1995a). This Cr is strongly bound within the interlayer region and can not be displaced via simple cation exchange reactions. Under most conditions, therefore, the Cr is secure and does not pose an environmental threat. However, oxidation of the Cr(III) would lead to its release to solution as the toxic Cr(VI) oxyanion. Manganese oxides are unlikely oxidants for this intercalated Cr(III); the small pore size within the interlayer region would prevent the entry of all but the smallest Mn oxide units. In this respect, the montmorillonite provides the Cr(III) with a measure of stability against oxidation. However, many industries use powerful aqueous oxidants which would have easy access to the interlayer region of montmorillonite. For example, water treatment facilities commonly employ chlorine compounds such as NaOCl to assist in the removal of Fe and organic contaminants (Laubusch 1971). The oxidation of Cr(III) by OCl^- is known to be thermodynamically favorable. In the presence of powerful aqueous oxidants such as OCl^-, therefore, one would expect the oxidation and subsequent release of interlayered Cr(III).

In assessing the potential toxicity of a redox-sensitive metal such as Cr(III) which is present largely in the solid phase, one must not be satisfied with an understanding of the redox behavior of only its aqueous forms; Cr held in the solid

phase poses a much greater potential threat. The aim of this investigation, therefore, was two-fold. The primary goal was to elucidate the characteristics of oxidative dissolution of interlayered hydroxy-Cr polymers. Because Al and Cr are known to coprecipitate within the interlayers of montmorillonite (Dubbin et al. 1994), a secondary goal was to determine the effect of this coprecipitated Al on the oxidation of the Cr.

7.2 Materials and Methods

7.2.1 Clay synthesis

The montmorillonite (SWy-1, Crook County, Wyoming) was obtained from the Source Clays Repository of The Clay Minerals Society. Prior to fractionation, the clay was Na-saturated by washing five times with 1 *N* NaCl then washed free of Cl^- as determined by the $AgNO_3$ test. For each sample, five grams of the <2 μm fraction was first suspended in 2 L deionized water. Two sets of hydroxy-Cr interlayered clays were prepared. The first set was prepared by treating each of seven montmorillonite suspensions with a different $CrCl_3$ concentration (67, 100, 133, 200, 400, 600, and 800 cmol Cr/kg clay). For the second set, $AlCl_3$ and $CrCl_3$ were added to separate montmorillonite suspensions to give three Al/(Al+Cr) molar ratios (0.67, 0.5, 0.33). Each of these three had a total trivalent cation concentration of 200 cmol M^{3+}/kg clay. All ten clay-M^{3+} suspensions were stirred vigorously and titrated at 1 mL/min with 0.1 *N* NaOH until a final NaOH/M^{3+} molar ratio of 2.5 was reached.

To assist in the elucidation of the oxidation mechanism, bulk $Cr(OH)_{3(s)}$ was prepared by titrating $CrCl_3$ with 0.1 *N* NaOH until a $NaOH/Cr^{3+}$ molar ratio of 3.0 was reached. All suspensions were brought to final volumes of 3 L and then transferred to capped bottles. The suspensions were aged at 23 $\pm$ 0.5°C for 30 days and were agitated daily. After aging, each suspension was separated into its filtrate and solid phase by ultrafiltration through a Millipore filter of 0.025 μm pore size. The solid phase of each sample was washed free of Cl^- as determined by the $AgNO_3$ test.

7.2.2 Oxidation of the hydroxy-Cr polymers

Oxidation of the bulk $Cr(OH)_{3(s)}$ was conducted by suspending several milligrams of the oxide in 50 mL of NaOCl which, while dilute (1.07 % Cl), was in large excess of that required for complete oxidation of the Cr. A magnetic stirring bar maintained a homogeneous suspension. At selected times 1 mL of the suspension was withdrawn and passed through a Millipore filter of 0.025 μm pore diameter. Four mL of deionized H_2O were subsequently passed through the same filter to ensure all of the Cr in solution had been washed from the clay. Oxidation of the interlayered clays involved following this same procedure except that approximately 30 mg clay was added to the NaOCl. Chromium and Al in all extracts were determined with atomic absorption spectroscopy.

7.3 Results

7.3.1 Oxidation of bulk (non-interlayered) $Cr(OH)_{3(s)}$

At the start of all oxidative dissolutions the Eh and pH values were approximately 0.74 V and 11.3, respectively. These conditions fall within the stability field for chromate (Figure 7.1). Therefore, one would expect chromate species to be the stable end-product of these oxidation reactions. The oxidation of Cr(III) by OCl^-, which is thermodynamically favorable, consumes hydroxyls. One would expect, therefore, the oxidation of Cr(III) to coincide with a decrease in pH. During dissolution of the bulk $Cr(OH)_{3(s)}$, the pH of the suspension did, in fact, decrease from 11.3 to 7.8 (Figure 7.2). The first 2 h of the reaction produced a decrease in pH of approximately 1 unit. During the next 2 h, proton production accelerated and pH decreased by more than 2 units to 7.8 at 5 h reaction time.

Supernatant Cr concentration increased only gradually during the first 3 h (Figure 7.2). However, there was a marked increase in oxidation rate between 3 and 4 h prior to the maximum rate which occurred between 4 and 5 h. The highest rate of Cr(III) oxidation was observed only when the pH was near its minimum value. This observation indicates that the generation of protons is a prerequisite to enhanced oxidation.

7.3.2 Oxidative dissolution of pure hydroxy-Cr interlayers

Dissolution curves of all seven clays which contained pure hydroxy-Cr

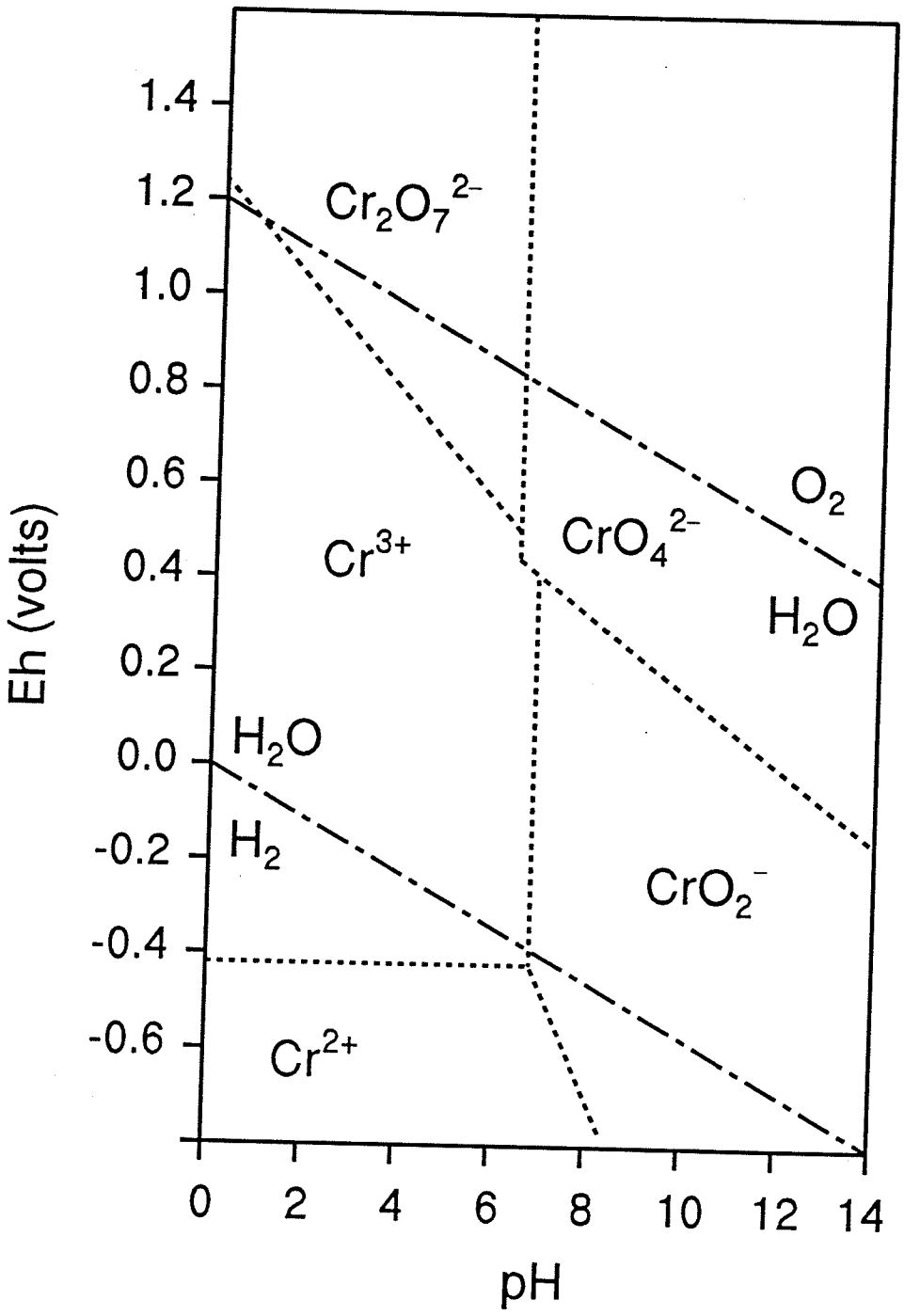

Figure 7.1. Eh - pH diagram of Cr species in water at 25°C (modified from Bartlett and Kimble 1976).

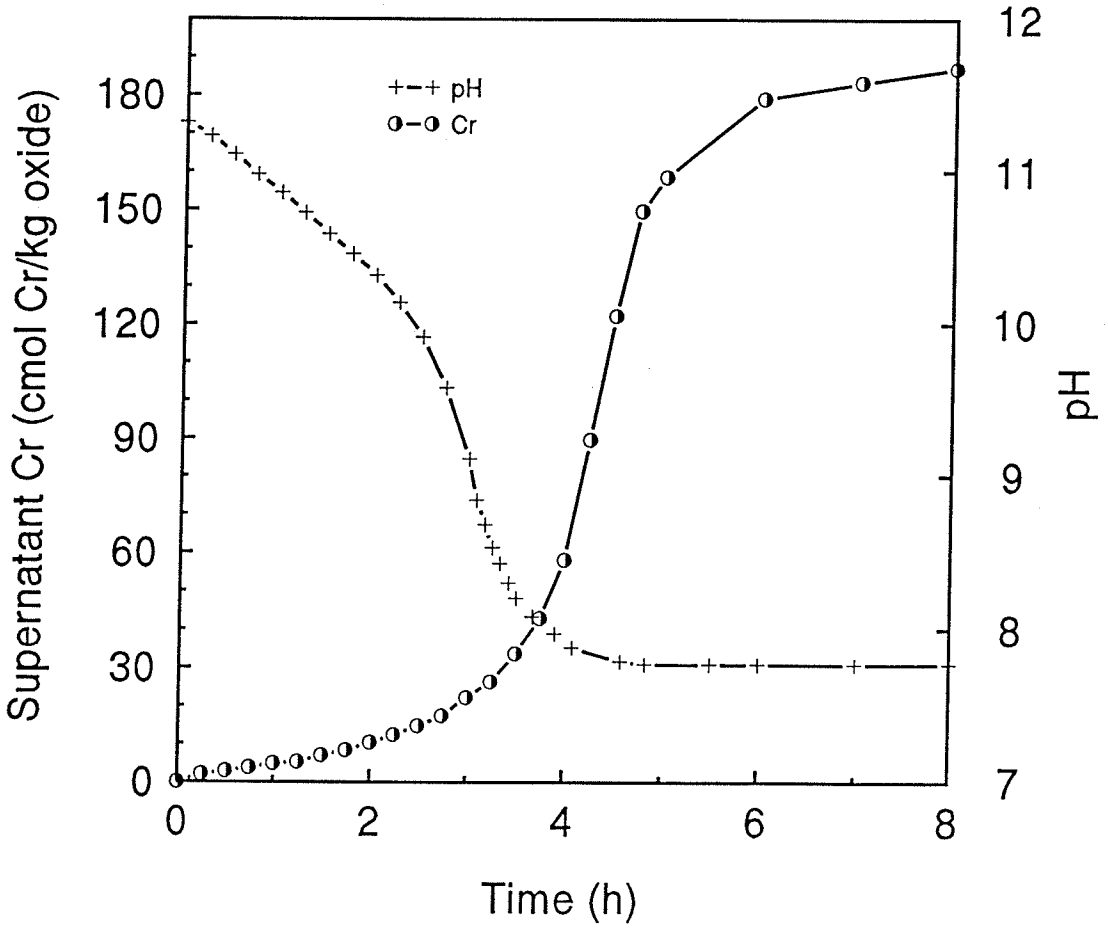

Figure 7.2. Supernatant Cr concentration and pH as a function of time for the dissolution of bulk $Cr(OH)_{3(s)}$.

interlayers are shown in Figure 7.3. The four clays treated with the least amount of Cr sorbed all of that which was added. However, the three clays treated with the largest amounts of Cr sorbed only a portion of that which was added. Specifically, the 400, 600, and 800 clays sorbed only 334, 355, and 416 cmol Cr/kg clay, respectively. Therefore, in the oxidation of these three highest-Cr clays, the final supernatant Cr concentrations were considerably lower than what one would expect from the original Cr concentrations of the aging suspensions.

Oxidation was allowed to proceed to completion for all seven clays. Oxidation of the 67 clay progressed slowly initially then accelerated somewhat between 3 and 6 h leading to complete dissolution of the interlayers by 10 h. Likewise, oxidation rates of the 100 and 133 clays were slow initially, then accelerated between 2 and 5 h. Interlayers of the 100 and 133 clays were completely oxidized by 8 and 7 h, respectively. The oxidative behavior of the 200 clay mimicked that of the previous three. That is, a slow initial oxidation rate was followed by a rapid rate followed, once again, by a slower rate leading to termination by 5 h. Dissolution curves of the three most Cr-rich clays displayed only a gross resemblance to those of the previous four. For these three highest-Cr clays the maximum oxidation rate occurred much earlier and its magnitude was much greater than for the others. Oxidation was complete by 2 h for all three of these clays.

Figure 7.3 shows a relationship between the amount of sorbed Cr and duration of oxidation which at first appears contradictory. As the amount of sorbed Cr

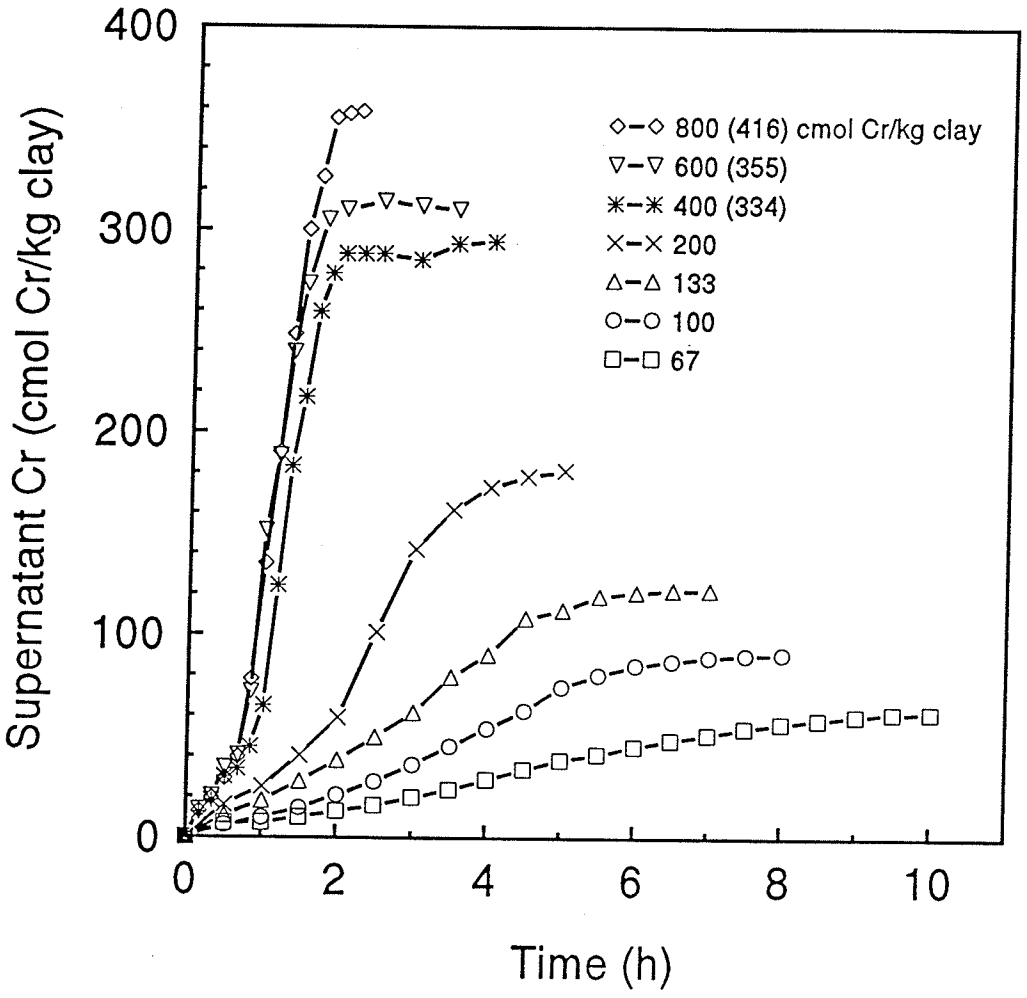

Figure 7.3. Supernatant Cr concentration as a function of time for the seven pure Cr clays. Values in parentheses indicate actual amount of sorbed Cr.

increased, the time required for its complete oxidation decreased. Two important parameters, which may explain these different oxidation rates, are known to vary among the seven clays. First, the pore space within the interlayer region would greatly affect the supply of oxidant to the interlayered hydroxy polymers. The relative total pore space in these clays can be inferred from N_2-BET specific surface areas. The N_2-BET specific surfaces were determined previously for the 67, 100, 133, 200, 400, 600, and 800 clays and found to be 44, 62, 85, 91, 122, 111, and 103 m^2/g, respectively (Dubbin and Goh 1995a). It can be seen, therefore, that the oxidation rates increased with increasing pore space. Secondly, the surface charge of the hydroxy polymers, which is governed by pH, ultimately determines the amount of OCl^- which is complexed. A lower pH imparts a greater positive charge to the hydroxide surface, thereby allowing for greater complexation of the negatively charged hypochlorite molecule. The minimum pH values attained during the oxidative dissolutions of each of the seven clays, listed in order of increasing Cr concentration, were 9.3, 8.7, 8.2, 7.8, 7.4, 7.1, and 7.2. Clearly, the lowest pH values correspond to the greatest oxidation rates.

7.3.3 *Oxidative dissolution of coprecipitated hydroxy-Cr and -Al interlayers*

Each curve in Figure 7.4 represents the dissolution of hydroxy interlayers from clays which held 100 cmol Cr/kg. The solid-circle curve is for a clay that also held 100 cmol Al/kg. There were significant differences in the Cr oxidation rates between

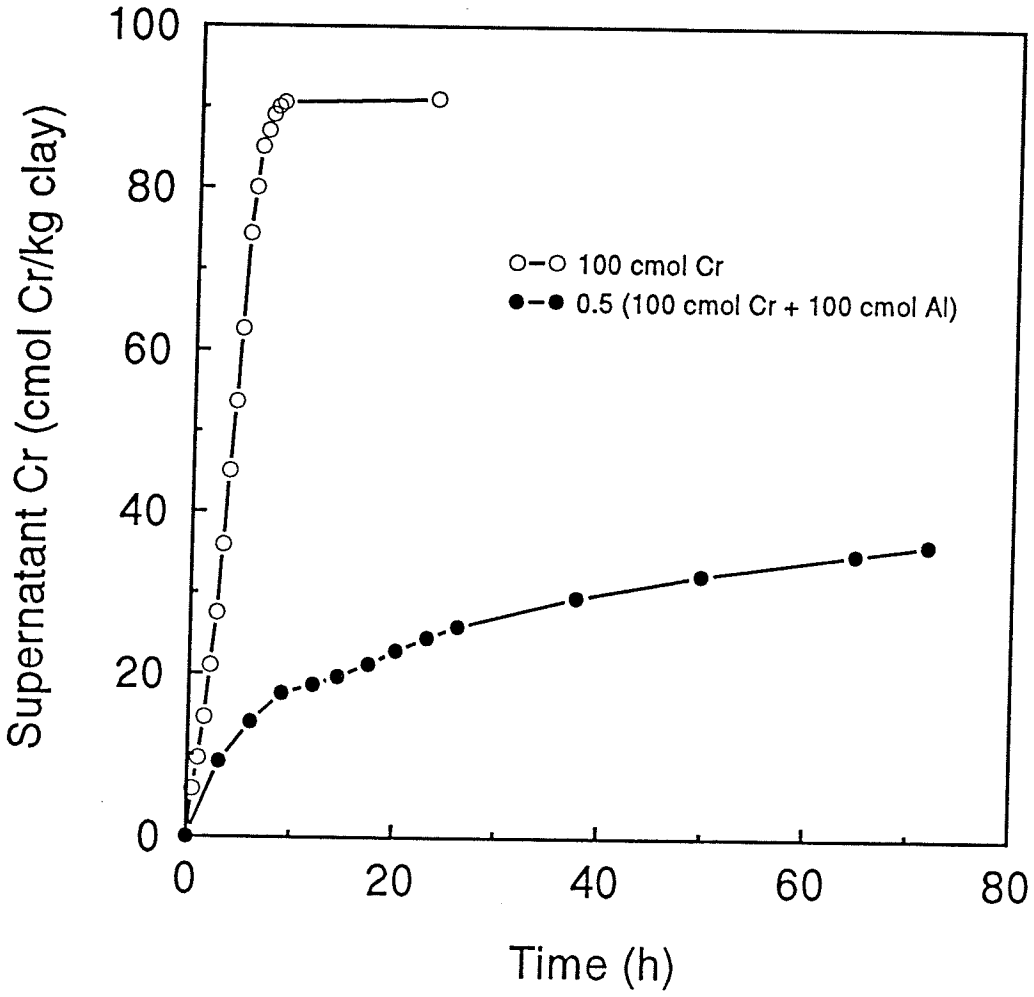

Figure 7.4. Supernatant Cr concentration as a function of time for both clays which held 100 cmol Cr/kg. The solid-circle curve is for a clay which also held 100 cmol Al/kg and therefore had an Al/(Al+Cr) molar ratio of 0.5.

these two clays. The rate of oxidation of Cr from the pure Cr interlayers was fast and constant, relative to that of the coprecipitated hydroxy-Cr and -Al interlayers. The oxidation rate of Cr from the Al-Cr interlayers was rapid only during the first 10 h, beyond which the rate was significantly slower. The pure Cr interlayers were dissolved extremely fast relative to the Al-Cr interlayers. Oxidative dissolution of the pure Cr interlayers was complete by 8 h (Figures 7.3 and 7.4) whereas oxidation of Cr from the Al-Cr interlayers was only partially complete by 70 h. As there was considerable Cr remaining on the Al-Cr clay after 70 h, the Al was shown to provide an effective hindrance to Cr oxidation.

As a means of determining the long-term stability of coprecipitated hydroxy-Cr and -Al interlayers, the supernatant Cr concentrations of the clays with Al/(Al+Cr) molar ratios of 0.33, 0.5, and 0.67 were monitored for several weeks (Figure 7.5). Chromium oxidation rates for all three clays were relatively rapid initially then decreased markedly at 3 to 5 days. The duration of this enhanced oxidation period varied with the Al/(Al+Cr) ratio of the interlayers. The clay with the most Cr (i.e. 0.33) gave the longest period of enhanced oxidation whereas the 0.67 clay gave the shortest period. Oxidation of Cr from all three clays continued, although at a much slower rate, throughout the remainder of the study period. The slow but sustained oxidation of Cr from these Al-Cr clays indicates that this Cr was oxidized via a mode of oxidation which was different from that for the pure Cr clays. After 30 days of reaction, substantial amounts of Cr remained sorbed on all three Al-Cr clays. The

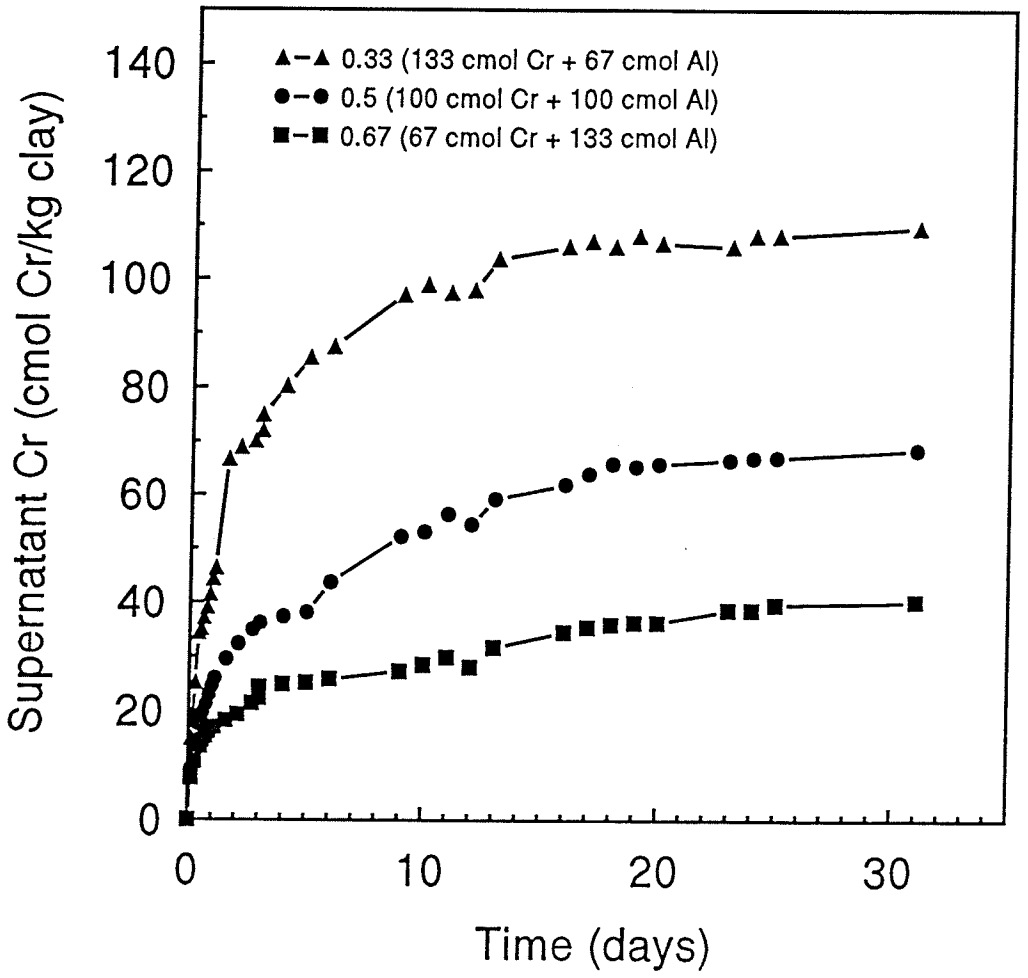

Figure 7.5. Supernatant Cr concentration as a function of time for clays which held Al/(Al+Cr) molar ratios of either 0.33, 0.5, or 0.67. Each clay held 200 cmol M^{3+}/kg.

amount of Cr remaining on each clay, as a percent of that initially present, varied with the initial Al/(Al+Cr) ratio. Specifically, the amount of Cr remaining after 30 days for the 0.33, 0.5, and 0.67 clays was 10-15, 30-40, and 40-45 %, respectively. Once again, the Al is shown to provide a significant hindrance to the oxidation of Cr. There were no detectable amounts of Al released from any of the Al-Cr clays during the 30 day oxidation period.

7.4 Discussion

7.4.1 *Oxidation mechanism*

The oxidative dissolution of all hydroxy-Cr polymers by NaOCl may be described with four elementary steps (Figure 7.6). As a precursor to dissolution, the OCl^- anions, accompanied by cations, diffuse into the interlayer region. The hypochlorite molecule has a net negative charge and is, therefore, electrostatically attracted to positive sites on the hydroxide surface (Figure 7.6a). Due to differences in the electronegativity of O and Cl, the hypochlorite anion is also polar, with a partial positive charge on the Cl. When in close proximity to the hydroxide surface, the OCl^- molecule will orient itself with the Cl atom close to an electron-rich hydroxyl group (Figure 7.6b). Once Cl-O orbital overlap has occurred, electron transfer is virtually instantaneous. Because the complexed hydroxyl group serves as ligand for both Cr and Cl, the electron transfer depicted in Figure 7.6c is classed as an inner-sphere (ligand-bridged) mechanism (Cotton and Wilkinson 1988). Water molecules are

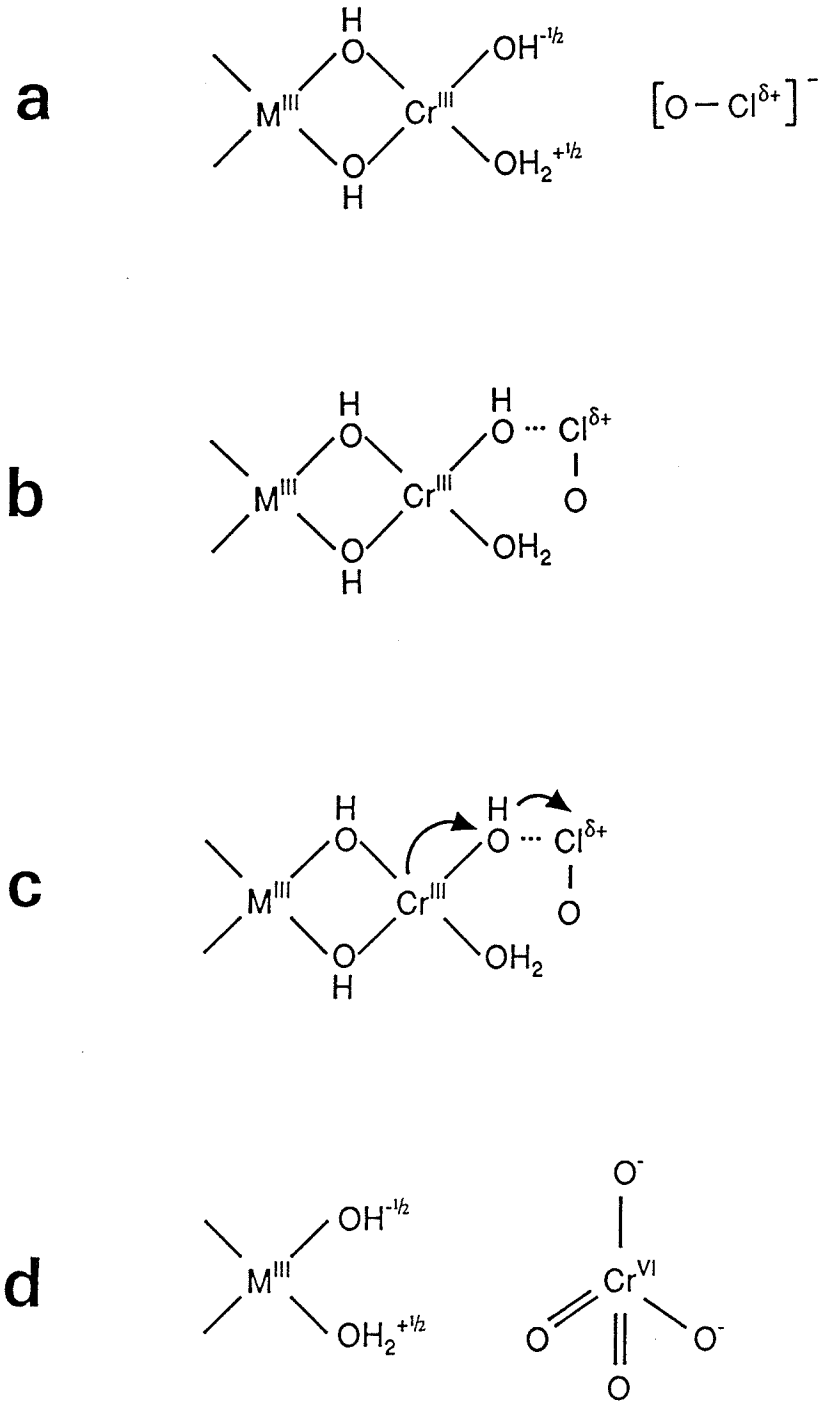

Figure 7.6. Schematic illustration of the proposed four-step oxidation mechanism. In order of occurrence the steps are: (a), electrostatic attraction; (b), complexation; (c), electron transfer and (d), dissolution.

also known to be bridging ligands. However, because the H_2O on the hydroxide carries a partial positive charge, it is much less likely to serve as a conduit for electrons. The electron transfer depicted in Figure 7.6c only grossly represents the actual process. Because two Cl atoms are required to complete the oxidation of one Cr(III), a multistep mechanism is involved, wherein an unstable intermediate is formed. Once the oxidation of Cr(III) is complete, the resultant Cr(VI) atom will adopt tetrahedral geometry, thereby destroying the hydroxide locally (Figure 7.6d). Whether oxidative dissolution continues depends on the identity of M^{3+}. Oxidation will continue if M is Cr and terminate if it is Al.

7.4.2 Oxidation kinetics

From the previous discussion, it is apparent that the rate of Cr(III) oxidation is most directly controlled by the rate at which the OCl^- complexes with the Cr-OH groups. This may be written as:

$$\frac{-dCr(III)}{dt} = k[Cr(III)-OH-OCl] \qquad (1)$$

This relationship assumes that all Cr atoms are oxidized with equal ease. However, within the sorbed hydroxy-Cr polymers, Cr may exist in one of two principal chemical environments (Dubbin and Goh 1995a). These different environments

determine the ease with which Cr(III) is oxidized. In the first environment, the six ligands around Cr consist of either OH or H_2O. In this case, the Cr is sorbed electrostatically via the net positive charge of the hydroxy polymer. Because the siloxane oxygen of the montmorillonite have not entered the coordination sphere of Cr, the Cr is held through an outer-sphere complex. In the second principal environment, a siloxane O replaces either OH or H_2O within the coordination sphere of Cr such that the Cr is sorbed covalently to the montmorillonite. Deprotonated O-groups, such as the siloxane O of montmorillonite, are known to serve as σ-donor ligands and provide these covalently bonded Cr atoms with greater electron density (Hering and Stumm 1990). Consequently, Cr(III) atoms sorbed through inner-sphere complexes are stronger reductants than those held through outer-sphere complexes. The redox potential of inner-sphere Cr, with respect to OCl^-, will, therefore, also be greater than that for outer-sphere Cr. Therefore, it is more accurate to express equation (1) with two terms, one for each mode of Cr(III) complexation:

$$\frac{-dCr(III)}{dt} = k[Cr(III)_{IS}\text{-}OH\text{-}OCl] + k'[Cr(III)_{OS}\text{-}OH\text{-}OCl] \qquad (2)$$

The relative proportion of inner- and outer-sphere Cr(III) varies with the total amount sorbed. Due to a small interlayer distance (Dubbin and Goh 1995a), all of the Cr in the lowest-Cr clays is in close proximity to the montmorillonite surface. It is possible,

therefore, for all this Cr to be sorbed through inner-sphere complexes. In the most Cr-rich clays, however, the interlayer distance is considerably greater and only that Cr which is adjacent to the siloxane surface could be sorbed specifically. Therefore, as the amount of sorbed Cr increases, the proportion which is bound inner-spherically decreases.

The concentration of all Cr(III)-OH-OCl complexes depends firstly on the concentrations of Cr(III) and OCl^-. Equation (2) should, therefore, be refined further:

$$\frac{-dCr(III)}{dt} = k[Cr(III)_{IS}][OCl] + k'[Cr(III)_{OS}][OCl] \qquad (3)$$

The Cr(III) on the right hand side of equation (3) refers only to that Cr which is located at the margins of the polymer and, therefore, accessible to the oxidant. As discussed in the next section, the Al-Cr clays may hold appreciable amounts of Cr(III) yet the oxidation rate is extremely slow because very little Cr(III) is located at the polymer margin. As indicated previously, the total OCl^- in the reaction vessel is in large excess of that required for complete Cr(III) oxidation and will, therefore, decrease only slightly during oxidation. Of relevance is the OCl^- concentration only within the interlayer space, which may vary considerably. Therefore, OCl^- in equation (3) refers only to OCl^- within the interlayer region.

Figure 7.2 indicates, and the proposed oxidation mechanism predicts, that the

oxidation of hydrolyzed Cr(III) is catalyzed by protons. As proton activity increases, the positive surface charge of the polymer also increases, thereby enhancing electrostatic attraction with the OCl^-. However, a lower pH reduces the number of hydroxyl groups to which the Cl can complex and through which the electrons can shuttle. It is apparent, therefore, that the pH at which oxidation is greatest will occur when both the electrostatic attraction and the number of hydroxyls are maximized.

From the previous discussion, it is apparent that the dissolution behavior of the pure hydroxy-Cr interlayers varies with the concentration of Cr(III), OCl^-, and H^+. Dissolution of the Al-Cr interlayers, however, involves a fourth variable, as will be discussed in the next section. The present discussion explains the dissolution curves of only the pure Cr clays. The most obvious trend illustrated in Figure 7.3 is that oxidation rates increased with the amount of sorbed Cr. This has occurred for two main reasons. First, as equation (3) illustrates, clays which held more Cr displayed greater oxidation rates simply because there was more Cr which could be oxidized. Second, the more Cr-rich clays generally had larger interlayer pore spaces, as indicated by greater N_2-BET specific surfaces. This greater pore space allowed for a more rapid movement of OCl^- into the interlayer region, thereby increasing oxidation rate. It is also obvious from Figure 7.3 that each clay displayed a marked acceleration in oxidation rate. These accelerations were caused by two main factors. First, protons liberated during the Cr(III) oxidation increased the positive charge of the polymer surface, thus allowing for greater complexation of OCl^-. Second, as the oxidation

progressed, interlayer material was removed and Na^+ was subsequently added to the newly-vacant exchange sites. The large hydration shell of Na^+ expanded the interlayer space, thus further increasing the supply of OCl^- to the polymers. During the period of most rapid oxidation for the 400, 600, and 800 clays, about 1.5×10^{16} Cr(III) atoms were oxidized from each clay every second. This number is remarkable, especially when one considers the number of steps required for oxidation to occur and the small sample size employed ($\sim$30 mg).

The maximum oxidation rate attained by each clay varied considerably. Much of this difference can be attributed to differences in the amount of Cr sorbed. However, if the maximum Cr(III) oxidation rate for each clay is expressed as cmol of Cr released to the supernatant per hour and per cmol of Cr sorbed (Figure 7.7), one can then attempt to explain these rate differences in terms of pH, polymer surface area, and mode of Cr complexation. Note, however, that the amount of sorbed Cr may indirectly affect these other parameters. For example, as Cr(III) content increases, the potential for a greater reduction in pH also increases.

Generally, for the pure Cr clays, maximum oxidation rates increased with the Cr content (Figure 7.7). This can be attributed to lower pH values and a greater OCl^- supply in the more Cr-rich clays. For the two most Cr-rich clays, however, additional sorbed Cr led to reductions in oxidation rate, despite similar pH values for each. These reductions were due primarily to a decrease in pore space, as indicated by smaller N_2-BET specific surfaces. Another observation from Figure 7.7 is that the

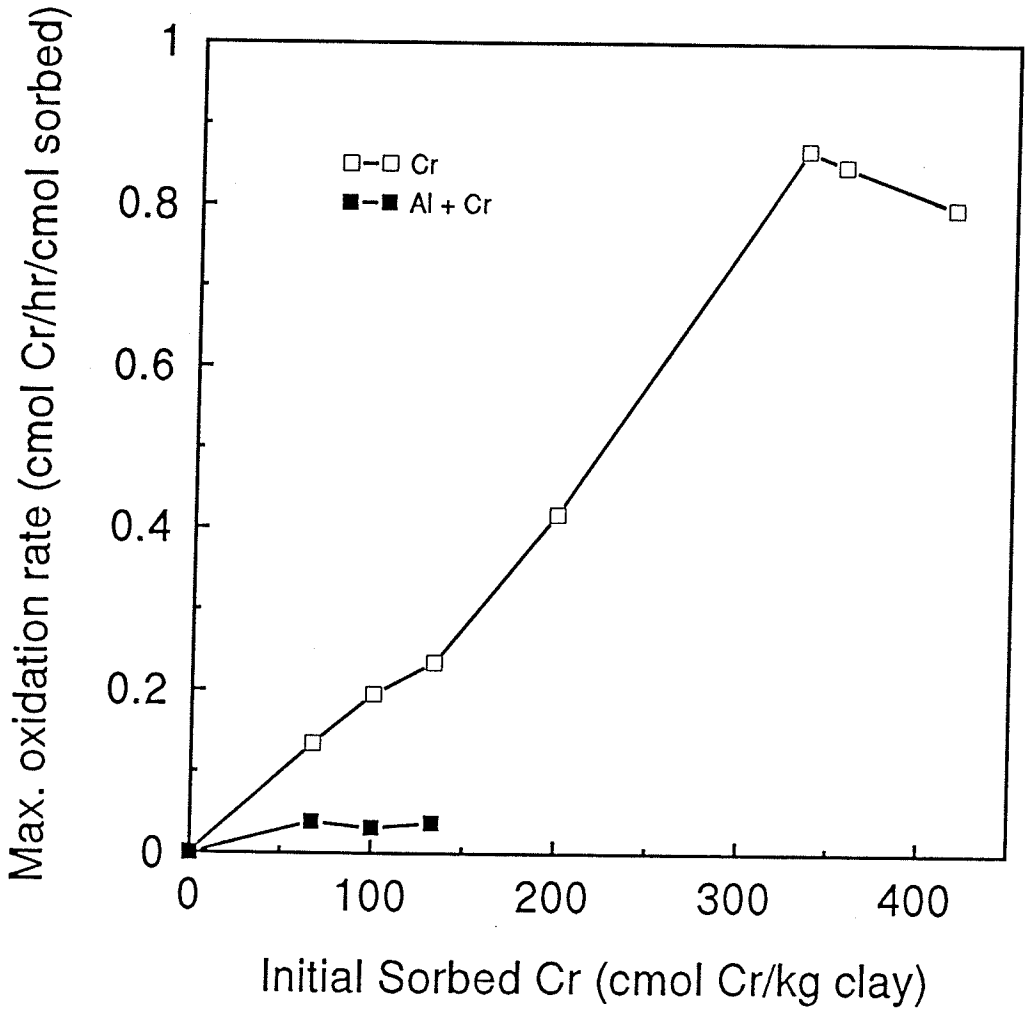

Figure 7.7. Maximum Cr oxidation rate for all samples, expressed as cmol of Cr released to the supernatant per hour and per cmol of Cr sorbed, as a function of the initial sorbed Cr concentration.

maximum oxidation rates observed for chromium in the pure Cr clays exceeded that of Cr in the Al-Cr clays. The reasons for this are explained next.

7.4.3 Effect of coprecipitated Al

Previous work (Dubbin et al. 1994) has shown that coprecipitated hydroxy-Cr and -Al interlayers exist as simple octahedral sheets wherein Cr has substituted for Al. One such sheet is shown schematically in Figure 7.8a. In this arrangement, considerable amounts of Cr are located at the periphery of the polymer. At the onset of oxidation, therefore, one observes the release of substantial amounts of Cr(VI) because much of the Cr(III) is easily accessible to the oxidant. However, the oxidation rate of Cr(III) from the Al-Cr clays began to decrease almost as soon as oxidation started, despite a decrease in the suspension pH. The mechanism proposed to explain this observation is illustrated in Figure 7.8. As Cr(III) atoms are removed via oxidation, the polymer becomes smaller and Al concentrates at the margins. As more Al accumulates, the Cr(III) atoms become less accessible, thereby decreasing the rate of oxidation. Eventually, an Al "shield" forms around the central, unaltered core of Al and Cr (Figure 7.8b).

The oxidation of Cr(III), whether it be from pure Cr clays or Al-Cr clays, is extremely fast. One can reasonably assume, therefore, that the Al shield will form within hours, or possibly even minutes, after the start of oxidation. However, it is clear from Figures 7.4 and 7.5 that the oxidation of Cr(III) continued long after the

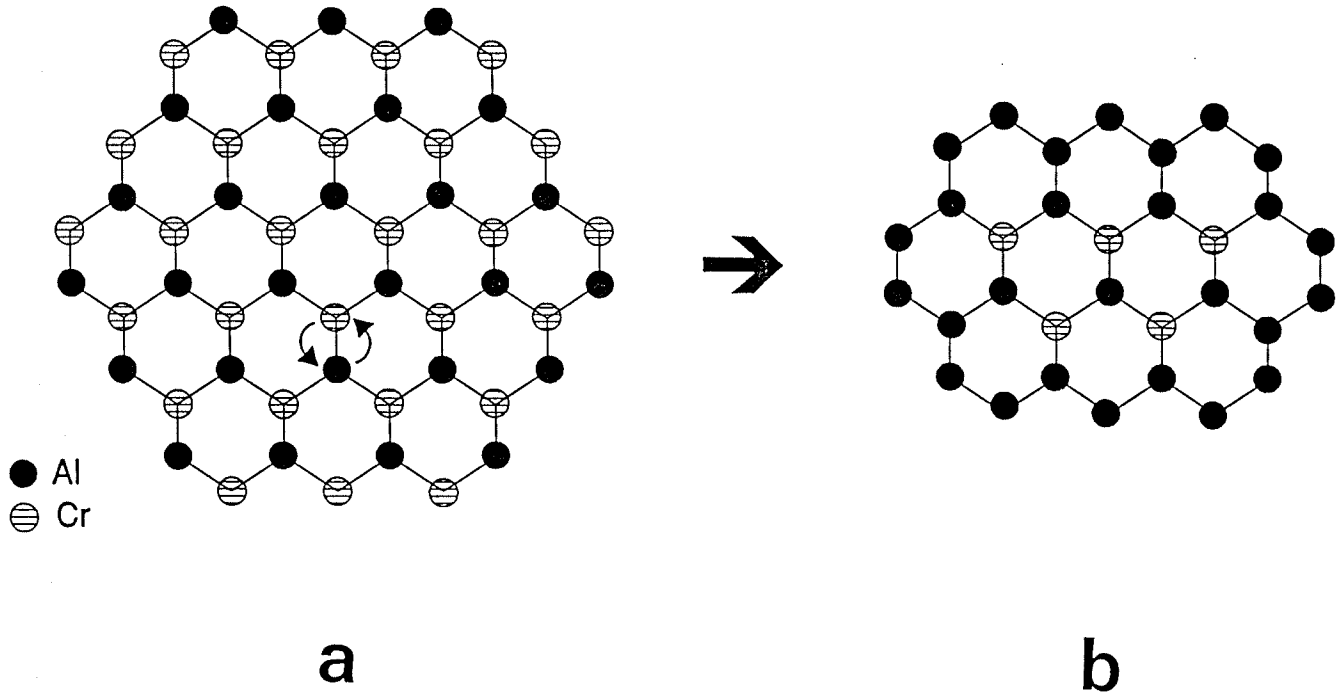

Figure 7.8. Schematic illustration of a hydroxy-Cr and -Al polymer before oxidation (a). Arrows depict interchange of atoms. An Al shield is visible in polymer (b), after oxidation.

shield would have formed. The continued oxidation of Cr(III) is believed to occur due to diffusion of Cr(III) atoms from the interior to the margins of the hydroxy polymers. The relative ease with which atoms can diffuse through solids is well known (Moore 1983). At the atomic level, the diffusive transport of Cr(III) requires Al to exchange lattice positions with Cr, as illustrated by the arrows in Figure 7.8a.

The diffusion of atoms in solids, like that in liquids and gases, occurs in response to a chemical gradient. The concentration gradient which drives the diffusion process in these Al-Cr polymers is generated by the depletion of Cr(III) at the polymer margin. And, like diffusion in liquids and gases, diffusion in solids can be described by Fick's law:

$$j_{Cr} = -D_{Cr} \frac{dc_{Cr}}{dx} \qquad (4)$$

where j is the diffusive flux, D is the diffusion coefficient, and dc/dx is the concentration gradient. To provide an accurate description of diffusion in solids, however, one must consider crystal defects such as vacancies. These vacancies can serve as channels through which the atoms travel to their new lattice positions. Vacancies may be considered as catalysts in two respects. First, they lower the activation energy of atom transfer and, second, their concentration does not change. The vacant sites in a dioctahedral sheet such as the interlayered hydroxy polymers,

though not strictly considered defects, would greatly increase the cation diffusion rate by lowering the activation energy for atom transfer. Therefore, in the presence of vacancies, the interchange of Al and Cr, while remaining difficult electronically, would become much easier sterically. To account for these vacancies in a quantitative way, the diffusion coefficient, D, in equation (4) must be related to the average jump frequency, Γ, of Cr in the polymer. Modifying the equation of Schmalzried (1974) gives the following:

$$j_{Cr} = -\Gamma_{Cr}\, g\, a_{Cr}^2 \frac{dc_{Cr}}{dx} \qquad (5)$$

where g is a geometrical factor which gives the probability that Cr will jump in a particular direction. For the polymer illustrated in Figure 7.8a, g is 1/3 or 1/2, depending on the initial location of the Cr atom. The a_{Cr} term gives the distance between two planes of Cr atoms.

The previous discussion makes clear that the ever-decreasing rate of Cr(III) oxidation is due to a continual decrease in the dc/dx term over time. As oxidation proceeds the Al shield thickens and the Cr(III) concentration within the polymer decreases. The average jump frequency, Γ, will remain constant provided the temperature does not vary. Therefore, oxidation will continue, although at an ever-decreasing rate, until all the Cr(III) has been oxidized. The Al shield slows, but does

not stop, the oxidation of Cr(III). The Al around the margin of the polymer simply provides a hindrance to Cr(III) oxidation. However, if the oxidizing conditions to which the Al-Cr clays are exposed are only transitory, some Cr(III) may remain unoxidized, depending on the duration of oxidation. In this regard, the coprecipitated Al affords the interlayered Cr(III) with a measure of protection against oxidation.

7.5 Conclusions

Interlayered hydroxy polymers of Cr(III) were oxidized rapidly in the presence of the powerful aqueous oxidant, NaOCl. The interlayer region of montmorillonite did not offer any protection against oxidation. On the contrary, the interlayer environment increased the oxidation rate of Cr(III) by (i), increasing the polymer surface area, (ii), allowing for the possibility of inner-sphere complexes, and (iii), providing a relatively confining environment in which the protons from oxidation could accumulate more rapidly. It may be concluded, therefore, that, with respect to aqueous oxidants such as NaOCl, interlayered hydroxy-Cr poses a greater environmental threat than does external phase $Cr(OH)_{3(s)}$. For the pure Cr clays, the layer structure of montmorillonite offers protection only from oxidants, such as Mn oxides, which are too large to enter the network of interlayer spaces.

Pure hydroxy-Cr interlayers are unlikely to form in natural environments. In natural systems, Cr(III) would coprecipitate with other hydrolyzable metals such as Al. Therefore, the Al-Cr clays prepared in this study more closely mimic the true

situation. The Al in these clays was shown to provide a significant hindrance to Cr(III) oxidation. The magnitude of this hindrance depends on the diffusion rate of Cr through the hydroxy polymers. This diffusion rate, in turn, is a function of temperature. Higher temperatures increase the kinetic energy of the polymer cations, thus increasing their rate of interchange. The jump frequency of the interlayer cations is also strongly dependent on their relative ionic radii. The activation energy of cation interchange would increase as the difference in ionic radii increases. To more closely replicate field conditions in future studies, therefore, both the oxidation temperature and the type of coprecipitated cation should reflect those found in natural systems. Another important area for future study would be to test the proposed oxidation mechanism in a more quantitative way. This could be achieved most effectively by fitting the proposed rate equations with the experimental data. However, uncertainty regarding the relative populations of inner- and outer-sphere Cr(III) may make this task difficult.

8. SUMMARY AND CONCLUSIONS

Soils and sediments rich in both smectite and Cr can be expected to hold large amounts of intercalated hydroxy-Cr polymers. The investigations described in the previous chapters provide new and important insights into the nature of these intercalated species. The structure and stability of the hydroxy-Cr interlayers varied considerably in response to changes in only two parameters: the amount of sorbed Cr and the presence or absence of Al. Under natural conditions of synthesis, where one would encounter a full suite of minerals, cations, ligands, as well as temperature and moisture regimes, the polymer diversity would increase dramatically. However, the range of polymers examined in the present study offered a glimpse into the nature of those interlayers which would form under natural conditions.

All sorbed Cr which was detected by XPS was shown to be present as Cr(III). Due to the slow polymerization of Cr(III), all pure Cr hydroxy polymers were small and poorly ordered. However, these polymers became less disordered as the amount of sorbed Cr increased. Montmorillonite was an effective sorbent for hydroxy-Cr species up to 1200 cmol(+)/kg. Above this concentration sorption continued, though less efficiently. When large amounts of Cr(III) were sorbed, hydroxy polymers 5 to 10 nm in diameter formed on the external surface of the montmorillonite. These polymers provided an effective means for binding adjacent tactoids, as revealed by the formation of montmorillonite microclusters.

As shown by XRD data, the presence of Al induced the formation of gibbsite-like sheets in all Cr-clays. Several other techniques indicated that both Al and Cr were present within the same hydroxy polymer. Specifically, data from cation exchanges, oxidative dissolutions, as well as from IR and ^{27}Al MAS NMR spectroscopy, support the notion of Al and Cr existing within the same polymer. Thus, the Al served to integrate Cr into relatively well ordered hydroxy interlayer polymers. In this respect, the Al has acted as a template in the formation of gibbsite-like sheets in the interlayer region of the Al-Cr clays.

The way in which a metal complexes with a surface greatly influences its behavior. A metal held through an inner-sphere complex is much less available to the surrounding solution than one which is held through only electrostatic forces. The mode of complexation becomes even more important when the metal, such as Cr, presents a potential threat to ecosystem health. Previous work suggested, but did not confirm, that Cr(III) forms inner-sphere complexes with the siloxane surface of montmorillonite. In this study, data from cation exchanges, as well as from IR and ^{29}Si MAS NMR spectroscopy, provide further evidence that Cr does, in fact, form covalent bonds with siloxane oxygen. Consequently, Cr can be expected to be much less bioavailable than a metal which forms only outer-sphere complexes.

The structure of the hydroxy polymers, summarized above, dictates their stability. Due to their small size and lack of long-range order, the pure Cr interlayers provided the montmorillonite little resistance to collapse upon heating. The addition

of Al, with the resulting increase in polymer size and order, greatly increased the thermal stability of the montmorillonite interlayer. Because Cr was held strongly through inner-sphere complexes, the polymers were highly resistant to displacement by K or Ca. Chromium could be displaced, in very small amounts, only from the Al-Cr clays and the three most Cr-rich clays. Therefore, Cr was found to be secure within the interlayer region when subjected to simple cation exchange reactions. However, the hydroxy interlayers were highly vulnerable to attack from the aqueous oxidant, NaOCl. The most Cr-rich clays were the most vulnerable due to their greater interlayer pore space and greater potential for pH reduction during the course of oxidation. The sustained oxidation of Cr(III) in the Al-Cr clays indicates that Al and Cr do not occupy fixed positions within the hydroxy polymers. Rather, Cr(III) is believed to move via solid-state diffusion to the polymer margin, where it can be oxidized. Therefore, the coprecipitated Al serves only to decrease the rate of, and not stop completely, the oxidation of Cr(III).

Although the primary focus of this study was to determine the fundamental properties of hydroxy-Cr interlayers, insights gained from this investigation are not without their application. As described above, sorbed hydroxy-Cr polymers can, in general, be considered unavailable to the solution. Although polymer dissolution may occur at a sufficiently low pH via proton attack, the Cr would be released as the relatively inert Cr(III) cation. However, under strongly oxidizing conditions, Cr would enter solution as the toxic Cr(VI) oxyanion. Therefore, to safeguard the quality of

waters in which hydroxy-Cr clays are present, efforts must be made to ensure that the redox conditions do not allow for the oxidation of Cr(III).

In any study which aims to address a wide range of topics, it is inevitable that some of the original questions will remain unanswered and new questions will arise. This study was no exception. Of the original goals, the attempt to determine the gross structure of the pure hydroxy-Cr polymers was the least successful. The techniques employed were not well-suited for the structural determination of these poorly ordered materials. Future attempts to elucidate the structure of the hydroxy-Cr polymers would be more successful if they were to incorporate x-ray absorption spectroscopy. This technique is capable of determining the local structure around a specific absorbing element, such as Cr. Alternatively, in the absence of such advanced instrumentation, one may increase the size and crystallinity of the hydroxy polymers by increasing the aging time, temperature, or both. The resultant polymers would then lend themselves more readily to effective study with conventional techniques.

Several new questions also arose from these investigations. As indicated previously, Al served as a template in the formation of gibbsite-like sheets in the Al-Cr clays. In future studies it may be useful to determine the concentration below which Al is no longer effective as a template. Data from such an investigation would allow one to characterize the Al-Cr interactions more completely. The rate of Cr(III) oxidation from the Al-Cr clays was shown to be dependent on the rate of Cr(III) diffusion through the hydroxy polymers. Therefore, a second possible area of further

investigation would be to establish how this diffusion rate changes in response to temperature, layer charge of the host clay, and the identity of other cations within the polymer. As a final suggestion for future work, one may wish to examine naturally-occurring hydroxy-Cr interlayers. Obviously, such a study would have the potential to be the richest source of information concerning these interlayers as they occur in natural systems. However, due to the heterogeneity of the environments in which these clays would occur, the certainty with which one could infer cause and effect relationships would be reduced.

BIBLIOGRAPHY

Ahlrichs, J.L. 1968. Hydroxyl stretching frequencies of synthetic Ni-, Al-, and Mg-hydroxy interlayers in expanding clays. Clays Clay Miner. 16: 63-71.

Asher, L.E. and Bar-Yosef, B. 1982. Effects of pyrophosphate, EDTA, and DTPA on zinc sorption by montmorillonite. Soil Sci. Soc. Am. J. 46: 271-276.

Baes, C.F. and Mesmer, R.E. 1976. The Hydrolysis of Cations. John Wiley & Sons, Toronto, ON. 489 pp.

Bailey, S.W. 1980. Summary of recommendations of AIPEA nomenclature committee. Clay Miner. 15: 85-93.

Bailey, S.W. 1988. Hydrous phyllosilicates (exclusive of the micas). Reviews in Mineralogy 19, Mineralogical Society of America, Washington, DC. 725 pp.

Barnhisel, R.I. and Bertsch, P.M. 1989. Chlorites and hydroxy-interlayered vermiculite and smectite. Pages 729-788 *in* J.B. Dixon and S.W. Weed, eds. Minerals in soil environments. 2nd ed. Soil Science Society of America Book Series No. 1, Madison, WI.

Bartlett, R.J. and Kimble, J.M. 1976. Behavior of chromium in soils: I. Trivalent forms. J. Environ. Qual. 5: 379-383.

Bassett, W.A. 1958. Copper vermiculites from northern Rhodesia. Am. Miner. 43: 1112-1133.

Bertsch, P.M. 1989. Aqueous polynuclear aluminum species. Pages 87-115 *in* G. Sposito, ed. The environmental chemistry of aluminum. CRC Press, Boca Raton, Fl.

Blatter, C.L. 1973. Hg-complex intergrades in smectite. Clays Clay Miner. 21: 261-263.

Boyd, S.A., Mortland, M.M. and Chiou, C.T. 1988. Sorption characteristics of organic compounds on hexadecyltrimethylammonium-smectite. Soil Sci. Soc. Am. J. 52: 652-657.

Brindley, G.W. and Brown, G. 1980. Crystal structures of clay minerals and their X-ray identification. Mineralogical Society, London. 495 pp.

Brindley, G.W. and Kao, C.C. 1980. Formation, compositions and properties of hydroxy-Al- and hydroxy-Mg-montmorillonite. Clays Clay Miner. 28: 435-443.

Brindley, G.W. and Sempels, R.E. 1977. Preparation and properties of some hydroxy-aluminum beidellites. Clay Miner. 12: 229-237.

Brindley, G.W. and Yamanaka, S. 1979. A study of hydroxy-chromium montmorillonites and the form of the hydroxy-chromium polymers. Am. Miner. 64: 830-835.

Carr, R.M. 1985. Hydration states of interlamellar chromium ions in montmorillonite. Clays Clay Miner. 33: 357-361.

Carrado, K.A., Suib, S.L., Skoularikis, N.D. and Coughlin, R.W. 1986. Chromium (III)-doped pillared clays (PILC's). Inorg. Chem. 25: 4217-4221.

Carstea, D.D., Harward, M.E. and Knox, E.G. 1970. Comparison of iron and aluminum hydroxy interlayers in montmorillonite and vermiculite: I. Formation. Soil Sci. Soc. Am. Proc. 34: 517-521.

Carter, D.L., Mortland, M.M. and Kemper W.D. 1986. Specific surface. Pages 413-423 *in* A. Klute, ed. Methods of Soil Analysis. Part 1, 2nd ed. Agronomy Society of America and Soil Science Society of America, Madison, WI.

Cary, E.E., Allaway, W.H. and Olson, O.E. 1977. Control of chromium concentrations in food plants. 2. Chemistry of chromium in soils and its availability to plants. J. Agric. Food Chem. 25: 305-309.

Charlet, L. and Manceau, A.A. 1992. X-ray absorption spectroscopic study of the sorption of Cr(III) at the oxide-water interface. II. Adsorption, coprecipitation, and surface precipitation on hydrous ferric oxide. J. Colloid Interface Sci. 148: 443-458.

Cheslock-Fitzgerald, M.M. 1990. Trivalent and hexavalent chromium, their reactions with minerals and potential phytotoxicity in soils. M.Sc. thesis, University of Manitoba, Canada.

Cotton, F.A. and Wilkinson, G. 1988. Advanced inorganic chemistry. 5th ed. Wiley-Interscience, New York, NY. 1455 pp.

Dixon, J.B. and Jackson, M.L. 1962. Properties of intergradient chlorite-expansible layer silicates of soils. Soil Sci. Soc. Am. Proc. 26: 358-362.

Dixon, J.B. and Weed, S.B. 1989. Minerals in soil environments. 2nd ed. Soil Science Society of America Book Series No. 1, Madison, WI. 1244 pp.

Drljaca, A., Anderson, J.R., Spiccia, L. and Turney, T.W. 1992. Intercalation of montmorillonite with individual chromium(III) hydrolytic oligomers. Inorg. Chem. 31: 4894-4897.

Dubbin, W.E. and Goh, Tee Boon. 1995a. Sorptive capacity of montmorillonite for hydroxy-Cr polymers and the mode of Cr complexation. Clay Miner. 30: 175-185.

Dubbin, W.E. and Goh, Tee Boon. 1995b. Electron microscope observations of chromium hydroxide-induced montmorillonite microclusters. Clays Clay Miner. 43: 131-134.

Dubbin, W.E., Goh, Tee Boon, Oscarson, D.W. and Hawthorne, F.C. 1994. Properties of hydroxy-Al and -Cr interlayers in montmorillonite. Clays Clay Miner. 42: 331-336.

Eary, L.E. and Rai, D. 1987. Kinetics of chromium(III) oxidation to chromium(VI) by reaction with manganese dioxide. Environ. Sci. Technol. 21: 1187-1193.

Egozy, Y. 1980. Adsorption of cadmium and cobalt on montmorillonite as a function of solution composition. Clays Clay Miner. 28: 311-317.

El Swaify, S.A. and Emerson, W.W. 1975. Changes in the physical properties of soil clays due to precipitated aluminum and iron hydroxides: I. Swelling and aggregate stability after drying. Soil Sci. Soc. Am. Proc. 39: 1056-1063.

Farmer, V.C. 1974. The layer silicates. Pages 331-363 *in* V.C. Farmer ed. The Infrared Spectra of Minerals. Mineralogical Society Monograph No.**4**.

Farmer, V.C. and Russell, J.D. 1967. Infrared absorption spectrometry in clay studies. Clays Clay Miner. 15: 121-141.

Fendorf, S.E., Fendorf, M., Sparks, D.L. and Gronsky, R. 1992. Inhibitory mechanisms of Cr(III) oxidation by δ-MnO_2. J. Colloid Interface Sci. 153: 37-54.

Fendorf, S.E., Lamble, G.M., Stapleton, M.G., Kelley, M.J. and Sparks, D.L. 1994. Mechanisms of chromium sorption on silica. 1. Cr(III) surface structure derived by extended x-ray absorption fine structure spectroscopy. Environ. Sci. Technol. 28: 284-289.

Fendorf, S.E. and Sparks, D.L. 1994. Mechanisms of chromium(III) sorption on silica. 2. Effect of reaction conditions. Environ. Sci. Technol. 28: 290-297.

Fendorf, S.E. and Zasoski, R.J. 1992. Chromium(III) oxidation by δ-MnO_2. 1. Characterization. Environ. Sci. Technol. 26: 79-85.

Fendorf, S.E., Zasoski, R.J. and Burau, R.G. 1993. Competing metal ion influences on chromium(III) oxidation by birnessite. Soil Sci. Soc. Am. J. 57: 1508-1515.

Fong, D.W. and Grunwald, E. 1969. Kinetic study of proton exchange between the $Al(OH_2)_6^{3+}$ ion and water in dilute acid. Participation of water molecules in proton transfer. J. Am. Chem. Soc. 91: 2413-2422.

Frenkel, H. and Shainberg, I. 1980. The effect of hydroxy-Al and hydroxy-Fe polymers on montmorillonite particle size. Soil Sci. Soc. Am. J. 44: 626-629.

Fripiat, J.J. 1988. High resolution solid state NMR study of pillared clays. Catalysis Today 2: 281-295.

Ghesquiere, C., Lemaitre, J. and Herbillon, A.J. 1982. An investigation of the nature and reducibility of Ni-hydroxymontmorillonites using various methods including temperature-programmed reduction (TPR). Clay Miner. 17: 217-230.

Glenn, R.C. and Nash, V.E. 1964. Weathering relationships between gibbsite, kaolinite, chlorite and expansible layer silicates in selected soils from the lower Mississippi coastal plain. Clays Clay Miner. 12: 529-548.

Goh, Tee Boon and Huang, P.M. 1986. Influence of citric and tannic acids on hydroxy-Al interlayering in montmorillonite. Clays Clay Miner. 34: 37-44.

Goodman, B.A. and Stucki, J.W. 1984. The use of nuclear magnetic resonance (NMR) for the determination of tetrahedral aluminium in montmorillonite. Clay Miner. 19: 663-667.

Griffen, R.A. and Au, A.K. 1977. Lead adsorption by montmorillonite using a competitive Langmuir equation. Soil Sci. Soc. Am. J. 41: 880-882.

Grim, R.E. 1968. Clay mineralogy. 2nd ed. McGraw-Hill, New York, NY. 596 pp.

Grove, J.H. and Ellis, B.G. 1980. Extractable chromium as related to soil pH and applied chromium. Soil Sci. Soc. Am. J. 44: 238-242.

Hamilton, J.W. and Wetterhahn, K.E. 1988. Chromium. Pages 239-250 *in* H.G. Seiler, H. Sigel, and A. Sigel, eds. Handbook on toxicology of inorganic compounds. Marcel Dekker, New York, NY.

Hering, J.G. and Stumm, W. 1990. Oxidative and reductive dissolution of minerals. Pages 427-465 *in* M.F. Hochella, Jr. and A.F. White, eds. Mineral-water interface geochemistry. Reviews in Mineralogy 23, Mineralogical Society of America, Washington, DC.

Herrera, R. and Peech, M. 1970. Reaction of montmorillonite with iron(III). Soil Sci. Soc. Am. Proc. 34: 740-742.

Herrero, C.P., Gregorkiewitz, M., Sanz, J. and Serratosa, J.M. 1987. ^{29}Si MAS-NMR spectroscopy of mica-type silicates: Observed and predicted distribution of tetrahedral Al-Si. Phys Chem Minerals. 15: 84-90.

Herrero, C.P., Sanz, J. and Serratosa, J.M. 1985. Si, Al distribution in micas: analysis by high-resolution ^{29}Si NMR spectroscopy. J. Phys. C: Solid State Phys. 18: 13-22.

Hochella, M.F. 1988. Auger electron and x-ray photoelectron spectroscopies. Pages 573-637 *in* F.C. Hawthorne, ed. Spectroscopic methods in mineralogy and geology. Reviews in Mineralogy 18, Mineralogical Society of America, Washington, DC.

Hsu, P.H. 1989. Aluminum hydroxides and oxyhydroxides. Pages 331-378 *in* J.B. Dixon and S.W. Weed, eds. Minerals in soil environments. 2nd ed. Soil Science Society of America Book Series No. 1, Madison, WI.

Hsu, P.H. and Bates, T.F. 1964. Formation of x-ray amorphous and crystalline aluminum hydroxides. Miner. Mag. 33: 749-768.

Inskeep, W.P. and Baham, J. 1983. Competitive complexation of Cd(II) and Cu(II) by water-soluble organic ligands and Na-montmorillonite. Soil Sci. Soc. Am. J. 47: 1109-1115.

James, B.R. and Bartlett, R.J. 1983. Behavior of chromium in soils: V. Fate of organically complexed Cr(III) added to soil. J. Environ. Qual. 12: 169-172.

Jaynes, W.F. and Boyd, S.A. 1991. Hydrophobicity of siloxane surfaces in smectites as revealed by aromatic hydrocarbon adsorption from water. Clays Clay Miner. 39: 428-436.

Jensen, W.B. 1978. The Lewis acid-base definitions: A status report. Chem. Rev. 78: 1-22.

Johnson, C.A. and Xyla, A.G. 1991. The oxidation of chromium(III) to chromium(VI) on the surface of manganite (γ-MnOOH). Geochim. Cosmochim. Acta. 55: 2861-2866.

Keren, R. 1980. Effects of titration rate, pH, and drying process on cation exchange reduction and aggregate size distribution of montmorillonite hydroxy-aluminum complexes. Soil Sci. Soc. Am. J. 44: 1209-1212.

Kinsey, R.A., Kirkpatrick, R.J., Hower, J., Smith, K.A. and Oldfield, E. 1985. High resolution aluminum-27 and silicon-29 nuclear magnetic resonance spectroscopic study of layer silicates, including clay minerals. Am. Miner. 70: 537-548.

Kirkpatrick, R.J. 1988. MAS NMR spectroscopy of minerals and glasses. Pages 341-403 *in* F.C. Hawthorne, ed. Spectroscopic methods in mineralogy and geology. Reviews in Mineralogy 18, Mineralogical Society of America, Washington, DC.

Klein, C. and Hurlbut, C.S. 1985. Manual of mineralogy. 20th ed. John Wiley & Sons, New York, NY. 596 pp.

Lahav, N. and Shani, U. 1978. Cross-linked smectites. II. Flocculation and microfabric characteristics of hydroxy-aluminum-montmorillonite. Clays Clay Miner. 26: 116-124.

Laubusch, E.J. 1971. Chlorination and other disinfection processes. Pages 158-224 *in* Water quality and treatment. 3rd ed. McGraw-Hill, Toronto, ON.

Lester, J.N. 1987. Heavy metals in wastewater and sludge treatment processes. Vol. I. Sources, analysis, and legislation. CRC Press, Boca Raton, Fl.

Liang, J.-J. and Sherriff, B.L. 1993. Lead exchange into zeolite and clay minerals: A ^{29}Si, ^{27}Al, ^{23}Na solid-state NMR study. Geochim. Cosmochim. Acta. 57: 3885-3894.

Lou, G. and Huang, P.M. 1988. Hydroxy-aluminosilicate interlayers in montmorillonite: implications for acidic environments. Nature. 335: 625-627.

Malla, P.B. and Komarneni, S. 1993. Properties and characterization of Al_2O_3 and SiO_2-TiO_2 pillared saponite. Clays Clay Miner. 41: 472-483.

Manceau, A. and Charlet, L. 1992. X-ray absorption spectroscopic study of the sorption of Cr(III) at the oxide-water interface. I. Molecular mechanism of Cr(III) oxidation on Mn oxides. J. Colloid Interface Sci. 148: 425-442.

Martin-Luengo, M.A., Martins-Carvalho, H., Ladriere, J. and Grange, P. 1989. Fe(III)-pillared montmorillonites: preparation and characterization. Clay Miner. 24: 495-504.

Mengel, K. and Kirkby, E.A. 1987. Principles of Plant Nutrition. 4th ed. International Potash Institute, Bern, Switzerland, 687 pp.

Misono, M., Ochiai, E., Saito, Y. and Yoneda, Y. 1967. A new dual parameter scale for the strength of Lewis acids and bases with the evaluation of their softness. J. Inorg. Nucl. Chem. 29: 2685-2691.

Moore, W.J. 1983. Basic physical chemistry. Prentice-Hall, Inc. Toronto. 711 pp.

Morris, H.D., Bank, S. and Ellis, P.D. 1990. ^{27}Al NMR spectroscopy of iron-bearing montmorillonite clays. J. Phys. Chem. 94: 3121-3129.

Nordstrom, D.K. and May, H.M. 1989. Aqueous equilibrium data for mononuclear aluminum species. Pages 29-53 *in* G. Sposito, ed. The environmental chemistry of aluminum. CRC Press, Boca Raton, Fl.

Occelli, M.L. and Tindwa, R.M. 1983. Physicochemical properties of montmorillonite interlayered with cationic oxyaluminum pillars. Clays Clay Miner. 31: 22-28.

Oestrike, R., Yang, W.-H., Kirkpatrick, R.J., Hervig, R.L., Navrotsky, A. and Montez, B. 1987. High-resolution ^{23}Na, ^{27}Al, and ^{29}Si NMR spectroscopy of framework aluminosilicate glasses. Geochim. Cosmochim. Acta. 51: 2199-2209.

Paustenbach, D.J., Rinehart, W.E. and Sheehan, P.J. 1991. The health hazards posed by chromium-contaminated soils in residential and industrial areas: conclusions of an expert panel. Regul. Toxicol. Pharmacol. 13: 195-222.

Pinnavaia, T.J., Tzou, M.-S. and Landau, S.D. 1985. New chromia pillared clay catalysts. J. Am. Chem. Soc. 107: 4783-4785.

Pinnavaia, T.J., Tzou, M.-S., Landau, S.D. and Raythatha, R.H. 1984. On the pillaring and delamination of smectite clay catalysts by polyoxo cations of aluminum. J. Mol. Catal. 27: 195-212.

Plee, D., Borg, L., Gatineau, L. and Fripiat, J.J. 1985. High resolution solid state ^{27}Al and ^{29}Si nuclear magnetic resonance study of pillared clay. J. Am. Chem. Soc. 107: 2362-2369.

Rai, D., Sass, B.M. and Moore, D.A. 1987. Chromium(III) hydrolysis constants and solubility of chromium(III) hydroxide. Inorg. Chem. 26: 345-349.

Rausell-Colom, J.A. and Serratosa, J.M. 1987. Reactions of clays with organic substances. Pages 371-422 *in* A.C.D. Newman, ed. Chemistry of clays and clay minerals. Monograph No. 6, Mineralogical Society, London.

Rengasamy, P. and Oades, J.M. 1978. Interaction of monomeric and polymeric species of metal ions with clay surfaces. III. Aluminium(III) and chromium(III). Aust. J. Soil Res. 16: 53-66.

Rich, C.I. 1961. Calcium determination for cation exchange capacity measurements. Soil Sci. 92: 226-231.

Rich, C.I. 1968. Hydroxy interlayers in expansible layer silicates. Clays Clay Miner. 16: 15-30.

Rich, L.D., Cole, D.L. and Eyring, E.M. 1969. Hydrolysis kinetics of dilute aqueous chromium(III) perchlorate. J. Phys. Chem. 73: 713-716.

Sanz, J. and Serratosa, J.M. 1984. ^{29}Si and ^{27}Al high-resolution MAS-NMR spectra of phyllosilicates. J. Am. Chem. Soc. 106: 4790-4793.

Schmalzried, H. 1974. Solid state reactions. Academic Press, New York, NY. 214 pp.

Schramm, L.L. and Kwak, J.C.T. 1982. Influence of exchangeable cation composition on the size and shape of montmorillonite particles in dilute suspension. Clays Clay Miner. 30: 40-48.

Schutz, A., Stone, W.E.E., Poncelet, G. and Fripiat, J.J. 1987. Preparation and characterization of bidimensional zeolitic structures obtained from synthetic beidellite and hydroxy-aluminum solutions. Clays Clay Miner. 35: 251-261.

Sheehan, P.J., Meyer, D.M., Sauer, M.M. and Paustenbach, D.J. 1991. Assessment of the human health risks posed by exposure to chromium-contaminated soils. J. Toxicol. Environ. Health. 32: 161-201.

Shewry, P.R. and Peterson, P.J. 1976. Distribution of chromium and nickel in plants and soil from serpentine and other sites. J. Ecol. 64: 195-212.

Shriver, D.F., Atkins, P.W. and Langford, C.H. 1990. Inorganic chemistry. W.H. Freeman, New York, NY. 706 pp.

Skoularikis, N.D., Coughlin, R.W., Kostapapas, A., Carrado, K. and Suib, S.I. 1988. Catalytic performance of iron (III) and chromium (III) exchanged pillared clays. Appl. Cat. 39: 61-76.

Sposito, G. 1984. The surface chemistry of soils. Oxford University Press, New York, NY. 234 pp.

Sposito, G. 1994. Chemical equilibria and kinetics in soils. Oxford University Press, New York, NY. 268 pp.

Sterte, J. and Shabtai, J. 1987. Cross-linked smectites. V. Synthesis and properties of hydroxy-silicoaluminum montmorillonites and fluorhectorites. Clays Clay Miner. 35: 429-439.

Sunder, S., Oscarson, D.W., Miller, N.H., Dubbin, W.E. and Goh, T.B. 1995. X-ray photoelectron spectroscopic study of chromium sorbed on montmorillonite. Can. J. Appl. Spectrosc. 40: 31-35.

Tan, K.H., Hajek, B.F. and Barshad, I. 1986. Thermal analysis techniques. Pages 151-183 *in* A. Klute, ed. Methods of Soil Analysis. Part 1, 2nd ed. Agronomy Society of America and Soil Science Society of America, Madison, WI.

Tsvetkov, F., Mingelgrin, U. and Lahav, N. 1990. Cross-linked hydroxy-Al-montmorillonite as a stationary phase in liquid chromatography. Clays Clay Miner. 38: 380-390.

U.S. Environmental Protection Agency. 1977. Municipal sludge management: environmental factors; NTIS/EPA 430/9-77-004; Office of Water Program Operations: Washington, DC. 19 pp.

van Bladel, R., Halen, H. and Cloos P. 1993. Calcium-zinc and calcium-cadmium exchange in suspensions of various types of clays. Clay Miner. 28: 33-38.

van Olphen, H. and Fripiat, J.J. 1979. Data handbook for clay materials and other non-metallic minerals. Pergamon Press, Toronto. 346 pp.

Weast, R.C. 1976. CRC Handbook of Chemistry and Physics. 57th edition. CRC Press, Inc. Boca Raton, Fl.

Weaver, C.E. and Pollard, L.D. 1973. Smectite. Pages 55-86 *in* The chemistry of clay minerals: Developments in sedimentology. Vol. 15. Elsevier, Amsterdam.

Weismiller, R.A., Ahlrichs, J.L. and White, J.L. 1967. Infrared studies of hydroxy aluminum interlayer material. Soil Sci. Soc. Am. Proc. 31: 459-463.

Wilson, M.A., Barron, P.F. and Campbell, A.S. 1984. Detection of aluminium coordination in soils and clay fractions using ^{27}Al magic angle spinning n.m.r. J. Soil Sci. 35: 201-207.

Woessner, D.E. 1989. Characterization of clay minerals by ^{27}Al nuclear magnetic resonance spectroscopy. Am. Miner. 74: 203-215.

Xiang, Y., Villemure, G. and Detellier, C. 1992. Observation by scanning electron microscopy of globular particles of calcium-montmorillonite and of montmorillonite exchanged with methyl viologen or tris (bipyridyl) ruthenium(II). Clays Clay Miner. 40: 362-364.

Yamanaka, S. and Brindley, G.W. 1978. Hydroxy-nickel interlayering in montmorillonite by titration method. Clays Clay Miner. 26: 21-24.

Yamanaka, S. and Brindley, G.W. 1979. High surface area solids obtained by reaction of montmorillonite with zirconyl chloride. Clays Clay Miner. 27: 119-124.

Yamanaka, S., Yamashita, G. and Hattori, M. 1980. Reaction of hydroxybismuth polycations with montmorillonite. Clays Clay Miner. 28: 281-284.